Identification of past climate variability of the eastern Pacific Ocean using both $\delta^{13}C$ and $\delta^{18}O$ records in corals from Clipperton Atoll (1994-1906)

A thesis presented to the Faculty

of the University at Albany, State University of New York

in partial fulfillment of the requirements

for the degree of

Master of Science

College of Arts & Sciences

Department of Earth and Atmospheric Sciences

Lei Ren

1998

Identification of past climate variability of the eastern Pacific Ocean using both $\delta^{13}C$ and $\delta^{18}O$ records in corals from Clipperton Atoll (1994-1906)

Abstract of

a thesis presented to the Faculty

of the University at Albany, State University of New York

in partial fulfillment of the requirements

for the degree of

Master of Science

College of Arts & Sciences

Department of Earth and Atmospheric Sciences

Lei Ren

1998

ABSTRACT

The ENSO (El Niño and the Southern Oscillation) is a fundamental ocean-atmosphere phenomenon that dominates interannual global climate variability. Reconstructing past ENSO events is therefore important for documenting and understanding the past behavior of the global climate system and enabling us to predict future climate change. However, the present understanding of ENSO events has been mainly based on the instrumental record of Pacific climate which provides detailed data only for the past few decades. Recent studies have shown that the stable isotope record in coral skeletons can be used as a valuable indicator of paleoclimatic changes in tropical regions, and therefore can potentially be used as a tool for reconstructing past ENSO events. This study presents a complete 88-year oxygen and carbon isotopic record in corals from Clipperton Atoll in the eastern Pacific for the period 1906-1994. The data were analyzed using time-series statistical methods and discussed in terms of the varying extent to which they reflect the past ENSO events as well as other climatic changes. Although both sea surface temperature (SST) and precipitation have influenced coral $\delta^{18}O$ at Clipperton, multisample analysis suggests that the effect of SST on coral $\delta^{18}O$ appears to have played a more important role than that of precipitation/salinity. Growth rate does not appear to have much effect on coral $\delta^{18}O$. In the case of $\delta^{13}C$ in these corals, there is a negative correlation between SST and $\delta^{13}C$, although not as apparent as with skeletal $\delta^{18}O$. Solar radiation intensity also shows weak negative correlation with $\delta^{13}C$, which suggests a view contrary to what is generally held. To identify possible ENSO events and other possible climate changes in this region, the 88-year $\delta^{18}O$ record was analyzed using singular spectrum analysis (SSA) which revealed pronounced interannual cycles, interpreted as reflecting past ENSO events, as well as other interdecadal cycles and a long term trend. Comparison of the ENSO components (period

between 3 and 5 years) with the historic records of ENSO and SST shows that at Clipperton coral $\delta^{18}O$ is generally sensitive to ENSO variability, although it also shows some local characteristics. Comparison with coral isotopic records from other regions in the Pacific and Indian Oceans further corroborates other studies which indicate that ENSO has occurred persistently for at least 100 years over the entire tropical ocean and that it has oscillated in the same characteristic 3- to 6-year frequency band. The interdecadal cycles in the $\delta^{18}O$ record may also be related to ENSO events, while the long-term trend may be related to the global temperature rise as the result of the CO_2 "greenhouse effects". Coral $\delta^{13}C$ also has a long-term trend. Comparison with a model of variation of $\delta^{13}C$ in dissolved inorganic carbon (DIC) at Clipperton based on measurements of atmospheric O_2 and CO_2 concentration shows that this trend may be due to the input of ^{13}C depleted CO_2 and the "Suess" effect.

ACKNOWLEDGMENTS

Without the help and encouragement of many people, this work would have been impossible. Thanks are due to the Departments of Geological Sciences here in Albany and in Beijing (China). The social and academic environment during the development of this thesis influenced me a great deal. I am especially indebted to my advisor Brad Linsley, whose consistent advice and encouragement have been invaluable in the completion of this work. I could not have done it without his help and guidance. The financial support that he provided is also gratefully acknowledged. Special thanks go to my other thesis committee members Andrei Lapenis and John Arnason for reading my thesis and for their thoughtful comments and constructive criticisms of my early draft. I am also grateful to Steve Howe for his assistance with isotopic analysis. His professional guidance and his patience in helping me using the mass spectrometer greatly improved the quality of my analysis results. Special thanks are also accorded Taohong Li for his encouragement and help in many aspects of my university life. Many other people also helped in one way or the other, either by furnishing advice or by discussing interesting problems. Their help is also gratefully acknowledged. This work was supported by the US National Science Foundation (NSF) and the U.S. Department of Energy's (DOE) National Institute of Global Environmental Change (NIGEC).

Finally, a special word of thanks goes to my parents who led me into the fantastic geological world. I am greatly grateful to them for their encouragement and endurance with me during my adventurous university career over the past years.

TABLE OF CONTENTS

LIST OF FIGURES

LIST OF TABLES

CHAPTER 1 INTRODUCTION

The tropical ocean-atmosphere is an active component of the Earth's climate system and it exerts a strong influence on climate variability worldwide (Troup, 1965; Bjerknes, 1966, 1972; Rasmusson and Carpenter, 1982; Cane et al., 1986; Enfield, 1989; Philander, 1990; Glantz, 1996 to site a few). The ENSO (El Niño and the Southern Oscillation) is a fundamental phenomenon in the tropical climate system, so the task of understanding ENSO is seen by climatologists as an important key to understanding uncertainty about tropical climate and weather patterns and, to a varying extent, their impacts on regions outside the tropics (called the extra-tropics) (Cane et al., 1986; Enfield, 1989; Philander, 1990; Glantz, 1996). Therefore, reconstructing past variations of ENSO is essential for documenting and understanding the past behavior of the tropical climate system, providing a more accurate baseline for current climatic models, and predicting future changes.

The ENSO phenomenon is usually defined by abnormal changes in the spatial patterns of sea surface temperature (SST) in the Pacific Ocean (El Niño or EN) and in sea-level atmospheric pressure across the Pacific basin (the Southern Oscillation or SO). The Walker Circulation, an important atmospheric circulation pattern in the Pacific links the Southern Oscillation with sea surface temperature (Bjerknes, 1966). Under normal conditions (here referred to as La Niña or ENSO cool-phase), strong trade winds flow from east to west across the Pacific, leading to the creation of a pool of warm water in the western Pacific, known as the western Pacific water pool (WPWP) (Fig. 1.1). Consequently, the thermocline is relatively deep in the west Pacific. Elevated SST in the WPWP causes air to rise which, in turn, produces rain-bearing clouds. As the warmed air rises to even higher levels of the atmosphere, pressure differences between the west Pacific

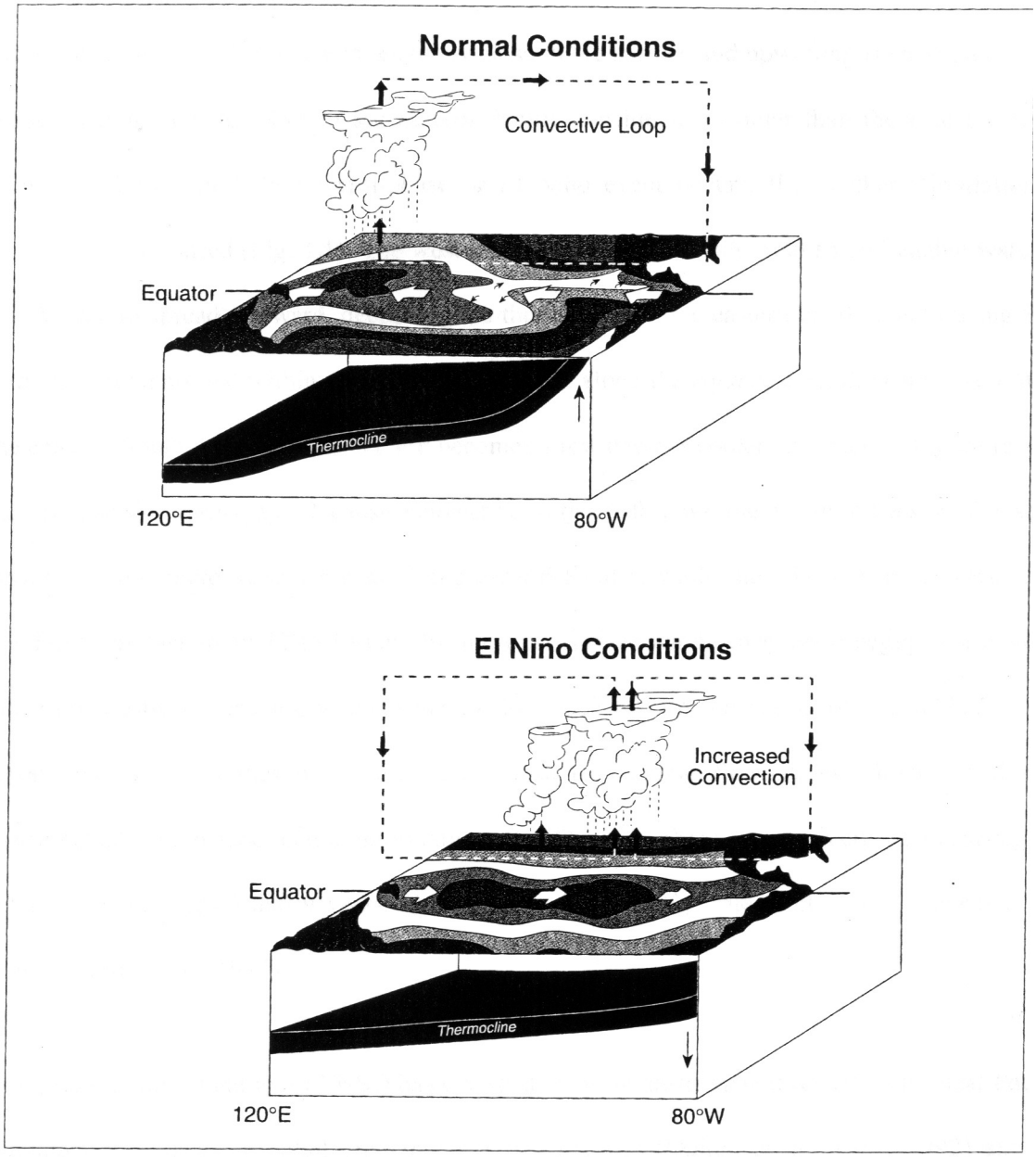

Fig. 1.1 Schematic of oceanic and atmospheric changes in the Pacific Ocean due to ENSO (after NOAA PMEL, 1996)

and the east Pacific move the now cooler air to higher altitudes and push it toward the eastern part of the Pacific basin. The cool, dry air ultimately descends in the eastern equatorial Pacific. In the eastern Pacific, the thermocline is relatively close to the surface and upwelling is strong along the coasts, making average SST in the eastern Pacific considerably cooler than those in the west. However, during an ENSO warm-phase or El Niño event occurs, the Walker Circulation is significantly modified (Fig. 1.1). The westward-flowing trade winds weaken and enable water in the WPWP to spread eastward, deepening the thermocline in the eastern Pacific, and raising SST 2 to 5°C above normal within a narrow latitude band along the equator extending from 160°W to the coast of South America. The WPWP becomes a few degrees cooler, as water in the central and eastern Pacific warms up. Because convective activity follows the warm waters at the sea's surface, clouds increase in the central and eastern Pacific, while they decline in the west. This condition can last about 12 to 18 months, until the surface winds once again begin to strengthen and flow westward, causing warm water to flow back toward the region of the WPWP. Thus, ENSO waxes and wanes over time in response to climatic fluctuations. Based on limited instrumental and paleoclimatic information, ENSO warm-phase events recur at quasi-regular intervals of between 3 and 9 years (Quinn et al., 1987; 1992; Cole et al., 1993; Dunbar et al., 1994; Charles et al., 1997).

The present understanding of ENSO has emerged from the instrumental record of tropical Pacific climate which spans in detail only the past few decades (Quinn, et al., 1987; 1992) and the continental recording systems such as tree rings and ice cores (Cook, 1992; Lough, 1992; Thompson et al., 1992 to site a few). Very little documentation is available from the oceans which cover 75% of the Earth's surface and are the place where ENSO events directly occur. Recent studies have shown that ENSO events can be identified using the isotopic records of the skeletons

of long-lived corals located in certain ENSO sensitive settings (McConnaughey, 1989a; Druffel et al., 1990; Cole and Fairbanks, 1990; Cole et al., 1993; Dunbar et al., 1994; Charles et al., 1997 among others). Massive reef corals can grow continuously at rates of several mm to several cm per year with most species producing annual growth bands. The oxygen isotopic composition ($\delta^{18}O$) of coral skeletons has been shown to be a good indicator of seasonal and interannual changes in SST and precipitation which are both associated with changes in ENSO (Dunbar and Wellington, 1981; Swart, 1983; McConnaughey, 1989a; Linsley et al., 1994; Charles et al., 1997 and others). In regions where precipitation and/or seawater oxygen isotopic composition ($\delta^{18}O_{water}$) remain relatively constant, the skeletal $\delta^{18}O$ may be converted into an estimate of past SST (McConnaughey, 1989a; Dunbar et al., 1994). Alternatively, in regions where there is little variation in SST, the skeletal $\delta^{18}O$ may be used to estimate changes in seawater oxygen isotope composition through time, usually related to variations in the input of isotopically light precipitation and/or run-off (Cole et al., 1993; Linsley et al., 1994; Tudhope et al., 1995). Several authors have in fact reconstructed seasonal variations in seawater temperature (Weber and Woodhead, 1972; Fairbanks and Dodge, 1979; Dunbar et al., 1994) and precipitation (Dunbar and Wellington, 1981; Cole et al., 1993; Linsley et al., 1994).

However, complications arise when coral skeletal $\delta^{18}O$ is influenced by two or more competing influences at the same time. One problem is how to separate the effects of fluctuations in SST from those of variations in precipitation. Another problem is related to the possible influence of biological processes such as the growth rate on the skeletal $\delta^{18}O$ composition (Land et al., 1975; McConnaughey, 1989a; Allison et al., 1996; Cohen and Hart, 1997). It is known that the $\delta^{18}O$ of the actual aragonitic coral skeleton is often several per mil more depleted than the $\delta^{18}O$ of aragonite in isotopic equilibrium with seawater (Weber and Woodhead, 1972; McConnaughey,

1989a). The usefulness of corals as recorders of SST and precipitation depends on the assumption that this departure from equilibrium remains constant in the axis of maximum coral growth (Land et al., 1975; McConnaughey, 1989a; Wellington et al., 1996). However, several studies have argued that the growth rate may be an important influence on coral $\delta^{18}O$, causing significant ^{18}O depletion with increase of growth rate (Barnes and Lough, 1992; Barnes et al., 1995; Shen et al., in press).

At present, there are only three complete long ENSO records derived from corals in open-ocean regions of the Pacific and Indian Oceans (Cole et al., 1993; Dunbar et al., 1994; Charles et al., 1997). These coral time-series not only record ENSO events but also contain longer period oscillations such as interdecadal cycles and long-term trends. However, the few longer records suggest additional complexities: (1) It is suggested that the sea level pressure changes appear to set the stage for a possible onset of El Niño, and thus El Niño and the Southern Oscillation are a coupled phenomenon (Rasmusson and Carpenter, 1982; Philander, 1990). However, Deser and Wallace (1987) suggested that the eastern and western Pacific ENSO are more loosely coupled than implied. They have observed that the major negative swings (reduced east-west pressure difference) of the Southern Oscillation are not always accompanied with El Niño events; (2) An interdecadal cycle is commonly identified in long coral records. Dunbar et al. (1994) suggested a possible long-term solar cycle-SST link while some other authors (Cooper et al., 1989; Trenberth, 1990; Jacobs et al., 1994) suggested an interdecadal climate variability in ENSO. The origin of these decadal shifts still remains controversial; (3) Both increasing and decreasing long-term trends in $\delta^{18}O$ data are observed in some corals (Linsley et al., 1994; Charles et al., 1997; Quinn et al., 1998). However, it is not clear whether this trend is due to biogenic processes in corals or is correlated with the gradual environmental changes. The solutions of these kinds of questions will

be of help in developing a better understanding of the ENSO events and other related climatic phenomenon.

The carbon isotopic composition ($\delta^{13}C$) of coral skeleton is another important isotopic signature in corals which has more potential forcing variables than $\delta^{18}O$ and is currently a source of controversy (Weber & Woodhead, 1972; Weber et al., 1976; Swart, 1983; McConnaughey, 1989a, b). Unlike $\delta^{18}O$, $\delta^{13}C$ is affected by both kinetic and metabolic fractionation (McConnaughey, 1989b). Therefore, physiological processes, such as photosynthesis, respiration, and heterotrophy, can also affect the skeletal carbon isotopic composition, in addition to SST and $\delta^{13}C$ of dissolved inorganic carbon (DIC) in seawater. At the present time the focus of most studies has concentrated on how metabolic rate influences $\delta^{13}C$ in corals (Erez, 1978; McConnaughey, 1989a, b; Swart et al., 1996; Allison et al., 1996). Some authors suggest that the metabolic effect increases the $\delta^{13}C$ in coral aragonite (McConnaughey, 1989a; Allison et al., 1996) while others believe the effect decreases $\delta^{13}C$ (Erez, 1978; Swart et al., 1996). Only when this fundamental question is solved, can $\delta^{13}C$ in corals be used in reconstructing climate changes. On the other hand, in most discussions an assumption which has been implicit regarding the origin of $\delta^{13}C$ in coral skeletons has been that the $\delta^{13}C$ of the DIC has not varied significantly. However, the results from recent studies show that this may be not the case (Swart et al., 1996). With the large increase of atmospheric CO_2 (in the period 1970-1990, the total fossil fuel CO_2 emissions are 102 Gt C (5.1 Gt/yr) (Quay, 1992)), and depletion of $\delta^{13}C$ in the atmosphere due to fossil fuel combustion and land use, the active exchange of CO_2 between atmosphere and ocean may result in a change of $\delta^{13}C$ in DIC and in turn a change of $\delta^{13}C$ in coral (Swart et al., 1996).

For this study, samples were collected by B.K. Linsley and others in 1994 from Clipperton Atoll located at 10°N latitude and 109°W longitude in the East Pacific (Fig. 1.2). This position distinguishes it as the eastern most atoll in the Pacific Ocean lying about 1,100 km west of Mexico. To the west, the nearest islands are the Line Islands (160°W) which are 5,700 km west of

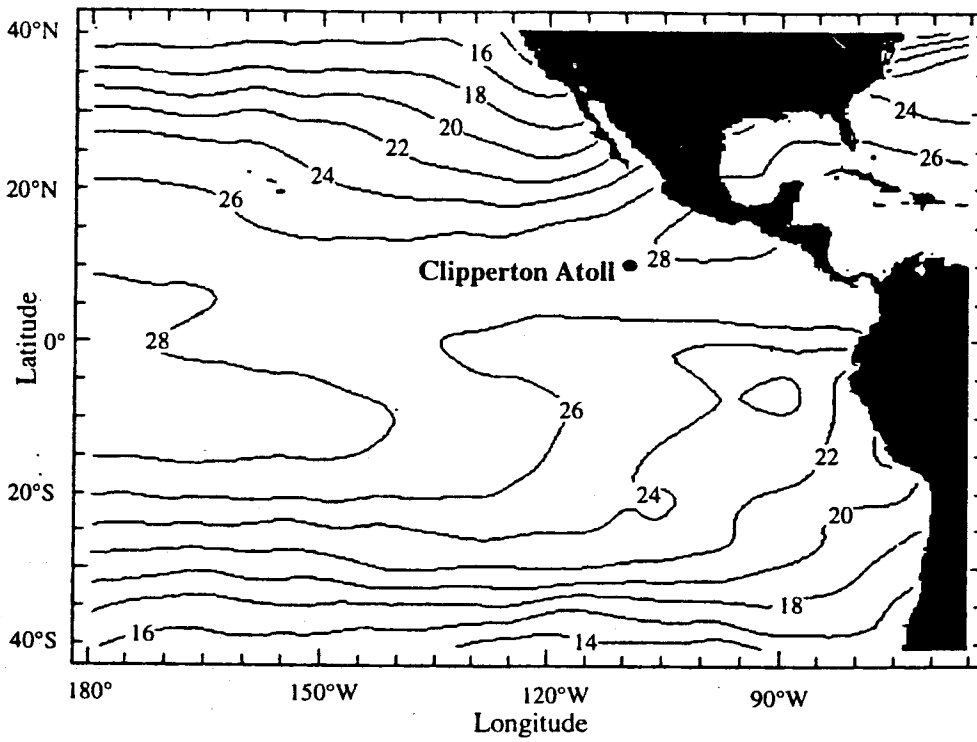

Fig. 1.2 The geographic location of Clipperton Atoll (after Linsley et al., in press)

Clipperton. As there are no other equatorial islands between Clipperton (109°W) and the Line Islands (160°W), corals from this site may offer a unique source of paleoenvironmental information especially concerning ENSO activities in the eastern Pacific.

Here, I present a continuous 88-year coral $\delta^{18}O$ and $\delta^{13}C$ record for the period 1906-1994 using a specimen of *Porites lobata* collected from Clipperton Atoll. In the following chapters all the factors potentially influencing $\delta^{18}O$ and $\delta^{13}C$ signals are discussed with a focus on how to

separate these factors from one to another, and also with reference to the possible influence of the coral skeletal growth rate. Then I used a statistical method called singular spectrum analysis (SSA) on the $\delta^{18}O$ results to identify past ENSO events and isolate other longer-term cycles, and I put forth climatic interpretations for these different individual cycles by comparing with the available historical instrumental records of ENSO, SST, and other published coral $\delta^{18}O$ records.

CHAPTER 2 STUDY AREA

2.1 Regional attributes

Clipperton Atoll is located near the northern edge of the Niño3 region (5°N to 5°S, 150°W to 40°W), a region known to be sensitive to monitoring El Niño processes) (Glantz, 1996) (See Fig. 2.1). Sea surface temperature data indicate that Clipperton is characterized by 0.5-1°C positive anomaly in SST during El Niño events. Since samples from Clipperton were the first long records collected at this site in the east Pacific, corals from this island may provide a new, regionally significant baseline on the past behavior of ENSO and past oceanographic conditions in this region. Before I describe the coral growth and collection of this region in more detail, let's first review the environmental factors that may influence coral growth and skeletal chemistry.

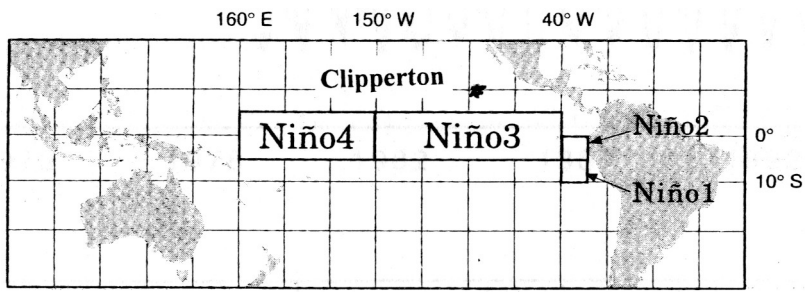

Fig. 2.1 Map depicting four regions (refered to as Nino1, Nino2, etc.) in the equatorial Pacific Ocean

Sea Surface Temperature (SST)

Sea surface temperature (SST) data for the 2°x2° grid box surrounding Clipperton Island was obtained from the Climate Analysis Center (CAC-SST) for the period 1970-1994 (Levitus and Boyer, 1994; Reynolds and Smith, 1994). The data shows that for the last 2 decades, the mean monthly SST has ranged mainly between 27°C and 29°C with a variation less than 2°C annually

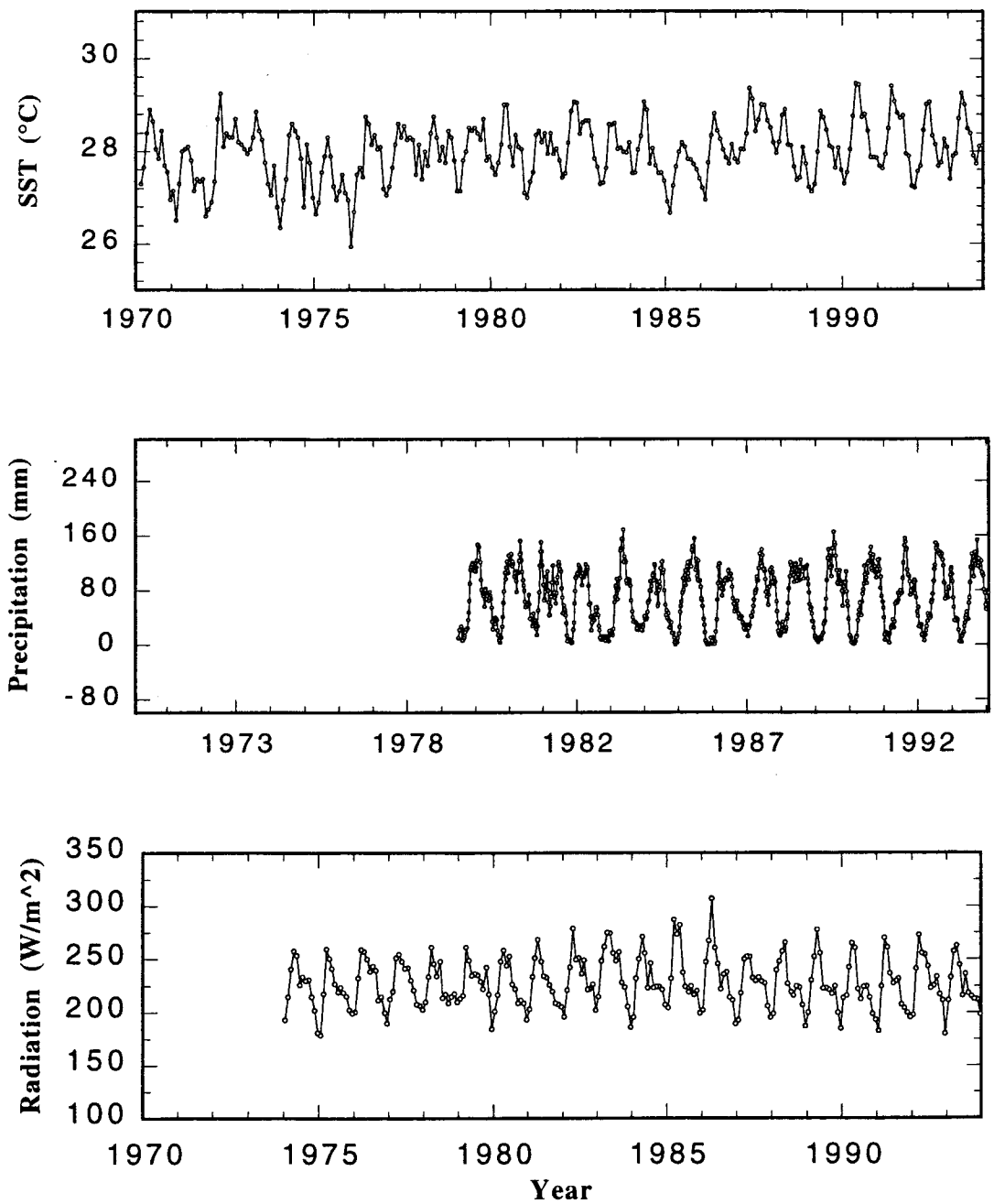

Fig. 2.2 Sea surface temperature (Reynolds, 1988; Reynolds and Smith, 1994), precipitation (Spencer, 1993), and radiation in the vicinity of Clipperton Atoll

(Fig. 2.2). This variation in SST suggests that temperature-related interannual variation in coral $\delta^{18}O$ will be equal to or less than 0.44‰ (For every 1°C of increase in temperature the $\delta^{18}O$ value of calcium carbonate precipitating in equilibrium with seawater decreases by 0.22‰ (Epstein et al., 1953; Tarutani et al., 1969; Grossman and Ku, 1986)). As also shown in Fig. 2.2, the SST maxima occur in May/June while the SST minima occur in January/February. Positive SST anomalies are generally associated with ENSO events. As Clipperton Atoll is located north of the Niño3 region, SST was only moderately influenced by ENSO events over the last 2 decades, with SST positive anomalies of 0.5°C during the 1982-83 and 1990 ENSO events, and 1°C during 1972-73 and 1986-87 ENSO events. Based on equilibrium considerations, it was expected that the SST anomalies of these magnitudes would result in temperature-related depletions of coral $\delta^{18}O$ of 0.11‰ and 0.22‰, respectively (Epstein et al., 1953; Tarutani et al., 1969; Grossman and Ku, 1986). Thus, the independent data of SST variation for the last 20 years provides the test to see how much influence SST has had on the actual $\delta^{18}O$ composition in corals in this region.

Recently a new compilation of global SST anomaly data has been developed by Kaplan et al. (in press) by combining SST data in 5°x5° latitude-longitude boxes with a statistical optimal smoothing infilling technique where data were sparse. This OS-SST dataset extends from 1856 to 1991 and the SST anomaly estimates for the 5°x5° grid box around Clipperton is shown in figure 2.3. Although the comparison of the data with CAC-SST data shows their consistency for the last 2 decades, it should be noted that the data before 1950 are based on sparse SST measurements. It can be seen from Fig. 2.3 that there is a long-term warming trend of ~0.5°C during the period of 1906-1994. Furthermore, this SST anomaly data shows pronounced 3 to 5-year period cycles. Comparison of these cycles with the historical ENSO records (Quinn et al.,

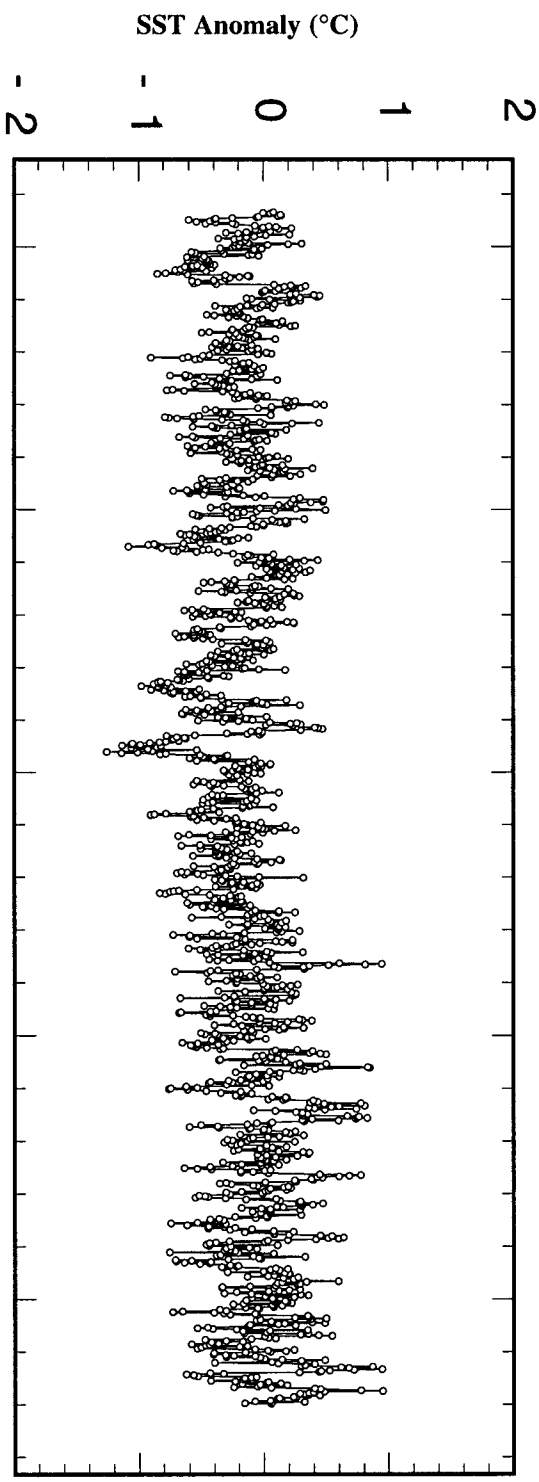

Fig. 2.3 Sea surface temperature anomaly near Clipperton Atoll during 1855-1991

1987; Quinn, 1992) suggests that these cycles are consistent with the historical ENSO events, with the SST anomaly increased during El Niño events.

Precipitation and sea surface salinity

The climate near Clipperton is also characterized by a pronounced wet season lasting from May/June through November (Mitchell and Wallace, 1990; Spencer, 1993). The satellite estimate of precipitation obtained from Clipperton is only for the period of 1979 to 1994 and no data are available for earlier periods (Fig. 2.2). As shown in Fig. 2.2, during 1979-1994 the annual variation in precipitation is relatively regular with maxima occurring in August/ September with up to 120 mm/month, while precipitation minima occur in March/April with only 10 mm/month. Both precipitation maximum and minimum lag the SST maximum and minimum by up to 2 months. As Clipperton is on the interface between the low pressure zone and the high pressure zone during ENSO events, it makes the precipitation pattern complicated during El Niño events with more rainfall in some El Niños while other events result in drought conditions.

Clipperton Atoll is located in an open ocean area that receives little terrestrial runoff (Glynn et al., 1996). Thus, although precipitation varies by >100 mm/month, the average sea surface salinity (SSS) obtained from a salinity climatology within the 2.5°x2.5° grid box that includes Clipperton, shows that salinity varies by <0.8‰ annually, ranging from 33.3‰ in September-December to 34.1‰ in January-March (Fig. 2.4) (Levitus and Boyer, 1994). If we assume the relationship between $\delta^{18}O_{water}$ and salinity is 0.11-0.12‰ $\delta^{18}O$ per ‰ salinity (Craig and Gordon, 1965; Dunbar and Wellington, 1981) or 0.27‰ $\delta^{18}O$ per ‰ salinity (Fairbanks et al.,

1997), the 0.8‰ annual salinity range in Clipperton was expected to lead to 0.09‰ or 0.22‰ annual $\delta^{18}O$ change in coral.

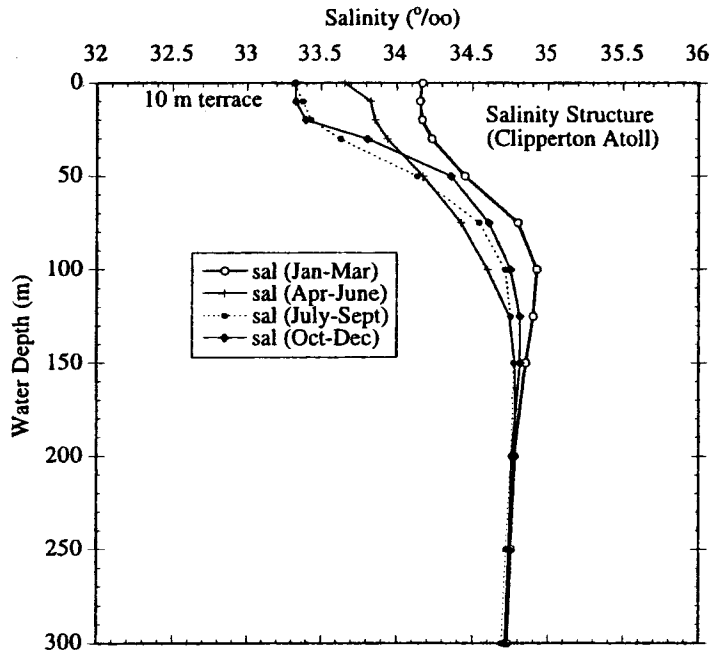

Fig. 2.4 Average seasonal vertical salinity profiles in the upper 300 m surrounding Clipperton (from Levitis et al., 1994)

Radiation

The radiation data was obtained for the period 1974-1994 from NOAA NCEP-NCAR CDAS-1 monthly diagnostic surface downward shortwave solar radiation (Fig. 2.2). As shown in Fig. 2.2, The average annual radiation is about 230 w/m^2 with the maximum of 270 w/m^2 in April/May and the minimum of 190 w/m^2 in December/January which are approximately concurrent with SST maximum and minimum. Downward solar radiation near Clipperton is relatively uniform during 1974 to 1994 with the exception in 1985-1986 when it shows anomously high radiation. At the present time, it is not known whether higher radiation will lead to an increase of $\delta^{13}C$ in

coral or decrease of it. Comparison of this radiation data with $\delta^{13}C$ in coral of this region may provide an answer to this fundamental question.

2.2 Sample description

Reef-building Corals

Clipperton Atoll has a total reef area of about 370 ha, and is the largest coral reef in the eastern Pacific. Although it is a well developed atoll with high coral cover, the reef-building fauna is depauperate, consisting of only 7 species of scleractinian corals belonging to the genera *Pocillopora, Porites, Pavona* and *Leptoseris*, and 1 species of hydrocoral in the genus *Millepora* (Glynn et al., 1996). Scleractinian corals predominate (10-100% cover) over insular shelf depths of 8 to 60 m (Glynn et al., 1996). *Porites lobata* is the most abundant species at Clipperton Atoll and is the principal framework builder. Due to its ubiquity, longevity, rapid growth rate and apparent reliability of isotopic records (Cole et al., 1993; Linsley et al., 1994; Dunbar et al., 1994; Tudhope et al., 1995; Charles et al., 1997 and others), *Porites* is an ideal coral to sample for analysis. According to Linsley et al. (in press), the mean linear skeletal extension rates in *Porites lobata* at Clipperton ranged from 11.7 mm/yr. to 22.5 mm/yr. The average annual extension rate of colony 4B, sampled in this study, ranged between 15 mm/yr and 30 mm/yr and averaged 25 mm/yr. However, there are frequent grazing scars by the pufferfish *Arothron meleagris* which results in the removal of small amounts of live tissue and skeleton from *Porites lobata*. Linsley et al. (in press) suggested that these "fish bites" have complicated the results of $\delta^{18}O$ in Clipperton corals and they can have a profound effect on the quality of the isotopic record that can be extracted from a given coral. In this study, I used a sampling technique (described in Chapter 3) designed to minimize the effects of pufferfish grazing.

Sample collection

In April 1994, a number of cores of *Porites lobata* were collected from Clipperton Atoll (Fig. 2.5). This study mainly focuses on the analysis of the longest core numbered C4B, which was collected from east side of the Atoll (Fig. 2.5). The other cores (C2A, C2B, C3C, CDT-20, and CDT-40) are discussed in Linsley et al. (in press). The colony C4B grew near the outer edge of a carbonate terrace surrounding the atoll. The total length of the core is 2.45 m and water depth of this colony top is about 8.2 m. There was no observed vertical SST gradient on this exposed terrace during field work. And none of the corals were observed to be influenced by shading or other micro-environmental factors (Linsley et al., in press).

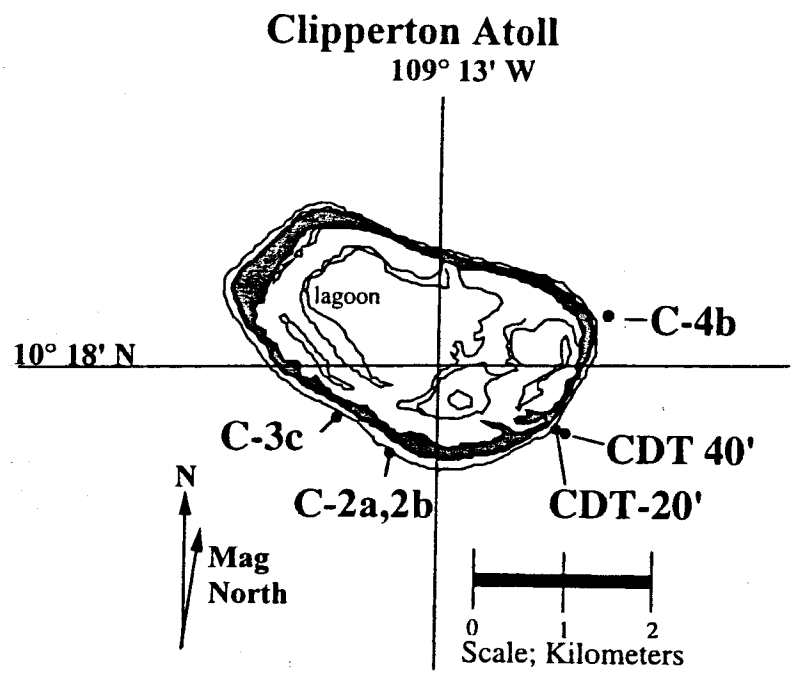

Fig. 2.5 Enlargement of Clipperton Atoll showing the location of C4B sampling site

CHAPTER 3 SAMPLE PREPARATION AND ANALYSIS

3.1 Sample Preparation

The cored coral sample (C4B) for this study was washed with fresh water, air dried, and then cut using a low-speed band saw into a 7 mm thick slab along the major axis of growth (Linsley et al., in press). Great care was taken to produce sections that were parallel to the growth axis to avoid distortion of the skeletal chronology. The slab segments were X-rayed (30 kV, 0.70-0.90 s) with a Phillips Radifluon medical X-ray unit using Kodak X-OMAT-G X-ray film. X-ray positives of the coral are shown in Fig. 3.1.

As deionized water soaking has little effect on the stable isotope ratios of evolved CO_2 (McConnaughey, 1989a), the slab segments of coral were cleaned with deionized water in an elongate ultrasonic bath for 15 minutes to remove saw-cuttings and were then oven dried at 40°C. For the purpose of seasonal-scale climate reconstruction, the slab must be sampled at subannual intervals. For this study subannual samples were collected for isotopic analysis by high-speed drilling using a Micro-drill with a 1-mm-diamond drill under a binocular microscope along tracks parallel to corallite traces as identified in X-ray positives (see Fig. 3.1). Previous studies have shown that high-resolution (i.e., approximately 10 samples/yr) sampling intervals are necessary to accurately reconstruct seasonal climatic histories with oxygen isotopes, while lower resolution sampling generally results in attenuation of the seasonal $\delta^{18}O$ amplitude (Goreau, 1977; Fairbanks and Dodge, 1979; Winter et al., 1991). Furthermore, in order to reconstruct time-dependent changes in skeletal isotope composition, it has been previously determined that sampling should occur along the major growth axis, where growth rates are at their maximum (Fairbanks and Dodge, 1979) and aragonite-seawater $\delta^{18}O$ isotope disequilibria

Figure 3.1; Comparison of banding patterns in Clipperton *Porites lobata*. Note that Core 4B was used for this study.

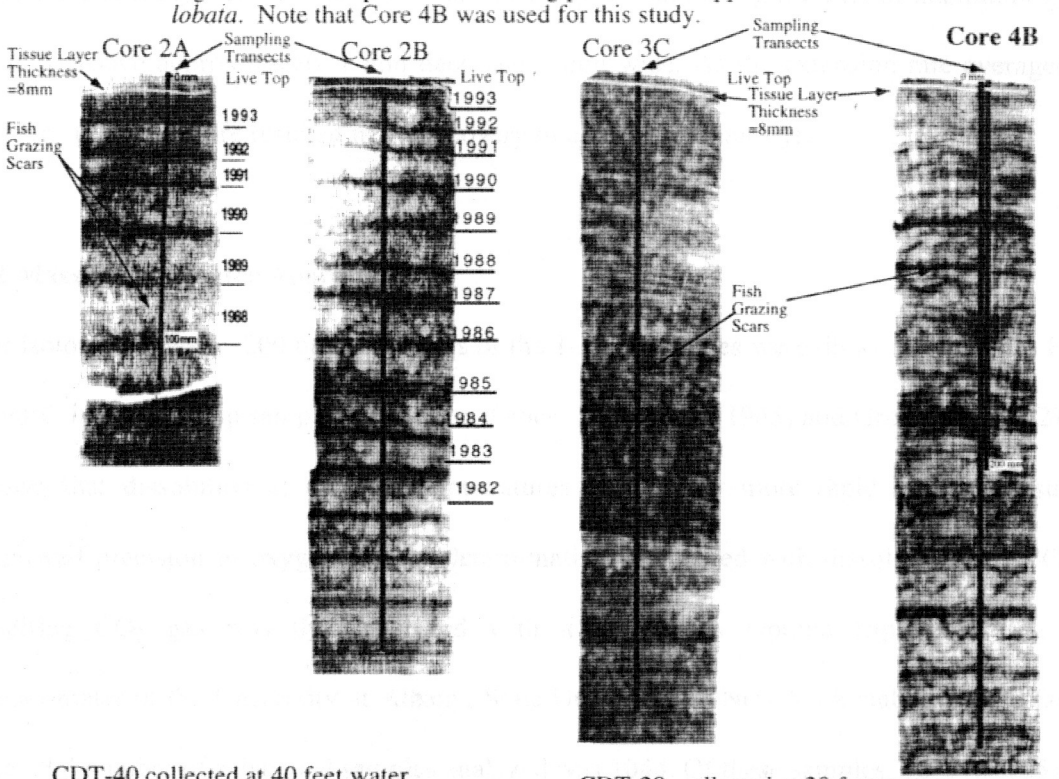

CDT-40 collected at 40 feet water depth (12.2m), SE side of atoll

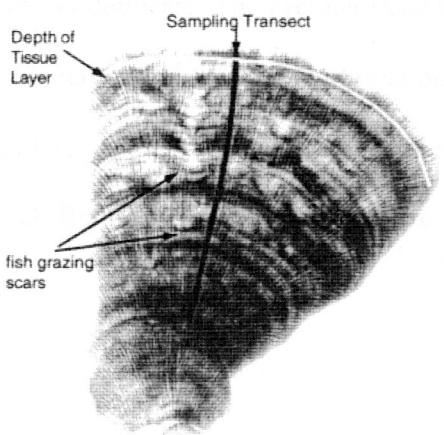

CDT-20, collected at 20 feet water depth (6.1m), SE side of atoll

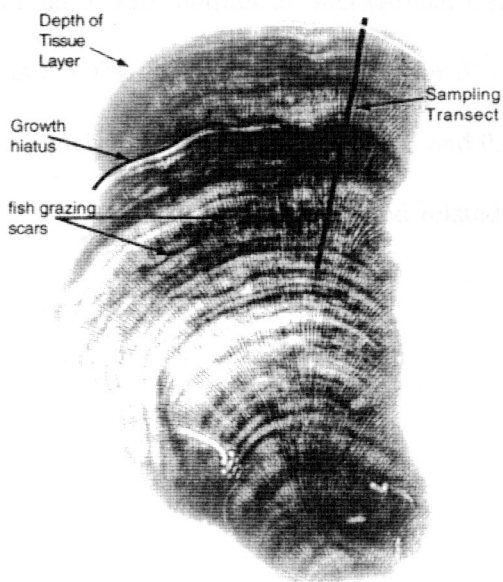

are believed to be constant (Land et al., 1975; McConnaughey, 1989a; Wellington et al., 1996; Allison et al., 1996). Furthermore, I used a sampling technique which averaged the 2.5 mm subsamples designed to minimize the effects of pufferfish grazing. The Clipperton coral core used for this study was continuously sampled every 2.5 mm along the axis of maximum growth from a groove approximately 1 mm deep and 3 mm wide. As the extension rate averaged ~25 mm/yr., this procedure resulted in the recovery of about 10 samples/yr.

3.2 Mass Spectrometer Analysis

For isotopic analysis ~200 ug subsamples of the 1-3 mg samples were dissolved in 100% H_3PO_4 at 90°C in a Multiprep sample preparation device. Shackleton (1965) and Grossman (1982) have shown that dissolution at elevated temperatures is not only more rapid but also results in improved precision in oxygen isotope determinations compared with dissolution at 25°C. The resulting CO_2 gas was then analyzed with a Micromass Optima triple-collecting mass spectrometer in the University at Albany, State University of New York stable isotope facility. The total number of subannual samples analyzed was 1044. Of these samples, 10% (n=105) were analyzed in duplicate. The average standard deviation of 136 samples of international reference NBS-19 analyzed over a 6 month time period was 0.018‰ for $\delta^{13}C$ and 0.039‰ for $\delta^{18}O$. The standard deviation of the duplicate samples (n=105) analyzed were 0.028‰ for $\delta^{13}C$ and 0.029‰ for $\delta^{18}O$. Both $\delta^{18}O$ and $\delta^{13}C$ results are shown in Fig. 3.2. All data are reported related to V-PDB.

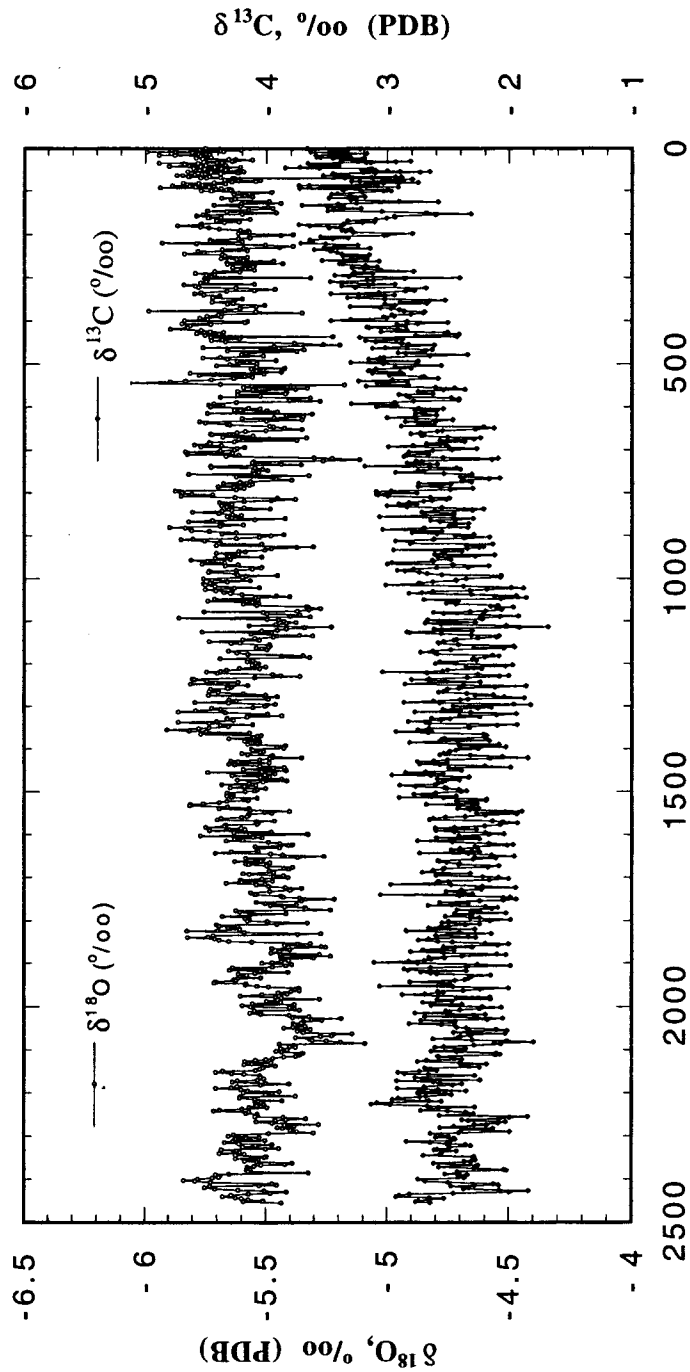

Fig. 3.2 Oxygen and carbon isotopic data in core C4B plotted vs. depth

CHAPTER 4 CHRONOLOGY

There are a variety of different types of annual banding and skeletal chemical constituents in coral skeletons which can be used to provide an annually resolved chronology, for example, density banding, fluorescent banding and seasonality in $\delta^{18}O$ and $\delta^{13}C$ records (Isdale, 1984; Cole and Fairanks, 1990; Tudhope et al., 1995 to site a few). The best choice of parameter(s) depends upon the specific reef site and corals concerned. Most Clipperton corals show poor annual density bands (see Fig. 3.1). Fortunately, both $\delta^{18}O$ and $\delta^{13}C$ have very clear seasonal cycles. To develop a chronology for the isotopic results of core C4B, I first determined that these seasonal cycles observed were annual. Counting $\delta^{18}O$ and $\delta^{13}C$ cycles results in a total of 88 years in this record (see Fig. 3.2). This places large $\delta^{18}O$ negative anomalies in the record during the intervals 1918-20, 1930, 1957-58, 1972-73, and 1990-91 when there were strong ENSO events and positive SST anomalies at Clipperton (CAC-SST and OS-SST). The 1976 cold event is also clearly identified in the record. As this coral was collected live from Clipperton in April 1994, I assigned a date of 1994 to the outer surface of the coral and the last year is counted down to 1906. To verify the accuracy of this chronology, I compared the last part of the record in the period 1970-1994 with another core (C2B) which had well-defined annual density bands (Linsley et al., in press) (Fig. 4.1). This comparison demonstrated the accuracy of this chronology at least in the period of 1970 to 1994. However, due to the lack of good density banding, the possibility cannot be excluded that the chronology may contain a small degree of error, probably on the order of ± 1 years, before 1970.

For the purpose of display and comparison with the other instrumental data such as SST, precipitation, and radiation which are all recorded as monthly data, subannual age estimates for

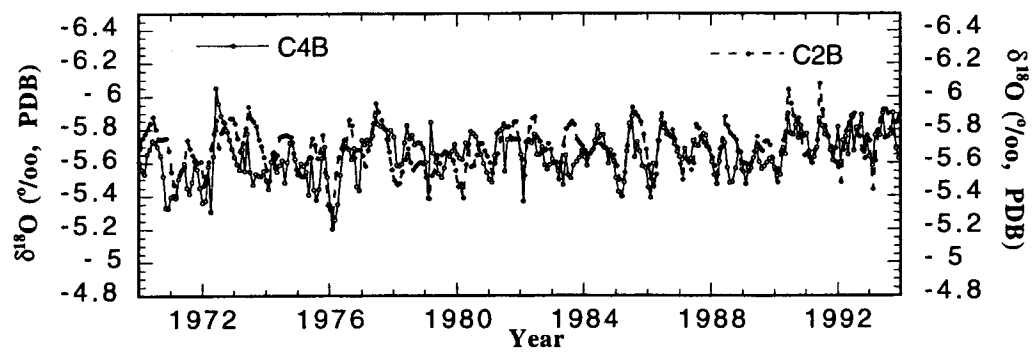

Fig. 4.1 Comparison of the oxygen isotopic composition of cores C4B and C2B in the period 1970-1994

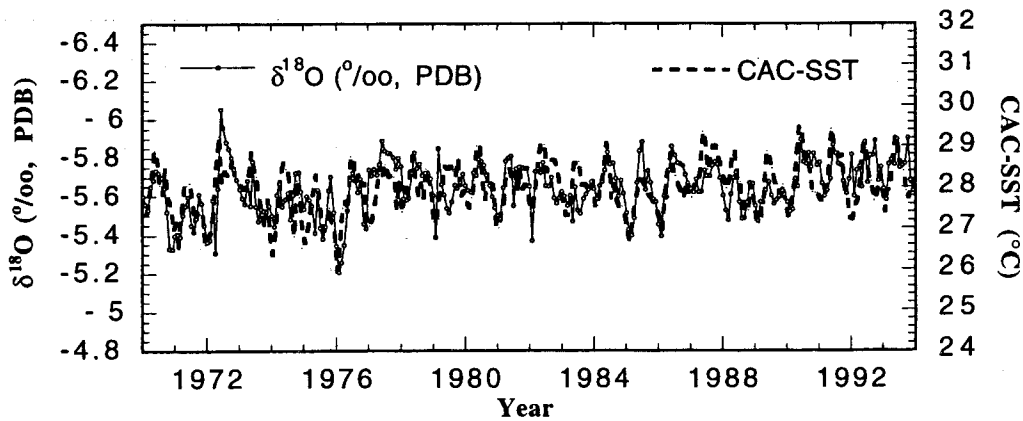

Fig. 4.2 Comparison of oxygen isotopic composition of cores C4B with CAC-SST in the period 1970-1994

core 4B were linearly interpolated into 12 points per year. As will be shown in Chapter 6 and 7, because SST has a greater influence on the $\delta^{18}O$ than does precipitation, and also because the mean annual $\delta^{18}O$ range in core C4B of 0.4‰ is approximately equal to the expected temperature-related $\delta^{18}O$ range using $\delta^{18}O$=0.22‰/°C (Epstein et al., 1953; Tarutani et al., 1969; Grossman and Ku, 1986), I refined this chronology by re-tuning this $\delta^{18}O$ data to the monthly SST record by assigning the lowest $\delta^{18}O$ to the highest SST and the highest $\delta^{18}O$ to the lowest SST every year using the available SST data from 1970 to 1994 (Fig. 4.2). For all other age assignments I assigned the lowest $\delta^{18}O$ extremes to May of each year (on average, the highest SST of a year) and the highest $\delta^{18}O$ extremes to January of each year (similarly, on average, the lowest SST of the year) and interpolated linearly between these anchor points for all other age assignments (Fig. 4.3). Skeletal $\delta^{13}C$ was not used in chronology development. Since the precise timing of highest and lowest SST may vary from year to year, this approach undoubtedly may create the potential for a 1- to 2-month time-scale error in any given year, but at present it is the most objective method that can be used. Therefore, I conclude that the whole record is from April 1906 to March 1994 (see Fig. 4.3).

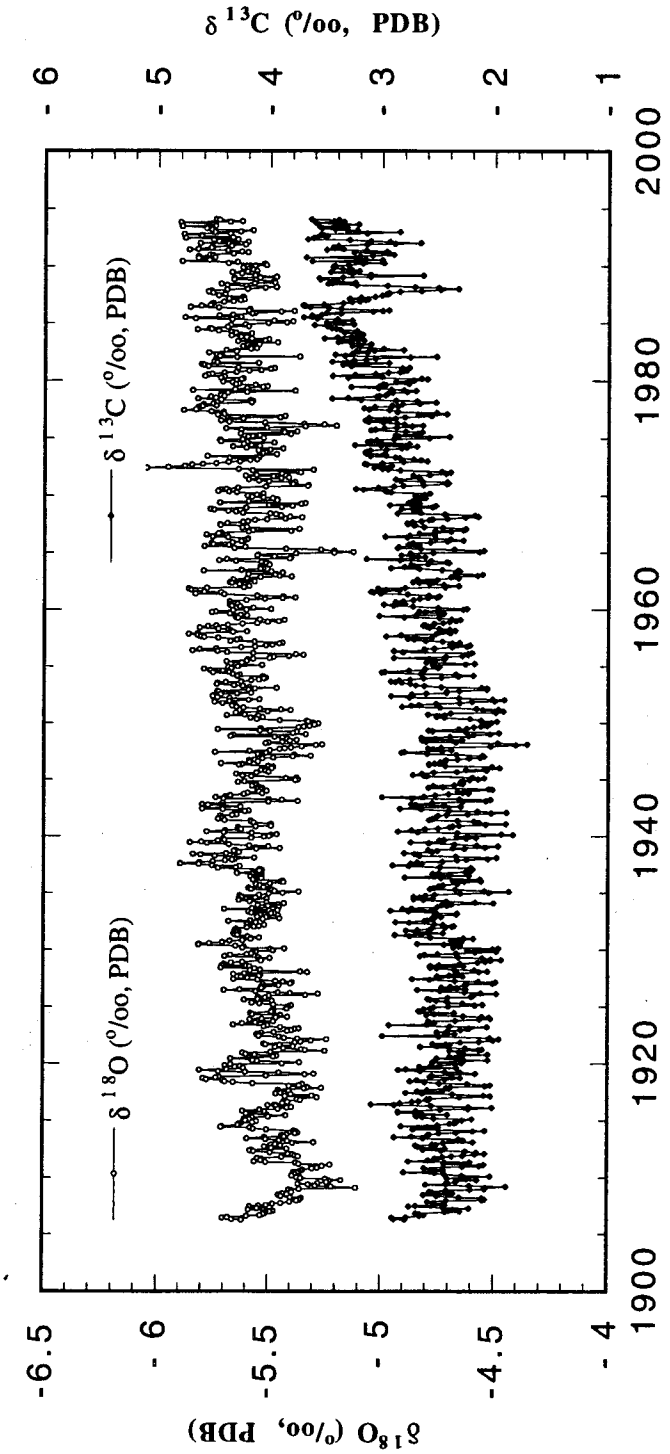

Fig. 4.3 The full record of monthly oxygen and carbon isotopic results for core C4B in the period 1906-1994

CHAPTER 5 THEORY AND BACKGROUND

In some cases the isotopic record preserved in corals has proven to be a useful indicator of paleoclimate conditions (McConnaughey, 1989a; Cole et al., 1993; Dunbar et al., 1994; Linsley et al., 1994; Charles et al., 1997 and others). To decipher more accurately the carbon and oxygen isotopic signature in coral skeletons, the processes by which isotopes are incorporated into coral skeletons and possible mechanisms of their isotopic fractionation must be understood. Only then can the oxygen and carbon isotopic data from analysis of samples be reasonably interpreted. This chapter first gives a brief introduction to the basic structure of corals and then discusses the detailed skeleton-forming processes and the associated mechanisms of isotopic fractionation.

5.1 Basic structure of corals

Most corals and their reef-forming skeletal accretions in the tropical, shallow-water benthic environment, belong to the Order Scleractinia of the Class Anthozoa of the Phylum Cnidaria and are represented by well over 1,000 species. The scleractinian corals are also known as true, hard or stony corals and are often divided into hermatypic (or reef-building) corals, and ahermatyic corals according to whether they normally contain zooxanthellae or not (see below) (McCarty et al., 1984). The basic structure of a typical reef-building scleractinian coral consists of hundreds to thousands of individual fleshy polyps that are housed in rigid cuplike massive skeleton known as corallites (Fig. 5.1). In the polyp there is an internal space for digestion called the coelenteron, which is terminated by an oral disc at the top and a basal disc at the bottom, respectively. In the center of the oral disc there is a mouth, surrounded by a circle of tentacles (Goreau et al., 1979; Johnston, 1980; Glynn and Wellington, 1983; Barnes and Chalker, 1990). The animal is essentially a "sack" with three-layered body walls (Fig. 5.2) consisting of an outer layer of

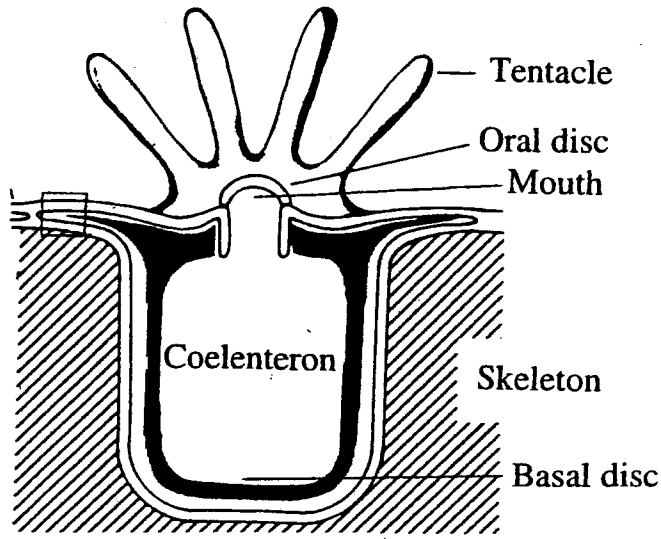

Fig. 5.1 The basic structure of a typical reef-building coral polyp (modified after Goreau, 1979)

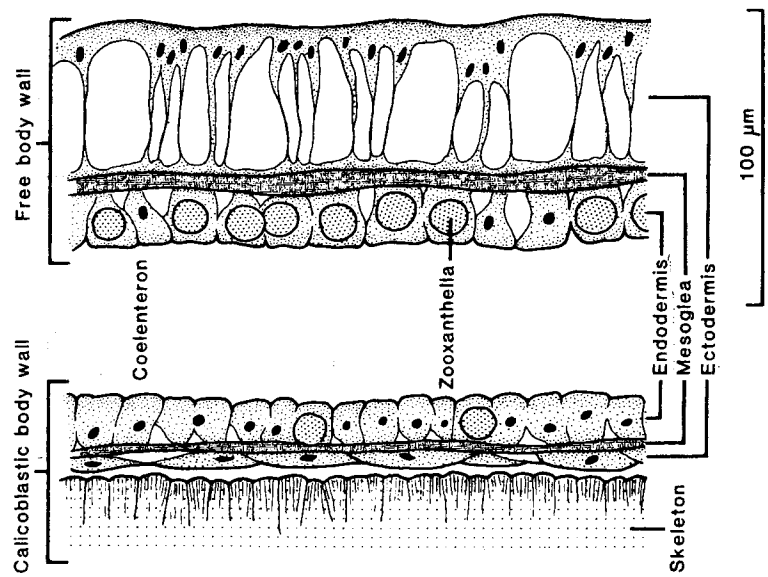

Fig. 5.2 Enlargement diagrammatic section of body wall showing three tissue layers (vertical section) and the relationship between tissues and skeleton (after Barnes and Chalker, 1990)

epidermis called the *ectodermis*, an inner layer of cells called the *endodermis*, and sandwiched between them, a so-called the *mesoglea* which is a cell-free, fibrous layer (Barnes and Chalker, 1990). The ectoderm exposed to the environment is histologically distinct from the calicoblastic ectoderm which covers the skeleton, the latter also known as a *calicoblastic*. It is generally believed that it is in a submembrane space (SMS) between this calicoblastic layer of the basal epidermis and the coral skeleton that $CaCO_3$ precipitates to form the skeleton (Wells, 1969; Barnes, 1970, 1971; Johnston, 1980; Barnes and Chalker, 1990).

A striking feature of many of the most effective reef-building corals is that they contain symbiotic algae called *zooxanthellae* within their endodermal cells (see Fig. 5.2). The photosynthetic activity of these algae have been found to play an important role in the process of calcification (McConnaughey, 1989a, b; Barnes and Chalker, 1990).

5.2 Mechanisms of skeletogenesis

Skeletogenesis refers to the processes of formation of calcium carbonate (aragonite) skeleton in corals. Two basic mechanisms of calcification have been proposed: Extracellular (Goreau, 1959; McConnaughey, 1989a, b) and intracellular (Hayes and Goreau, 1977) depending on whether calcareous skeletons precipitate extracellularly or from intracellular vesicles, separated from the cell cytosol by membranes (see Fig. 5.2) (Simkiss, 1976). It is generally believed that calcification mainly occurs extracellularly between the basal ectoderm and the skeleton in an area called the submembrane space (SMS) which is isolated from direct contact with seawater (Fig. 5.2) (Goreau, 1959, 1961; McConnaughey, 1989b; McConnaughey et al., 1997). In order for $CaCO_3$ to precipitate in the SMS, the product of the concentrations of calcium ions and carbonate ions in the calcifying fluid in the SMS must equal or exceed a certain value (the

solubility product). This will happen either if the calcium ion concentration is increased by the transport of that ion across the calicoblastic layer, or alternatively, if the carbonate ion activity is increased, for example by fixing CO_2 during photosynthesis which removes CO_2 from the calcifying fluid, or if both are increased.

Some possible processes that may lead to supersaturation of calcium carbonate at the site of their deposition of sites are as follows. It is known that the SMS is only permeable to small, uncharged molecules such as CO_2 while ions such as Ca^{2+} require enzymatic facilitation to cross membranes (Gutknecht et al., 1977). It is this membrane separation of different fluids that is a crucial characteristic in biomineralization. Thus Ca^{2+} can not be transported by simple diffusion. Most theories of biomineralization invoke a calcium pump or a proton/Ca^{2+} exchange pump to account for their Ca^{2+} transport across the calicoblastic layer (McConnaughey, 1989a, b). However, the exact nature of such pumps is uncertain. The energy for both mechanisms is the hydrolysis of ATP, which is a high-energy compound produced by metabolism (Isa et al, 1980; Kingsley and Watabe, 1985). In active transport, ATP is used as an energy source to move an ion such as Ca^{2+} against possible electrochemical gradients. In anion transport systems, however, the immediate source of energy is an electrical or electrochemical gradient. Thus, Ca^{2+} transport against a concentration gradient could be accomplished by a gradient of protons which exchange across the membrane for Ca^{2+} moving in the opposite direction (Fig. 5.3) (McConnaughey, 1989b; McConnaughey et al., 1997). This kind of $2H^+/Ca^{2+}$ pumping should raise both the pH and Ca^{2+} concentration in the SMS. Clearly, these activities in isolation or combination could account for processes that exceed the solubility product of $CaCO_3$ and initiate precipitation.

While the transport of Ca^{2+} involves the above enzymatic facilitation, CO_3^{2-} concentration in the

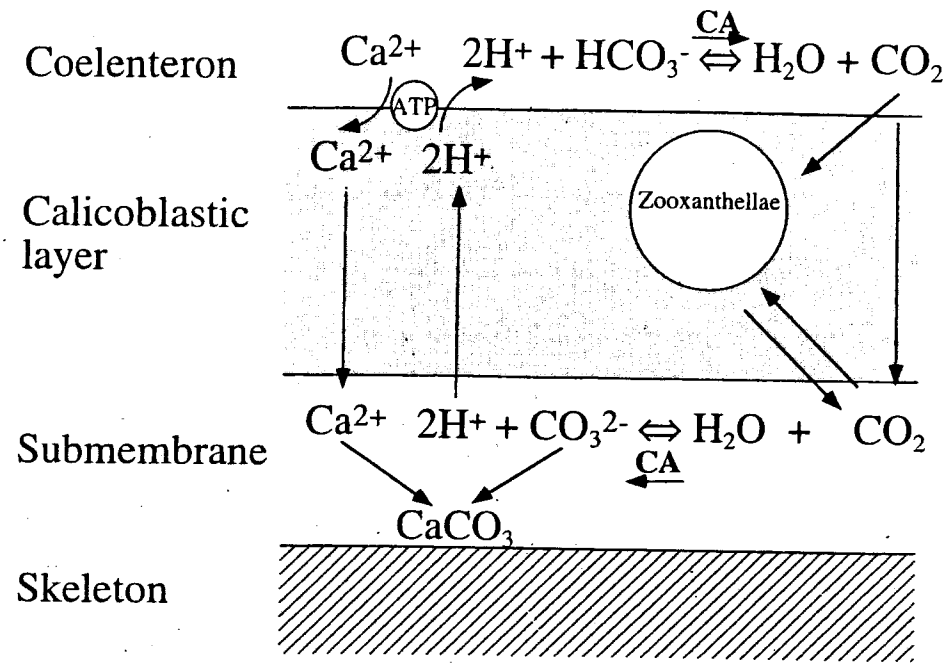

Fig. 5.3 Postulated transport mechanisms associated with the biological precipitation of $CaCO_3$ (modified after McConnaughey, 1989)

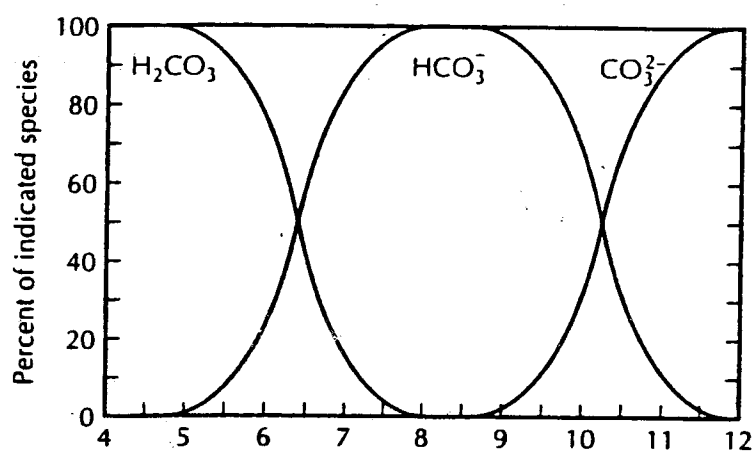

Fig. 5.4 Scheme diagram of distribution of major species of dissolved inorganic carbon at 20°C (after Faure, 1986)

calcifying medium is increased by quite different mechanisms. Inorganic carbon is present in seawater as a complex equilibrium (Skirrow, 1975) which is linked to atmospheric CO_2 concentrations:

$$H_2O + CO_2\,(aq) \Leftrightarrow H_2CO_3 \Leftrightarrow H^+ + HCO_3^- \Leftrightarrow 2H^+ + CO_3^{2-}$$

Surface waters tend to be close to equilibrium with atmospheric CO_2 and the solution of gaseous CO_2 lowers the pH and shifts the equilibrium so that it opposes additional solution. The relative proportions of the various species of dissolved inorganic carbon (DIC) in sea water depend on the pH which itself is controlled by photosynthetic removal and respiratory addition of CO_2 (Fig. 5.4) (Barnes and Chalker, 1990; McConnaughey, 1989b). At pH about 8.2 most of the inorganic carbon is present as bicarbonate with carbonate, carbonic acid and aqueous carbon dioxide together accounting for only a few percent of the total. When the pH is raised by photosynthetic removal of CO_2 or by an increase of alkalinity through proton-calcium ion exchange, the concentration of carbonate ion (CO_3^{2-}) will increase, relative to the concentration of bicarbonate ion. In fact, at pH>10, CO_3^{2-} becomes the dominant form of inorganic carbon. A pH shift from 8 to 9 will cause a five-fold increase in carbonic ion concentration (Barnes and Chalker, 1990). It is thus by this kind of pH increase and consequent shift in the carbonate equilibrium that causes increase of carbonate concentration in the calcifying medium.

Actually, the process of acquiring carbonate and calcium ions in corals is cyclic (Fig. 5.3). The two sides of the membrane are characterized by different fluid and reactions although the membrane is permeable to CO_2. On the coelenteron side, the decrease of Ca^{2+}, increase of protons will lower the pH, thus shifting carbonate equilibrium, aided by carbonic anhydrase (CA), in the direction of forming more CO_2. CO_2 then diffuses along the concentration gradient into the cells where it is either shunted into zooxanthellae and photosynthetically fixed, or

diffuses to the SMS for skeletogenesis. Some fixed carbon may be respired and also diffuse to the SMS. In the SMS, on the other side, where the pH is raised due to $2H^+/Ca^{2+}$ exchange pumping, CO_2 is easily converted to CO_3^{2-} in the presence of CA. Thus both the Ca^{2+} and CO_3^{2-} are maintained at high concentrations here (due to the biomembrane impermeability of anions), leading to continual precipitation of $CaCO_3$.

Therefore, calcification in corals involves complex processes of active transport of Ca^{2+} and H^+ and complex carbonate equilibrium reactions involving photosynthesis and respiration of the symbiotic algae in the cells. Photosynthesis has the potential to increase calcification in two ways. First, by provision of photosynthate either as an energy source or as a vital skeletal component. Second, by uptake of inorganic nutrients, especially carbon dioxide (Falkowski et al., 1990).

5.3 Fractionation of oxygen and carbon isotopes

It is well known that $\delta^{18}O$ and $\delta^{13}C$ in corals are frequently out of equilibrium with ambient water (Weber and Woodhead, 1972; Gonzalez and Lohmann, 1985; McConnaughey, 1989a, b)). Generally two types of fractionation are responsible for this disequilibrium: Kinetic fractionation and metabolic fractionation.

Kinetic fractionation

Kinetic fractionation results from discrimination against the heavy isotopes of C and O during the hydration and hydroxylation of CO_2, resulting in the simultaneous decrease of skeletal $\delta^{18}O$ and $\delta^{13}C$ relative to isotopic equilibrium (McConnaughey, 1989a, b). Slow exchange of oxygen isotopes between dissolved $CO_3^{2-}$and water in the SMS, and the fast rate of calcification as

discussed in the previous section, are most likely the main factors preventing oxygen and carbon isotope equilibrium during $CaCO_3$ precipitation (McConnaughey, 1989b). Thus, rapidly growing skeletons appear to be associated with strong kinetic depletion. McConnaughey (1989a) showed that $\delta^{18}O$ and $\delta^{13}C$ approached equilibrium values at growth rates below about 2 mm/yr and both decreased with the increasing growth rate. Allison et al. (1996) also reported the inverse correlation between skeletal growth rate and coral $\delta^{18}O$. On the other hand, many researchers also reported that the departure from the equilibrium appeared to remain constant after the growth rate exceeds 5 mm/yr (Land et al., 1975; McConnaughey, 1989a; Allison et al., 1996) although there is another opinion which suggested that this offset from equilibrium may not be constant over the long life of corals (Barnes and Lough, 1992; Barnes et al., 1995).

Therefore, when growth rate is relatively constant, isotopic fluctuations can be used to infer environmental variations such as SST and precipitation-related $\delta^{18}O_{water}$. SST affects both equilibrium and kinetic fractionation. The higher the SST, the greater the depletion of both ^{13}C and ^{18}O. According to Epstein et al. (1953), O'Neil et al. (1969) and other authors, every 1°C increase in temperature will cause a 0.22‰ decrease in $\delta^{18}O$ of calcium carbonate in equilibrium with seawater. ^{13}C fractionation with temperature has been reported but with considerable disagreement (Rubinson and Clayton, 1969; Turner, 1982). This temperature effect may be obscured by changes in $\delta^{18}O_{water}$. Rainfall, seawater evaporation, freshwater runoff and/or ocean circulation may all significantly alter the $\delta^{18}O$ composition of local seawater and subsequently precipitated carbonate (Allison et al., 1996). These changes are usually accompanied by changes in sea surface salinity (SSS) (Weber and Woodhead, 1972; Fairbanks and Dodge, 1979). It is generally expected that every 1‰ increase in SSS will result in 0.11-0.12‰ increase in $\delta^{18}O_{water}$ (Craig and Gordon, 1965; Dunbar and Wellington, 1981; Wellington et al., 1996). Recently

Fairbanks et al. (1997) reported a 0.27‰ increase in $\delta^{18}O_{water}$ per ‰ salinity increase from samples collected within convective regions in the tropical Pacific.

Metabolic fractionation

The other type of fractionation, called *metabolic fractionation,* results from changes in the $\delta^{13}C$ of dissolved inorganic carbon (DIC) in the vicinity of the coral skeleton, which is mainly caused by photosynthesis and respiration (Swart, 1983; McConnaughey, 1989a, b). As shown in the previous section on skeletogenesis mechanisms, fractionation occurs at the stage when CO_2 molecules are taken up by the zooxanthellae during photosynthesis (McConnaughey, 1989b). It is suggested that metabolic fractionation only effects $\delta^{13}C$, while $\delta^{18}O$ has no direct connection to photosynthesis and respiration (Swart, 1983; McConnaughey, 1989a, b). Swart (1983) observed that the removal of respired CO_2 from the mitochondria (where most respired CO_2 occurs) to the skeleton, is almost always associated with the exchange of oxygen atoms with water. In other words, oxygen is released back into the surrounding seawater and equilibrates with seawater oxygen when carbon is fixed. Furthermore McConnaughey (1989a) observed similar ranges of ^{18}O depletion between photosynthetic and non-photosynthetic corals but almost always higher ^{13}C in photosynthetic coral than that in non-photosynthetic ones.

The magnitude of metabolic fractionation is clearly related to the intensity of photosysthesis which in turn depends on various environmental factors such as radiation (solar irradiance levels), cloud cover, water transparency and upwelling events. As radiation levels increase and cloud cover decreases, photosynthesis and respiration generally increase. Increased water

transparency and decreased upwelling events will also increase the light level, thus increasing photosynthesis and respiration (Lelekin & Zvalinsky, 1981).

Currently there are two opposite opinions regarding the relationship between photosynthesis and skeletal $\delta^{13}C$. The more popular opinion suggests that photosynthesis will cause skeletal $\delta^{13}C$ in corals to increase (Weber and Woodhead, 1970; Goreau, 1977; McConnaughey, 1989a, b). This model was first proposed by Weber and Woohead (1970) and further developed by McConnaughey (1989b); they suggested that isotopically light CO_2 is efficiently removed by the zooxanthellae during photosynthesis, while heavier carbon is delivered to the internal pool (SMS) for skeletogenesis. So, an increase in photosynthesis would enrich the ^{13}C of the skeleton. Many observations did support this model. For example Fairbanks and Dodge (1979) observed that skeletal $\delta^{13}C$ decreased with depth, or with decreasing relative light intensity. Walsh (1975) also observed a positive correlation between the skeletal $\delta^{13}C$ in *Porites* and sunshine. However, a few authors disagreed with these conclusions (Erez, 1978; Erez & Honjo, 1981; Swart et al., 1996). Based on direct field experiments, Erez (1978) observed that the carbon isotopic composition in corals became lighter when the rate of photosynthesis increased. He suggested that the symbiotic algae increased the amount of light metabolic CO_2 in the organisms' SMS, which he explained as the main contribution to the variation of the carbon isotopic composition in the skeleton, and therefore caused the skeleton to become isotopically more depleted. Swart et al. (1996) also observed an inverse correlation between $\delta^{13}C$ of coral skeletons and photosynthesis. However, McConnaughey (1989a) disagreed with this model and explained that this apparent negative modulation of skeletal $\delta^{13}C$ by photosynthesis results from the confusion of photosynthesis with kinetic disequilibria as the kinetic depletion of ^{13}C can overpower the metabolic enrichment of ^{13}C, and result in the observed negative correlation between

photosynthesis and skeletal $\delta^{13}C$. At the present time, no satisfactory experiment exists to prove either of these two models. Only when this fundamental problem is solved, can $\delta^{13}C$ be used to indicate the intensity of photosynthesis or the related environmental factors such as radiation (solar irradiance levels), cloud cover, water transparency and upwelling events.

CHAPTER 6 ASSESSING DIFFERENT FACTORS OF INFLUENCE ON $\delta^{18}O$ AND $\delta^{13}C$

As discussed in chapter 5, coral skeletal $\delta^{18}O$ and $\delta^{13}C$ values are the result of the complex interaction of various factors. Due to the kinetic effect, the variations of $\delta^{18}O$ can be regarded as a function of changes of SST and precipitation-related $\delta^{18}O_{water}$ while due to both kinetic and metabolic effects the variations of $\delta^{13}C$ are more complicated and indecipherable. In this chapter, complete long-term results of $\delta^{18}O$ and $\delta^{13}C$ from corals in Clipperton Atoll are presented and discussed in terms of the different effects of the various factors on $\delta^{18}O$ and $\delta^{13}C$ in this region. An attempt is also made to examine the possible influence of extension rate or calcification rate on coral $\delta^{18}O$ and the variation of $\delta^{13}C$ with photosynthesis.

6.1 General characters of $\delta^{18}O$ and $\delta^{13}C$

The complete monthly records of coral oxygen and carbon isotopes are shown in Fig 4.3. As can be seen in the figure, for the whole period 1906-1994, both $\delta^{18}O$ and $\delta^{13}C$ show clear and regular seasonal variations. Based on the current age model (described in chapter 4) annual maxima occurring in the winter months of December through February, while their minima typically occur in May through July. The annual range of $\delta^{18}O$ varies between 0.3 and 0.4‰, which if entirely due to temperature corresponds to 1.5-2°C water temperature variations. Annual variation in skeletal $\delta^{13}C$ shows a larger range of 0.6-0.7‰. From 1906 to 1994 the annual average $\delta^{18}O$ decreases from -5.5‰ to -5.8‰, while the average $\delta^{13}C$ decreases from -2.35‰ to -3.2‰. This represents a long-term trend in both $\delta^{18}O$ and $\delta^{13}C$. Furthermore, some interannual cycles and interdecadal cycles are also observed which are more apparent and continuous in

$\delta^{18}O$. In the following two sections both $\delta^{18}O$ and $\delta^{13}C$ records are examined in more detail, respectively.

6.2 $\delta^{18}O$

Over the period 1970-1994 $\delta^{18}O$ and CAC-SST have an overall negative correlation although there exist discrepancies in a few years (Fig. 6.1a, b) (Levitus and Boyer, 1994; Reynolds and Smith, 1994). Increases of SST are generally associated with a depletion in $\delta^{18}O$, while decreases of SST correspond with enrichment in $\delta^{18}O$. The SST record for the period of 1970-1994 shows seasonal fluctuations of only about 1.5-2°C which are consistent with the corresponding range of variation of 0.3-0.4‰ in $\delta^{18}O$ assuming a slope of 0.22‰ per °C (Epstein et al., 1953; Tarutani et al., 1968; Grossman and Ku, 1986). The largest negative $\delta^{18}O$ anomaly (-6.05‰) in this period occurred during the 1972-73 strong ENSO event when SST increased to about 29.2°C (1.2°C above the overall mean 28°C). The largest positive $\delta^{18}O$ anomaly (-5.2‰) appeared in the coldest year of this period, the winter of 1976 when the SST was only 26°C (1.5°C below the overall mean 28°C). However, over these 24 years, there exist discrepancies in years 1974, 1977, 1979, 1985, 1987, and 1989. This may imply that besides the influence of SST, $\delta^{18}O$ values were also affected by some other factors such as precipitation-related $\delta^{18}O_{water}$ or/and coral growth rate. Comparison of the full record of monthly $\delta^{18}O$ anomalies with the OS-SST (Kaplan et al., in press) anomalies shows similar negative correlation (Fig. 6.2a, b). Of the nine historical strong ENSO events of this period (in the years 1911, 1913-15, 1918-20, 1925, 1940, 1957, 1965, 1972, and 1986) recorded in positive anomalies in SST, six can clearly be identified in coral $\delta^{18}O$.

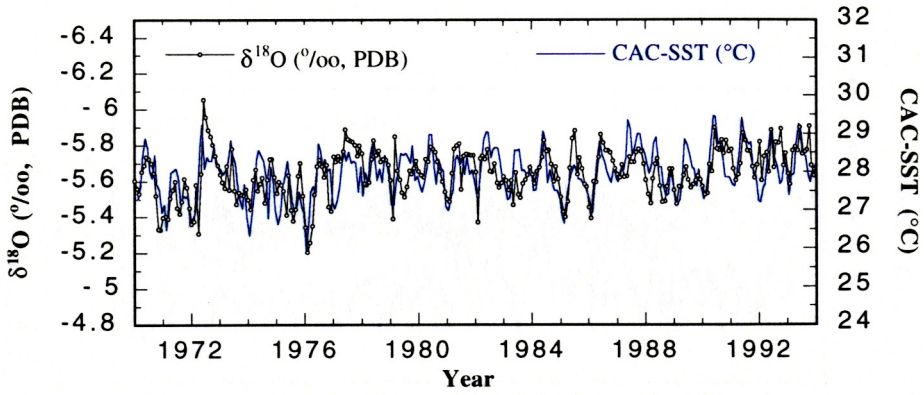

Fig. 6.1a Comparison of oxygen isotope with CAC-SST in the period 1970-1994

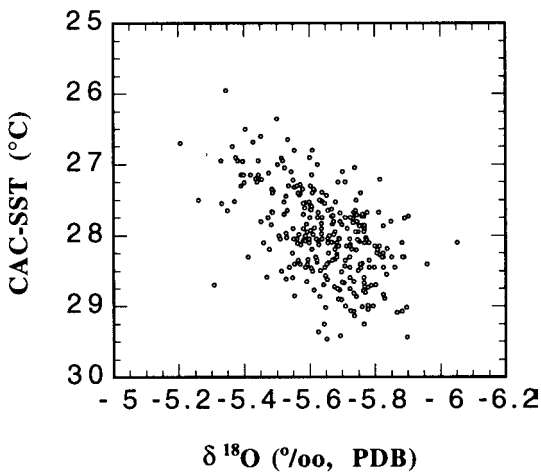

Fig. 6.1b Correlation between oxygen isotope and CAC-SST in the period 1970-1994

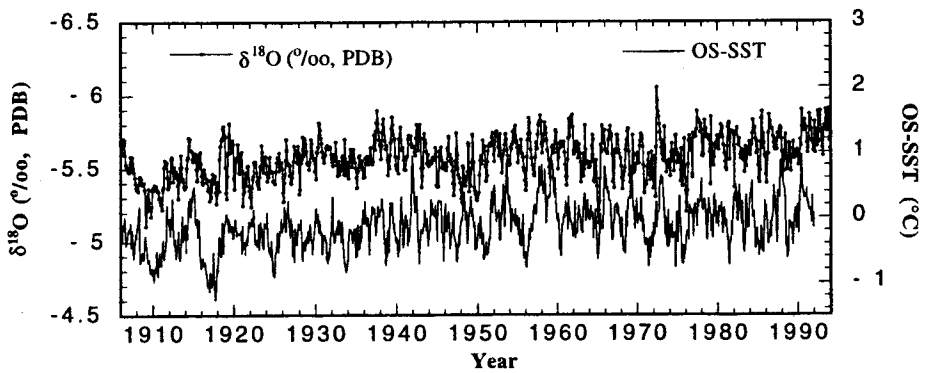

Fig. 6.2a Comparison of oxygen isotope with OS-SST amomaly in the period 1906-1991

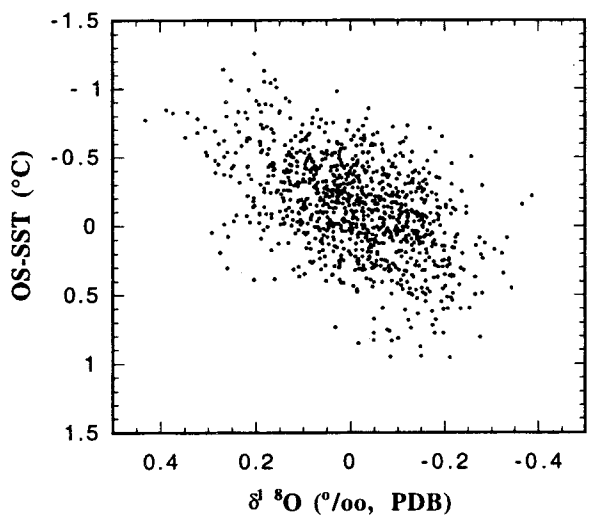

Fig. 6.2b Correlation between oxygen isotope and OS-SST anomaly in the period 1906-1991

In order to examine the effects of precipitation on coral $\delta^{18}O$ in this region, $\delta^{18}O$ was compared with satellite estimated precipitation (Mitchell and Wallace, 1990; Spencer, 1993). The available record of precipitation is only for the period of 1979 to 1994 and its correlation with $\delta^{18}O$ is relatively poor (correlation coefficient r^2 is only 0.146) (Fig. 6.3a, b). During these twenty years the seasonal variations of precipitation were relatively regular even during the ENSO years while $\delta^{18}O$ changed dramatically with relative enrichment in 1982-84 and 1988-89, and relative depletion in 1984-88 and 1990-94. During the years of poor correlation between SST and coral $\delta^{18}O$ in 1974, 1977, 1979, 1985, 1987, and 1989, there exists some correlation between $\delta^{18}O$ and precipitation in some years, but there also exists little correlation between them in other years. For example, for 1985 $\delta^{18}O$ values show more depletion relative to the inferred $\delta^{18}O$ from SST, which would imply larger precipitation in this year if this discrepancy was caused by the latter. The observed precipitation amount in 1985 is consistent with this, showing a relatively larger amount of precipitation. However, for 1989, $\delta^{18}O$ values show more enrichment relative to the inferred $\delta^{18}O$ from SST, which would suggest smaller precipitation in this year if the discrepancy was caused by the latter. But the observed precipitation amount is relatively larger rather than smaller compared with the other years. Therefore, it is likely that the influence of precipitation is relatively small compared with that of SST. However, it is difficult to determine the exact relationship between coral $\delta^{18}O$ and precipitation without knowing the degree of the sea surface salinity (SSS) influence.

Recently the potential growth rate effects on skeletal $\delta^{18}O$ has been discussed in several studies (Land et al., 1975; McConnaughey, 1989a; Barnes and Lough, 1992; Allison et al., 1996). As described in chapter 5, most authors believe that the departure from equilibrium remains constant when the growth rate exceeds 5 mm/yr (Land et al., 1975; McConnaughey, 1989a; Allison et al.,

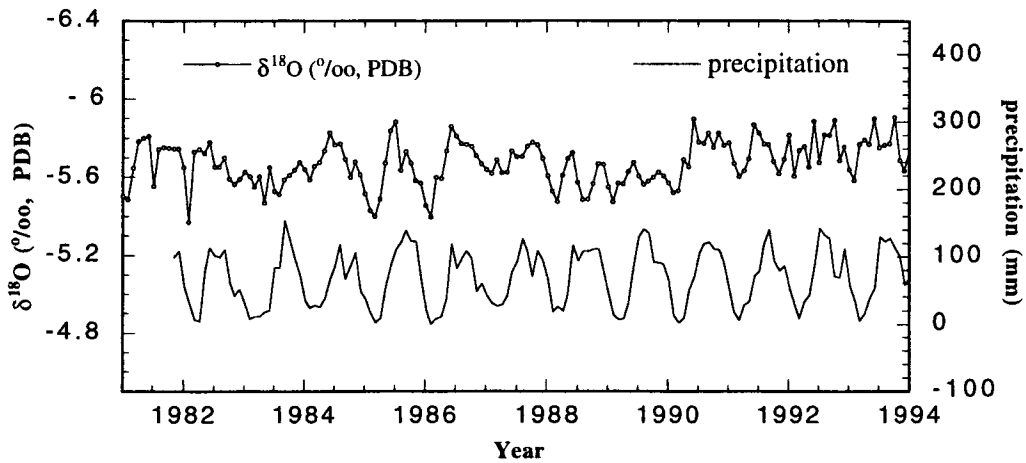

Fig. 6.3a Comparison of oxygen isotope with precipitation in the period 1981-1994

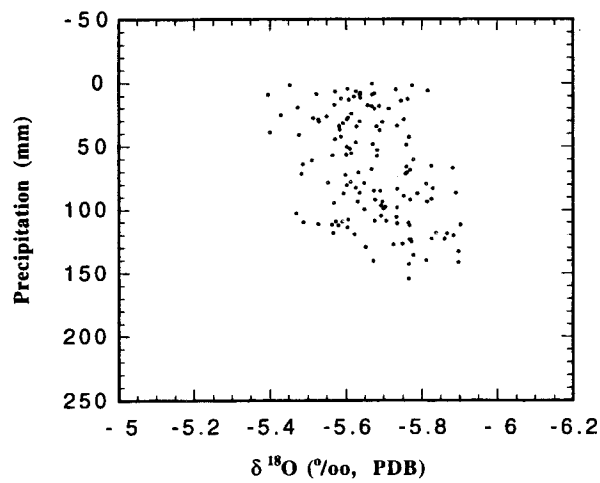

Fig. 6.3b Correlation between oxygen isotope and precipitation in the period 1979-1994

1996). However, some authors argue that this offset may be not constant (Barnes and Lough, 1992, Barnes et al, 1995). To assess this effect, I compared annual $\delta^{18}O$ with the annual linear extension rate estimated from the age model (Fig. 6.4). Compared to other published *Porites* records the mean annual growth rate is high and reaches 25 mm/yr. As can be seen in Fig. 6.4, the correlation between extension rate and $\delta^{18}O$ is poor. Due to the poor development of annual-bands in coral C4B, the seasonal extension rate variation is not available, and so the seasonal extension rate effects will not be examined here.

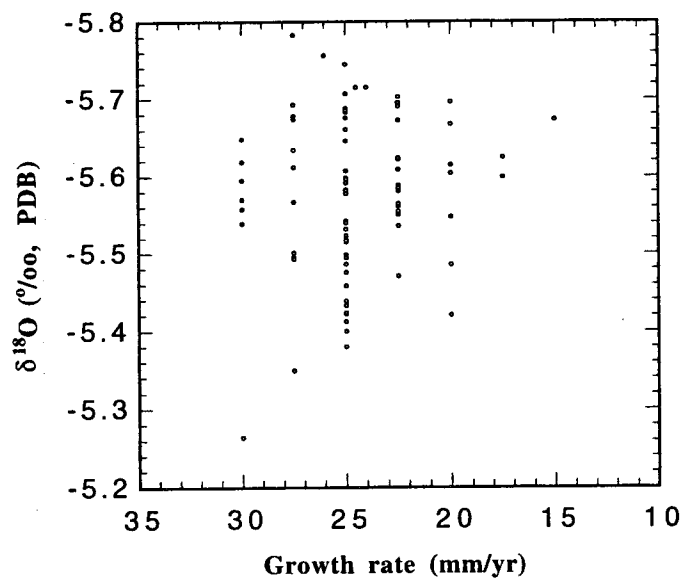

Fig. 6.4 Correlation between annual oxygen isotopic composition and annual growth rate in the period 1906-1994

6.3 $\delta^{13}C$

Due to the combined effects of kinetic and metabolic fractionation, the variation of skeletal $\delta^{13}C$ is more complicated than that of $\delta^{18}O$. Comparisons of $\delta^{13}C$ with SST in the period of 1970-1994 and the intensity of radiation in the period of 1974-1994 (from NOAA NCEP-NCAR CDAS-1) both show poor interannual correlations (Fig. 6.5a, b and Fig. 6.6a, b). However, there are consistent and coherent seasonal patterns: The decrease of $\delta^{13}C$ broadly coincides with the increase of both SST and the intensity of radiation. Especially from 1986 to 1987, $\delta^{13}C$ shows a dramatic enrichment from lowest -3.6‰ to highest -3.2‰ which coincides with a big drop from the highest intensity of the radiation (310 w/m^2) to the lowest intensity of radiation (250w/m^2) of this period. This relationship between $\delta^{13}C$ and radiation appears to be contrary to the more popular opinion which suggests that with the increase of intensity of radiation, $\delta^{13}C$ in corals will increase (McConnaughey, 1989a; Allison et al., 1996). As suggested by McConnaughey (1989a), metabolic behavior involves $\delta^{13}C$ departures from strict kinetic behavior, and thus, only when these two effects are separated can their individual effects on $\delta^{13}C$ be identified separately.

Besides the annual variations, $\delta^{13}C$ in corals for the whole period 1906-1994 shows a long-term trend. Core C4B $\delta^{13}C$ is relatively constant (averaging ~-2.35‰) during the years between 1906 and 1950 and becomes gradually more depleted after 1950 (reaching -3.2‰) in the 1990's. What has caused this kind of variation? We know that at present in most discussions an implicit assumption regarding the origin of $\delta^{13}C$ in corals has been that the $\delta^{13}C$ of DIC has not varied significantly (Weber and Woodhead, 1970; Erez, 1978; Allison, 1996). However, a recent study by Swart et al. (1996) showed that a large change in the $\delta^{13}C$ of DIC occurred and the pattern of this change was similar in timing and range to the variation of $\delta^{13}C$ in the corals. So it is possible that $\delta^{13}C$ of DIC in the vicinity of Clipperton Atoll may have changed over the time period of

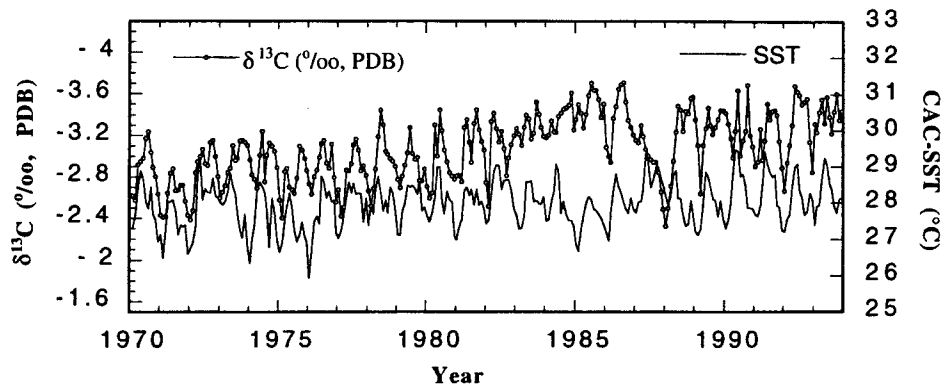

Fig. 6.5a Comparison of carbon isotopic composition with CAC-SST in the period 1970-1994

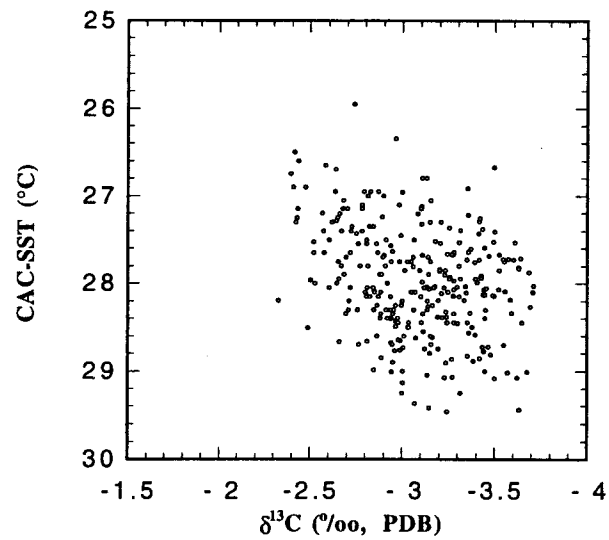

Fig. 6.5b Correlation between carbon isotope and CAC-SST in the period 1970-1994

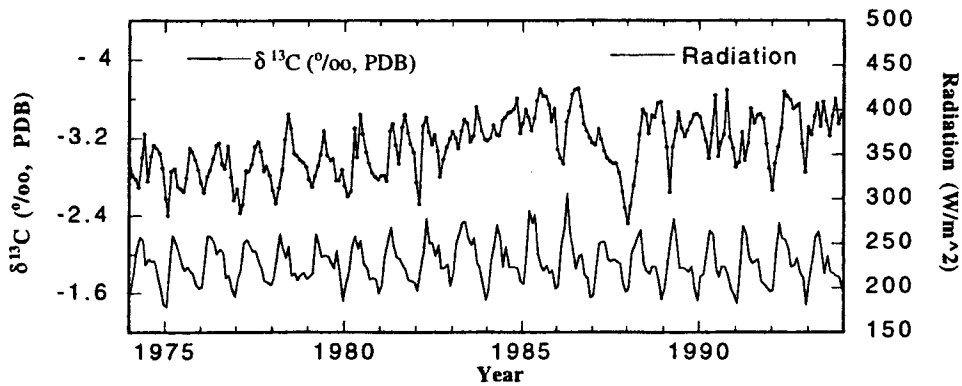

Fig. 6.6a Comparison of carbon isotope with radiation intensity in the period 1974-1994

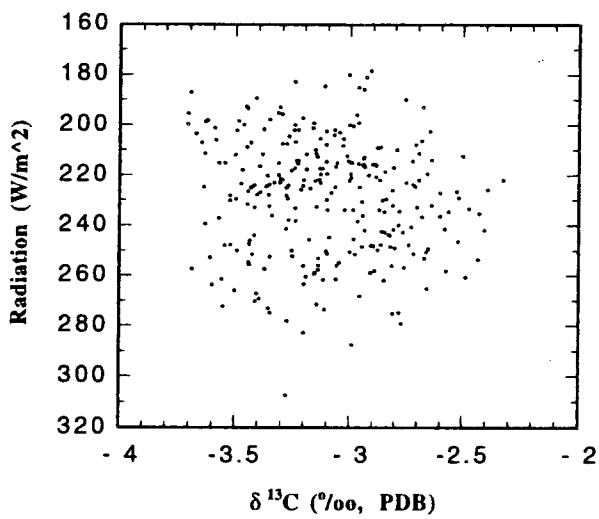

Fig. 6.6b Correlation between carbon isotope and radiation intensity in the period 1974-1994

this study and was recorded in coral $\delta^{13}C$ as in the case of Swart's samples collected from Florida Reef Tract. In fact, Druffel and Benavides (1986) also inferred a decrease of about 0.5‰ of $\delta^{13}C$ in DIC from 1900 to 1970 for the surface layer of the tropical ocean from the measurements of the $\delta^{13}C$ value of aragonite in a sclerosponge. Based on direct measurements made during three National Oceanographic and Atmospheric Administration (NOAA) research cruises in the period of 1970-1990, Quay et al. (1992) suggested the average $\delta^{13}C$ value of DIC in the surface waters of the Pacific decreased by about 0.4‰ between 1970 and 1990. Thus, the total decrease of $\delta^{13}C$ in DIC in the period 1900-1990 is estimated as approximately 0.9‰ (Quay et al., 1992), similar to the decrease in Clipperton coral $\delta^{13}C$ which is 0.85‰ during the same time. However, at present no direct measurements of $\delta^{13}C$ in DIC are available in the area of Clipperton Atoll. Recently, K. Caldeira introduced a global ocean carbon cycle model based on measurements of atmospheric O_2 and CO_2 concentration for estimating variations of $\delta^{13}C$ in DIC (Stephens et al., 1998). Using this model he calculated the DIC $\delta^{13}C$ values in the vicinity of Clipperton from 1941 to 1989 (K. Caldeira, per. comm.), ranging from 2.31‰ for 1941 to 1.89‰ for 1989. In the period 1941-1950, $\delta^{13}C$ was relatively constant and remains about 2.31-2.30‰, while after 1950 it progressively more depleted from 2.30‰ to 1.88‰ (Fig. 6.7). Although the estimated DIC $\delta^{13}C$ values only cover the period of 1941-1989, comparison of their variation with $\delta^{13}C$ in corals at Clipperton shows that the pattern of both trends is quite similar (see Fig. 6.7). From 1941 to 1950, both curves show a relatively flat pattern while after 1950 both become gradually more depleted. Therefore, if the model of DIC $\delta^{13}C$ variation is valid, this similar pattern between $\delta^{13}C$ in coral and that in DIC appears to imply that (1) due to the anthroprogenic influence, the assumption that $\delta^{13}C$ in DIC has not varied significantly over time may need to be re-examined, and (2) the variations of $\delta^{13}C$ in corals may be used as a new potential indicator of the increase of CO_2 uptaken by the oceans due to the increasing combustion of fossil fuels and

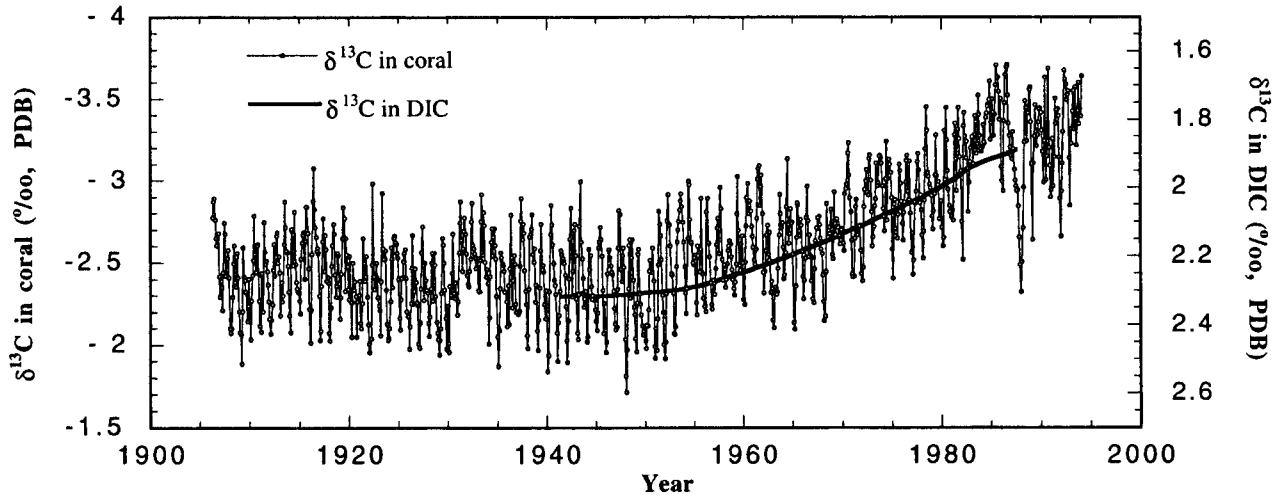

Fig. 6.7 Comparison of carbon isotopic composition of coral skeleton with carbon isotopic composition of DIC obtained from a model in the period 1941-1989

land use. However, it should be noted that the range of the variation in coral skeletal $\delta^{13}C$ for the period of 1941-1989 (which is about 0.85‰, from -2.35‰ – -3.2‰) is twice of that of model DIC $\delta^{13}C$ (which is about 0.43‰, from 2.31‰ to 1.88‰). As suggested by K. Caldeira (Per. Comm.) this model may underestimate the net southward transport of the sum of O_2 and CO_2 in the oceans. Therefore, more accurate models for estimating DIC $\delta^{13}C$ values, longer time scales for DIC $\delta^{13}C$ data, and additional $\delta^{13}C$ measurements of corals are all needed to evaluate further the contribution of DIC $\delta^{13}C$ to the variability of coral $\delta^{13}C$.

6.4 Analysis of multiple samples

As described above, due to the complex interactions of different individual effects on both $\delta^{18}O$ and $\delta^{13}C$, it is often difficult to separate one influence from another unless multiple samples are analyzed. In order to distinguish the effects of different factors on $\delta^{13}C$ and $\delta^{18}O$ in corals from Clipperton Atoll, some of the results of Linsley et al. (in press) will be discussed and reanalyzed in this section. The individual locations of each sample are shown in Fig. 2.5. Table 6.1 shows the total lengths of the six cores analyzed and the water depths from the top of the cores (after

Table 6.1 Total lengths and water depths of the six cores at Clipperton Atoll (after Linsley et al., in press)

Cores	*Water depth (m)*	*Total core length (m)*
C2A	13.1	2.26
C2B	13.1	2.26
C3C	12.5	2.67
C4B	8.2	2.45
CDT-20	6.1	small colony
CDT-40	12.2	small colony

Linsley et al., in press). For the purpose of this section, only data from samples spanning the 9 year period of 1986-1994 from the six coral samples is plotted and analyzed. For a complete discussion of the comparison of these coral isotopic results, the reader is referred to Linsley et al. (in press).

Results of analysis of multiple coral samples can potentially be used to separate the effects of different factors. For example, composition plots can highlight the effects of some factors, while keeping the effects of the other factors constant or negligible. One typical kind of plot is shown in Figs. 6.8. Here, coral $\delta^{18}O$ is plotted verses $\delta^{13}C$ for the six different coral samples for two months with different SSTs, but approximately the same intensity of radiation and precipitation. Only six pairs of months in this 9 year period (1985-1994) show this characteristic and are now plotted. In theory if it is assumed that the intensity of radiation is equal during two time intervals, the coral photosynthesis will be the same since the effects of metabolic fractionation should be approximately constant. Thus, when precipitation is also approximately equal, the differences in $\delta^{18}O$ and $\delta^{13}C$ of the samples between the two months in each plot in Figs. 6.8 can be regarded as mainly reflecting different SSTs in both $\delta^{18}O$ and $\delta^{13}C$ in these two months. To show the effect of SST on $\delta^{18}O$ and $\delta^{13}C$, the corresponding points on the plot are connected by arrows which consistently point from the month of the lower SST to that of the higher SST (Figs. 6.8). These arrows clearly illustrate the direction in which $\delta^{18}O$ changes with the increase of SST. In Figs. 6.8a, b, and c, which compare September vs. July, 1985, July vs. June, 1991, and August vs. July, 1992, respectively, with the increase of SSTs, $\delta^{18}O$ of all samples are more depleted. In Figs. 6.8d, which compares October vs. July, 1990, with the increase of SST, four of the six samples show the same trend of change as in Figs. 6.8a, b and c while the other two either show some enrichment in $\delta^{18}O$ or no difference at all. In Figs. 6.8e and f, which compare April vs.

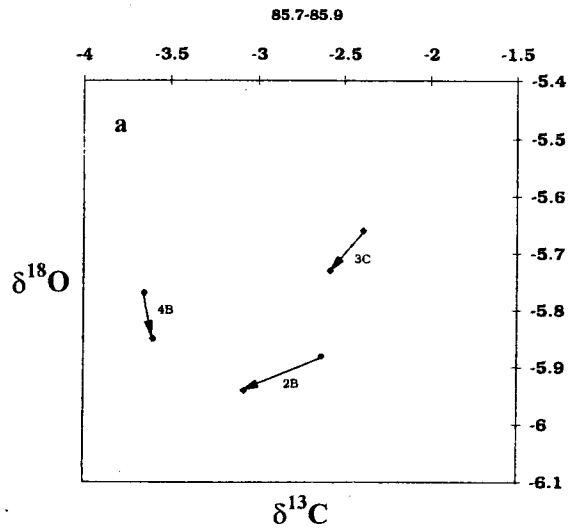

Sept. 1985 → July 1985

SST *28.00* *28.26*

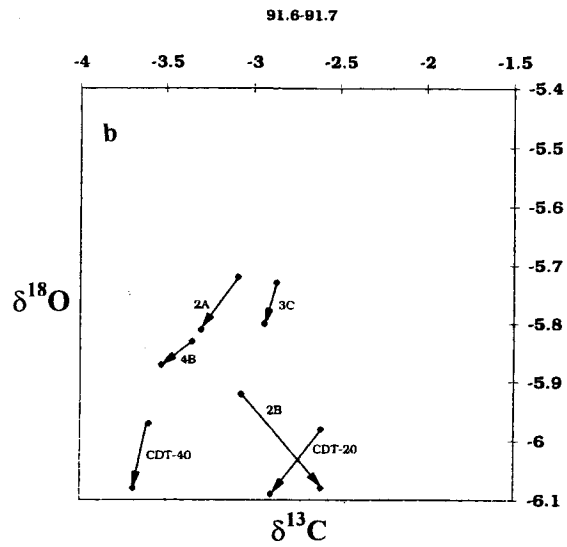

July 1991 → June 1991

SST *28.74* *29.81*

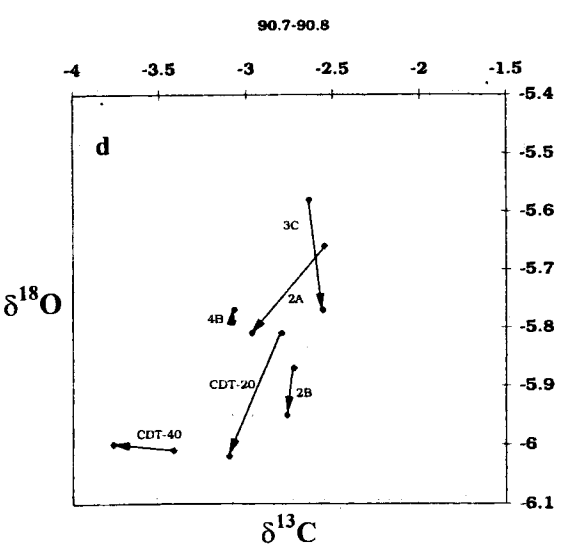

Oct. 1990 → July 1990

SST *28.01* *29.39*

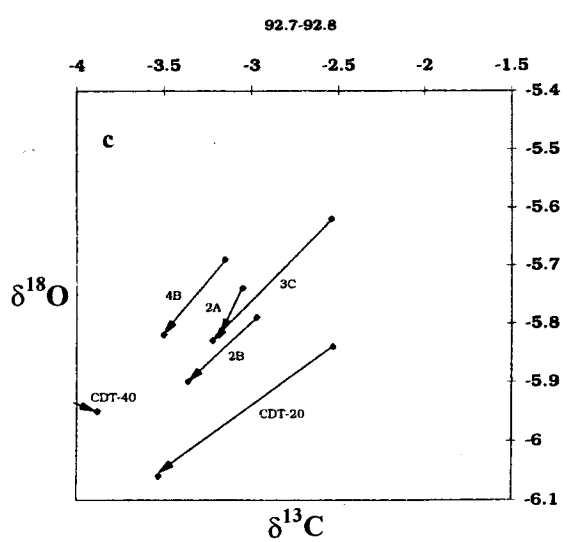

Aug. 1992 → July 1992

SST *27.97* *29.17*

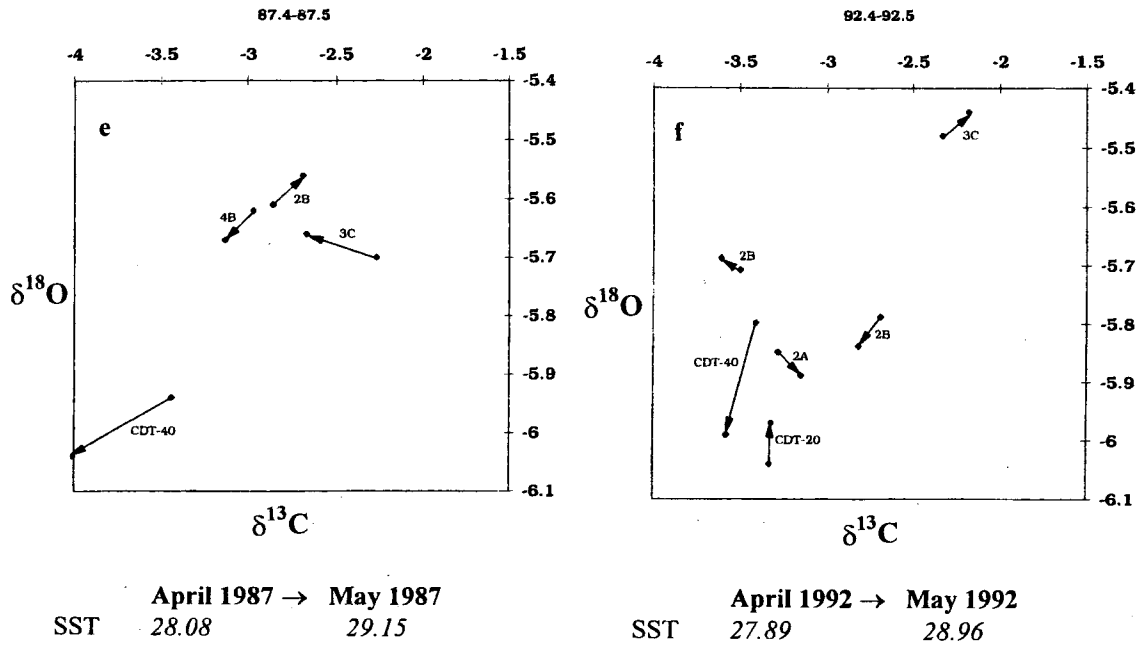

Fig. 6.8 $\delta^{13}C$ verses $\delta^{18}O$ in two time intervals with the same intensity of radiation and precipitation but different SST (arrows point to the months of higher SST)

may, 1987 and April vs. May, 1992, respectively, the patterns are complicated, with depletion of ^{18}O in some pairs and enrichment in some others. Overall, the magnitude of the variation in $\delta^{18}O$ is variable among the 6 plots with some changes larger than 0.22‰/°C and some smaller than that. In summary, with the increase of SST, 24 out of 31 pairs show depletion in ^{18}O while 5 show enrichment and 2 show no noticeable difference. Therefore, it is concluded that there is a clear negative correlation between $\delta^{18}O$ and SST in this region and this correlation identifies the SST as an important factor that influences the isotopic signatures recorded in corals in Clipperton Atoll.

The directional arrows in Figs. 6.8a-f also show how the $\delta^{13}C$ changes with the increase of SST. In Figs. 6.8 a, b, c, and e, respectively, two out of three, five out of the six, and three out of four pairs indicate that $\delta^{13}C$ is more depleted in the month with the higher SST. That is only 4 out of a

total of 19 show the more enrichment with the higher SST. In Figs. 6.8 d, and f, the pattern is more complicated, with some arrows indicating depletion in ^{13}C, some enrichment in ^{13}C, and others indicating no trend at all. The magnitude of difference also varies as with $\delta^{18}O$. In summary, of a total of 31 carbon isotope pairs, 21 show depletion, 5 show enrichment and the other 5 show no difference in $\delta^{13}C$ when the SST is the higher. Therefore, $\delta^{13}C$ also shows a negative correlation with SST although this is not so obvious as $\delta^{18}O$.

In order to isolate the effects of radiation and precipitation, other pairs of monthly data were plotted using similar $\delta^{18}O$–$\delta^{13}C$ diagrams. This time the two months chosen have approximately the same SST but different radiation intensities and precipitation. In theory, with 2 months of equal SST, the differences in $\delta^{13}C$ should reflect the effects of the different radiation intensities while the differences in $\delta^{18}O$ should represent those of the different precipitation-related $\delta^{18}O_{water}$. There are still only six pairs of months in this 9 year period (1985-1994) that have this characteristic and are compared.

First we can see how $\delta^{18}O$ changes with the increase of precipitation (Figs. 6.9). The arrows in all the plots point to the month with the higher precipitation. (1) In Figs. 6.9 a, b, and c, which compare January vs. November, 1988; March vs. April, 1990; and March vs. April, 1992, respectively, 12 out of a total of 16 pairs show depletion in $\delta^{18}O$ with the increase of precipitation, which is consistent with the prediction that $\delta^{18}O$ should be negatively correlated with precipitation. (2) In Figs. 6.9 d and e, which compare April vs. December, 1988 and April vs. December, 1989, respectively, only 3 out of the 12 arrows show the same trend while the other 9 show the opposite direction of change with the increase of precipitation, i.e. they show enrichment in $\delta^{18}O$. (3) In Figs. 6.9 f, which compares June vs. July, 1992, the pattern is more

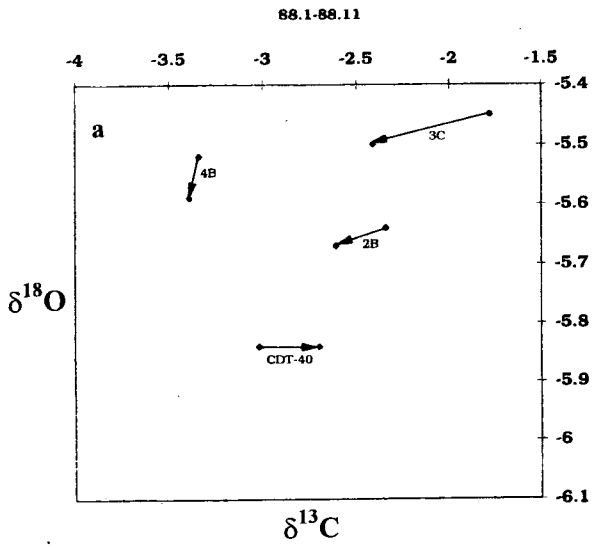

	Jan. 1988 →	Nov. 1988
Prep.	68.28	112.32

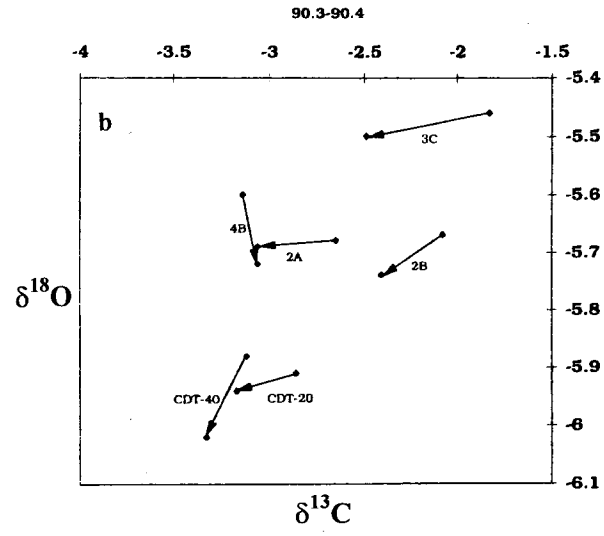

	Mar. 1990 →	April 1990
Prep.	2.00	9.42

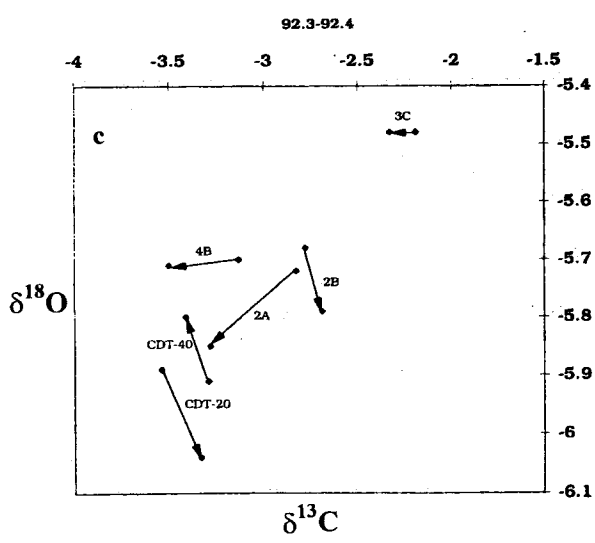

	Mar. 1992 →	April 1992
Prep	9.11	33.65

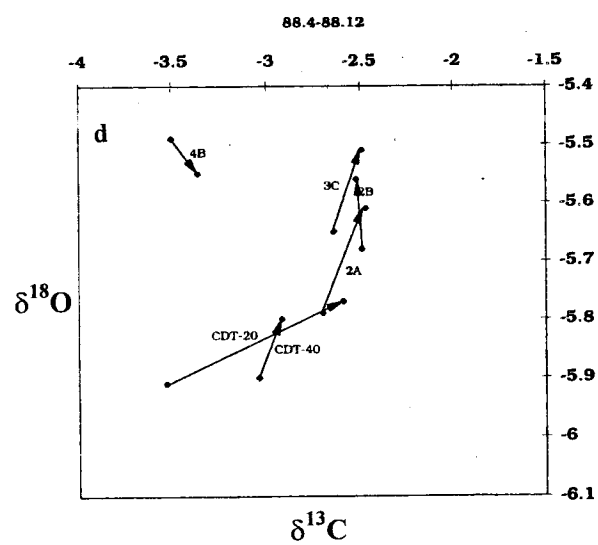

	April 1988 →	Dec. 1988
Prep.	19.04	80.86

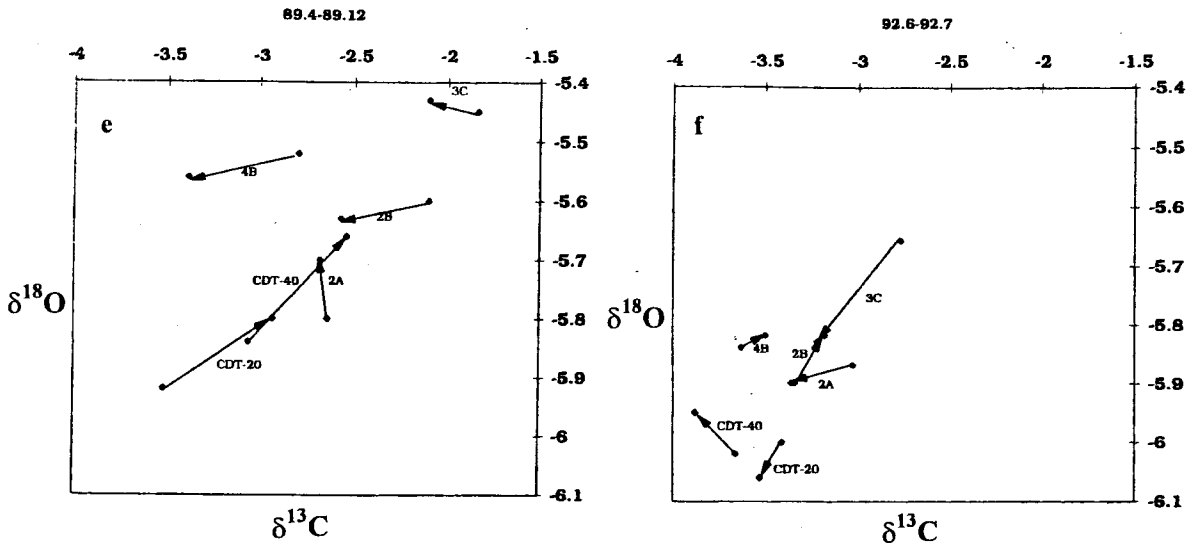

	April 1989 →	Dec. 1989		June 1992 →	July 1992
Prep.	8.64	89.18	*Prep.*	87.33	142.91

Fig. 6.9 $\delta^{13}C$ versus $\delta^{18}O$ in two time intervals with the same SST but different radiation intensity and precipitation (arrows point to the months of higher precipitation)

complicated with three arrows showing depletion in ^{18}O, two showing enrichment and one showing no obvious change. In summary, of a total of 34 pairs in all the plots, 16 show changes in $\delta^{18}O$ that indicate negative correlation with precipitation, 12 show positive correlation while the other 6 show no correlation. This mixed result suggests that overall, the correlation between coral $\delta^{18}O$ and precipitation is far less pronounced than that between $\delta^{18}O$ and SST. A recent study by Fairbanks et al. (1997) showed that the change in $\delta^{18}O_{water}$ with salinity can reach 0.27‰ $\delta^{18}O_{water}$ per ‰ salinity in convective regions of the tropical Pacific, which suggests that the variation of $\delta^{18}O_{water}$ in Clipperton should be about 0.22‰ using the average annual salinity change of 0.8‰ (see Chapter 2). However, the above plots show that the actual precipitation-related variation of $\delta^{18}O_{water}$, and thus the variation in coral $\delta^{18}O$, is neither obvious nor consistent, sometimes even showing positive correlation with the precipitation. Therefore, compared with the effect of SST on $\delta^{18}O$ in corals, the effect of precipitation does not appear to

be an important factor that influenced $\delta^{18}O_{water}$, which in turn influenced $\delta^{18}O$ in corals. The inconsistent variation $\delta^{18}O$ with precipitation further suggests that its effects may not be as large as that of the SST. However, it should be pointed out that due to the limitation of the current age model for Clipperton corals, it may produce the potential for a ± 1 month time-scale error in the period of 1985-1994. It thus can not excluded the possibility of error caused by the age model.

Next I examine how $\delta^{13}C$ changes when the radiation intensity is different. Again I use the same plotting technique as discussed in Figs. 6.9, but this time the arrows in the plots point to the month of higher radiation (Figs. 6.10). In Figs. 6.10 a, b, and d, with the increase of intensity of radiation, 13 out of the 16 pairs show depletion in ^{13}C, which is consistent with Erez (1978) but contrary to the more popular opinion that the increase of intensity of radiation tends to enrich the ^{13}C (McConnaughey, 1989a; Allison et al., 1996). In the other 3 plots (Figs. 6.10 c, e and f), however, 11 out of the 18 pairs show enrichment in ^{13}C with the increase of intensity of radiation, while only 6 show depletion in ^{13}C, and 1 shows no difference at all. In summary, of a total of 34 pairs of points, 19 show negative, while 11 show positive correlations between $\delta^{13}C$ and radiation intensity. Thus $\delta^{13}C$ in corals in this region appears negatively correlated with the intensity of radiation. However, it is still uncertain whether these observations reflect a true negative correlation between $\delta^{13}C$ and the metabolic fractionation. As discussed in Chapter 5, the metabolic fractionation is a very complex process, and the nature of this process is still unknown. Furthermore, only 34 pairs of observations were compared in the plots. Therefore further work needs to be done before $\delta^{13}C$ can be used as an indicator of photosynthesis.

Having compared the $\delta^{13}C$ and $\delta^{18}O$ of different time intervals, I now compare $\delta^{13}C$ and $\delta^{18}O$ in the six different samples for the same time interval. If we compare the plots of any individual

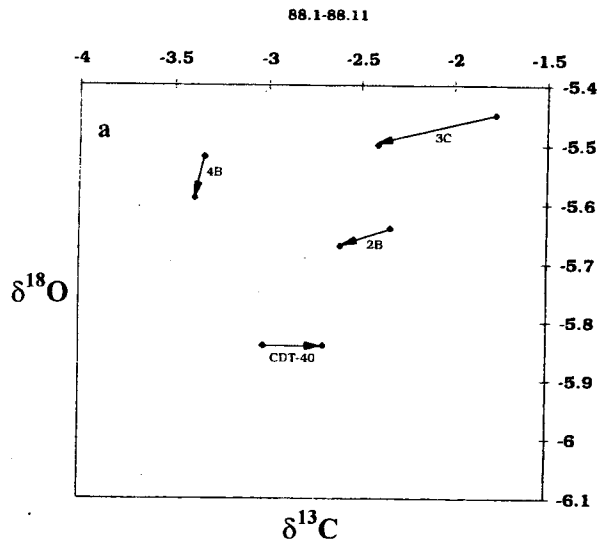

Jan. 1988 → Nov. 1988

Rad. 198.70 207.10

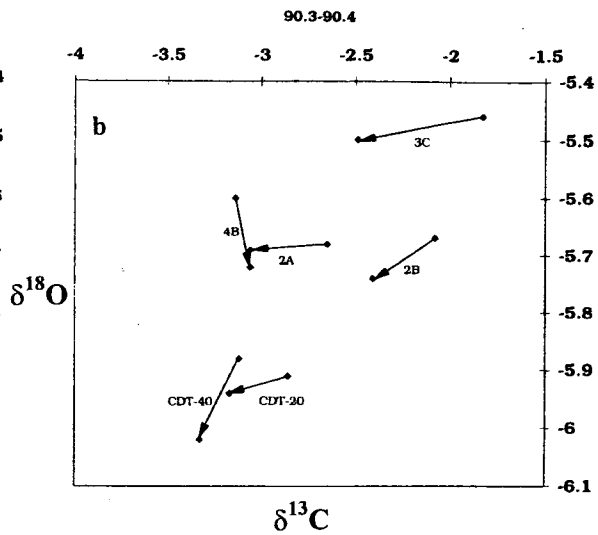

Mar. 1990 → April 1990

Rad. 242.80 265.30

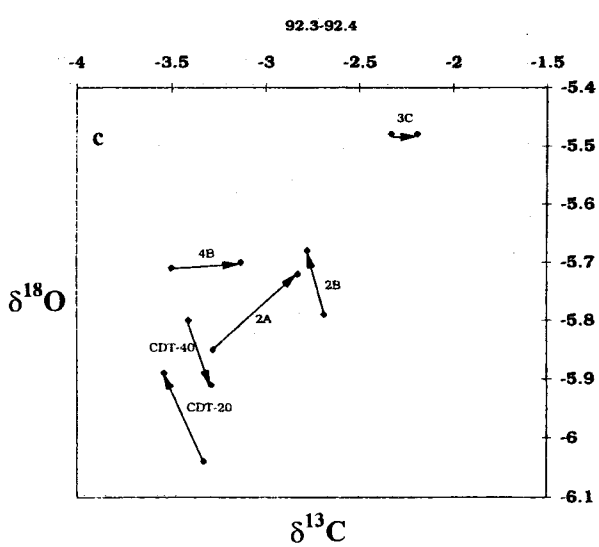

April 1992 → Mar. 1992

Rad. 255.60 273.19

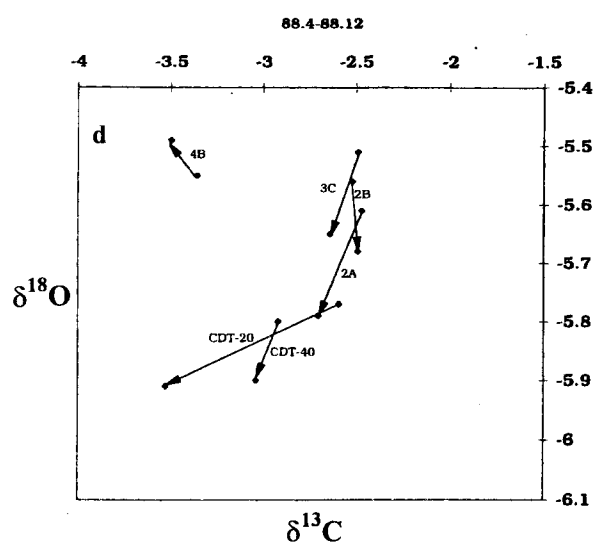

Dec. 1988 → April 1988

Rad. 187.20 257.40

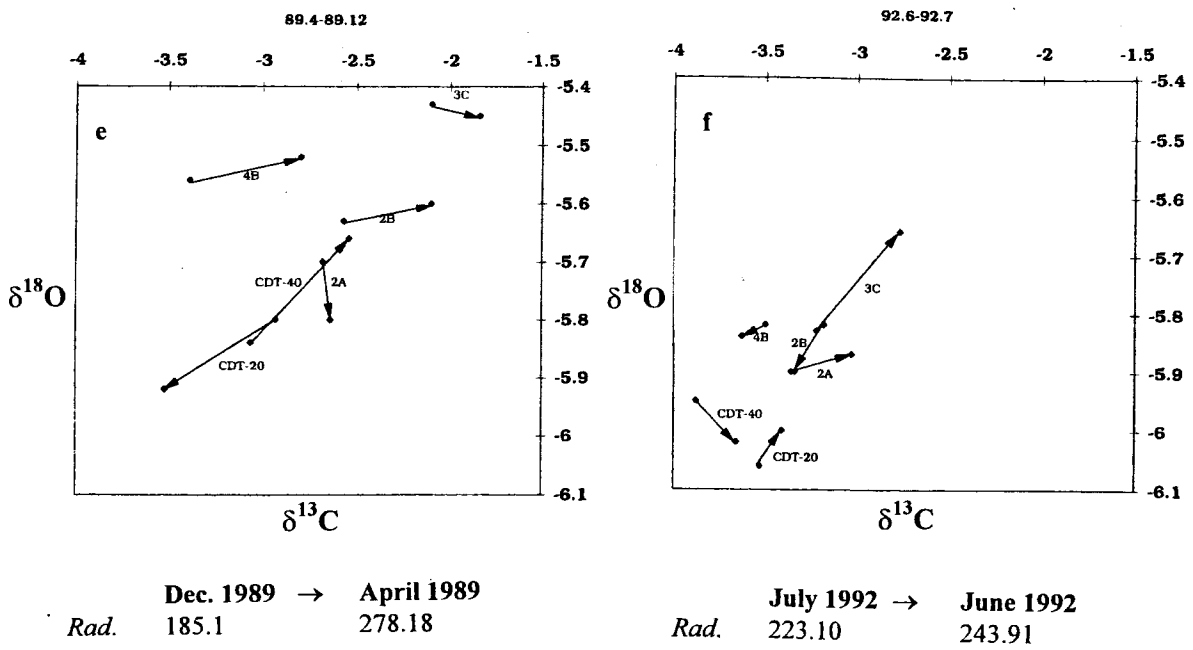

Fig. 6.10 The same figure as Fig. 6.9 but arrows point to the months of higher radiation intensity

month; for example June 1991 (Figs. 6.8b), we clearly see that they are widely scattered. Even for the four cores (2A, 2B, 3C and CDT-40) which grew in approximately the same water depth (approximately 12-13 m, see Table 6.1), they are still widely distributed. This indicates that for the four cores even though they represent the records in the different corals of exactly the same environmental conditions including the same SST, precipitation, radiation intensity and even the same isotopic composition of seawater, their signatures can be considerably different. For example, the maximum difference in $\delta^{18}O$ among the different samples for the month of June 1991 in Figs. 6.8b is equivalent to a change in SST of up to 2°C if calculated according to the change in $\delta^{18}O$ of about 0.22‰ with 1°C of change in SST under equilibrium conditions (Epstein et al., 1953; Tarutani et al., 1969; Grossman and Ku, 1986). For the four cores (2A, 2B, 3C and CDT-40) since all the other factors are the same, the observed discrepancies among the different corals can only be explained by differences in their intrinsic growth characteristics. One possible

such characteristic might be the extension rate. The mean annual extension rates of the four cores have been estimated by Linsley et al. (in press) and listed in Table 6.2. However, unfortunately no clear correlation between extension rate and $\delta^{18}O$ value can be seen. For example, the mean annual growth rate of 3C is the highest among the four cores 2A, 2B, 3C, and CDT-40, but its $\delta^{18}O$ is not the lightest, but the heaviest among the four samples in almost all the plots (see Linsley et al., in press). Another interesting fact is that the four points are consistently scattered

Table 6.2 The average annual growth rate of all six cores in Clipperton Atoll (after Linsley et al., in press)

	4B	*3C*	*2A*	*2B*	*CDT20*	*CDT40*
extension rate (mm/yr)	24.5	20.3	17.3	16.2	16.3	11.7

at approximately the same relative positions in all the plots compare (Figs. 6.8; 6.9; 6.10). 3C is always relatively enriched in both ^{13}C and ^{18}O while CDT 40 is always depleted in both ^{13}C and ^{18}O. 2A and 2B are always plotted near the center. Therefore, all these observations support the opinion (e.g. McConnaughey (1989a) and Allison et al. (1996)) that when corals grow faster than about 4-5 mm/yr (in Clipperton the annual growth rate reaches 25 mm/yr), variations in coral growth rate generally have only little effect on the $\delta^{18}O$ and $\delta^{13}C$ of corals.

Linsley et al. (in press) proposed that another possible reason of this scatter of the plots of the six samples may be due to the core sampling location on the dome shaped colony. As can be seen in the Figs. 6.8-6.10, for 2A and 2B, both of which grew in a same colony but different sampling location of cores, they show different signature of $\delta^{18}O$. Therefore, as Linsley et al. (in press) suggested, although the six samples are all drilled along the maximum growth axis, it is possible that core position within the maximum growth axis has resulted in this variations in disequilibrium vital effect scatter.

6.5 Summary

The above analysis suggests that the effect of SST on skeletal $\delta^{18}O$ in the Clipperton region appears to have played a more important role than that of precipitation and the SST may have been the main factor influencing $\delta^{18}O$ compared with precipitation/salinity. The scatter of $\delta^{18}O$ values among the six different samples for a given month does not appear to be related to the effects of the growth rate, but may be due to the core sampling location on the dome shaped colony. The patterns in $\delta^{13}C$ of corals are more complicated than their $\delta^{18}O$ signatures. Although there appears to be some negative correlation between SST and $\delta^{13}C$, it is not as apparent as with $\delta^{18}O$, and the radiation intensity also shows some negative correlation with $\delta^{13}C$, which suggests a view contrary to what is generally held.

CHAPTER 7 SINGULAR SPECTRUM ANALYSIS OF $\delta^{18}O$ DATA FROM CLIPPERTON, 1906-1994

7.1 Introduction

In Chapter 6 I discussed the various factors affecting the $\delta^{18}O$ and $\delta^{13}C$ records in corals in the Clipperton region and suggested that the $\delta^{18}O$ signature mainly reflects the variations of SST while $\delta^{13}C$ mainly reflects the changes of SST and intensity of the radiation. Therefore the long-term $\delta^{18}O$ and $\delta^{13}C$ data (1906-1994) in C4B (Fig. 4.3) can be used as valuable records of climatic changes during most of the 20th century. In this chapter I attempt to analyze the complete $\delta^{18}O$ record in C4B as a function of various climatic changes and ENSO events in the Clipperton region. The core C4B 88 year oxygen isotopic record represents the combined effects of various dynamic elements of climate change on various time scales. In terms of statistics, it is a time series which contains a complex combination of various deterministic components such as seasonal variations, ENSO events and a potentially significant long-term trend, in addition to stochastic components known as "white noise" (Hann, 1977). Some longer-term cycles as well as strong annual cycles in fact can be visually recognized (see Fig. 4.3). For example, from 1906 to 1912 and from 1930 to 1938 several pronounced interannual changes can be recognized while from 1918 to 1930 and from 1938 to 1955 there are some longer-term interdecadal changes (see Fig. 4.3). Although an estimate of the pacing and amplitude of these oscillations can be determined through visual examination, a more precise identification and assessment of the statistical significance of the various frequency components requires a more rigorous statistical analysis. To recognize accurately various components and their contributions to the total variability of the observed values, the data must be analyzed as a time series using statistical time-series analysis methods. One method of analyzing short time series with irregular frequency

components is a non-parametric technique called singular spectrum analysis (SSA). Recent studies have shown that using SSA, not only can ENSO cycles be recognized, but other cycles such as long-term trends and interdecadal oscillations can also be separately identified and evaluated (Linsley et al., 1994; Dunbar et al., 1994; Charles et al., 1997; Evans et al., in press). In this chapter, the fundamental principles of SSA are first briefly introduced, and then the $\delta^{18}O$ data from Clipperton analyzed using this method and the results presented. An attempt is also made to discuss the possible causes of the various cycles.

7.2 Principle of SSA

Basic concepts

In terms of statistics, an observed time series may be regarded as a realization or a single outcome of a stochastic process, which is a family of random variables indexed over time, denoted by {X(t)} (Chatfield, 1995). Fig. 7.1 shows several possible realizations for a stochastic process on a discrete time scale. The time series can be described by three main parameters: mean, variance and covariance which are defined as:

$$\text{Mean} = \Sigma X_i / N$$

$$\text{Variance} = \Sigma (X_i - \bar{X})^2 / N$$

$$\text{Covariance} = \Sigma (X_i - \bar{X})(Y_i - \bar{Y}) / N$$

While the variance is a measure of variability in a set of data, the covariance is actually a measure of degree of linear correlation between two sets of data X and Y (Godfrey et al., 1986) (Fig. 7.2). When covariance is positive, the two sets show positive correlation while when it is negative, the two sets show negative correlation. When covariance is zero, they have no correlation at all.

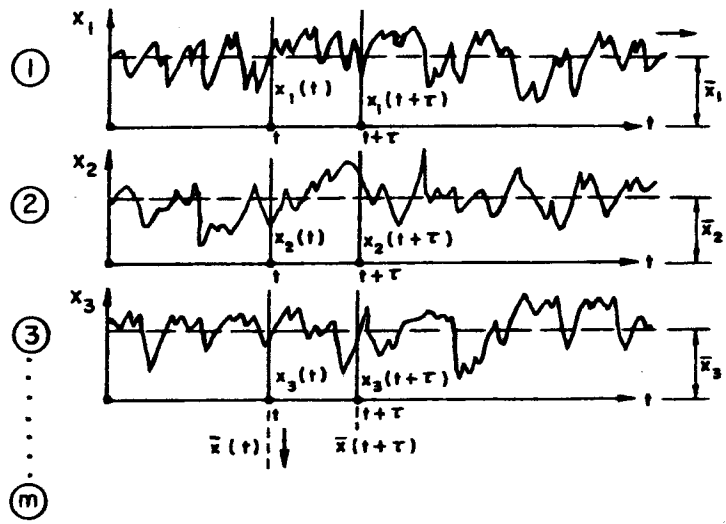

Fig. 7.1 Several realizations of a stochastic process (after Haan, 1977)

Quadrant	$(x-\bar{x})$	$(y-\bar{y})$	$(x-\bar{x})(y-\bar{y})$
1st	+	+	+
2nd	−	+	−
3rd	−	−	+
4th	+	−	−

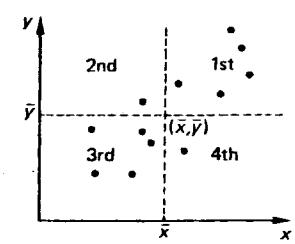

Fig. 7.2 The correlation of two sets of data (after Godfrey et al., 1986)

Principle Component Analysis

SSA is fundamentally based on a data-analysis method called principal component analysis (Vautard & Ghil, 1989; Vautard et al., 1992). Its principles are now reviewed. To visually show the degree of variability of two sets of data as well as the degree of correlation between them, a standard method is to plot them in a two-dimensional reference frame (see Fig. 7.2) (Golfrey et

al., 1986). Now the problem becomes one of how to describe the degree of scatter of the data points. First it is simply considered how they are scattered about their means along the x and y directions. In other words, it is considered the ranges of variability of projection of the data vectors along x and y axes. Clearly these can be exactly described by the variance of data set x and variance of data set y, respectively. Then we need the covariance of x and y to describe another aspect of the scatter pattern, the shape of the scatter pattern or the degree of correlation between x and y. Therefore, the degree of scatter of data points can be completely described by the following variance-covariance matrix:

$$\begin{pmatrix} s_{xx} & s_{xy} \\ s_{xy} & s_{yy} \end{pmatrix}$$

where S_{xx} represents the variance of x while S_{yy} represents the variance of y. S_{xy} is the covariance of x and y.

Alternatively, we can also describe the degree of scatter of the data points along directions other than those of the horizontal and vertical axes of the diagram. For this purpose we can rotate the reference frame by a certain angle and describe the degree of scatter of the data points in terms of the different variances and covariance along the new x' and y' directions in the new reference frame (see Fig. 7.2). It can be easily demonstrated that:

$$\begin{pmatrix} s_{x'x'} & s_{x'y'} \\ s_{x'y'} & s_{y'y'} \end{pmatrix} = \begin{pmatrix} \cos\theta & \sin\theta \\ -\sin\theta & \cos\theta \end{pmatrix} \begin{pmatrix} s_{xx} & s_{xy} \\ s_{xy} & s_{yy} \end{pmatrix} \begin{pmatrix} \cos\theta & -\sin\theta \\ \sin\theta & \cos\theta \end{pmatrix}$$

Thus even though the scatter degree is invariant, the variances along x' and y' directions and the corresponding covariance vary with the rotation angle. It is clear that there must exist a certain rotation angle or reference frame in which the scatter degree along one axis is the maximum while along the other it is the minimum. And it is also evident that under this circumstance the

covariance must be zero since the scatter pattern now shows no correlation at all. To find these two mutually orthogonal special directions of the new reference frame (*principal directions*) and the corresponding maximum and minimum variances or *principal variances,* it is simply a matter of finding the so-called *eigenvectors* and the *eigenvalues* of the above variance-covariance matrix, respectively (Vartard & Ghil, 1989; Vartard et al., 1992). Once we have the principal directions, we can represent the data points in terms of their new coordinates in the new reference frame with the principal directions as the x', y' axes:

$$\begin{pmatrix} x_1' & x_2' & x_3' & \dots & x_n' \\ y_1' & y_2' & y_3' & \dots & y_n' \end{pmatrix} = \begin{pmatrix} l_{11} & l_{12} \\ l_{21} & l_{22} \end{pmatrix} \begin{pmatrix} x_1 & x_2 & x_3 & \dots & x_n \\ y_1 & y_2 & y_3 & \dots & y_n \end{pmatrix}$$

where xi' and yi' are called the principal components which are actually the projections of data vectors (x, y) on the principal directions or eigenvectors (l_{11}, l_{12}) and (l_{21}, l_{22}), respectively. One of these principal components has the maximum variance while the other has the minimum variance, and their covariance is zero so that they are uncorrelated in this principal-variance frame of reference.

We can easily extend this to the analysis of M sets of data values in a M-dimensional space. In SSA, we analyze M lagged copies of a single centered time series X(t):

$x_{(1)}, x_{(2)}, x_{(3)}, \dots x_{(N-M+1)},$

$x_{(2)}, x_{(3)}, x_{(4)}, \dots x_{(N-M+2)},$

$x_{(3)}, x_{(4)}, x_{(5)}, \dots x_{(N-M+3)},$

.....

$x_{(M)}, x_{(M+1)}, x_{(M+2)}, \dots x_{(N)},$

where M is the maximum lag, also known as the window length. The variance of each of the above sub-series and the covariance among them can be calculated. Generally, we can assume

that the variance of each sub-series is the same and the covariance is also a constant which is dependent only on the lag τ between any two of the sub-series (Chatfield, 1989). Thus the variance-covariance matrix (called lagged-covariance matrix) is written as:

$$\begin{pmatrix} c(0) & c(1) & . & . & c(M-1) \\ c(1) & c(0) & c(1) & . & . \\ . & c(1) & . & . & . \\ . & . & . & . & c(1) \\ c(M-1) & . & . & c(1) & c(0) \end{pmatrix}$$

where $c_{(\tau)}$ ($0 < \tau < M-1$) is the covariance of x_i at lag τ (also called the autocovariance function) (Vartard & Ghil, 1989; Vartard et al., 1992). Then the eigenvalues (there are M of them) and the associated eigenvectors of this matrix can be found. Just as in the 2-D case, the former represent the principal variances of the series while the latter represent the associated directions which define the dominant modes of variability. The M eigenvectors are also called the *empirical orthogonal functions* (EOFs) (Vartard & Ghil, 1989; Vartard et al., 1992). Then we can represent each M-dimensional vector in terms of its new coordinates in the new reference frame with its axes parallel to the M eigenvectors:

$$\begin{pmatrix} x'(1) & x'(2) & . & . & x'(N-M+1) \\ x'(2) & x'(3) & . & . & x'(N-M+2) \\ . & . & . & . & . \\ . & . & . & . & . \\ x'(M) & x'(M+1) & . & . & x'(N) \end{pmatrix} =$$

$$= \begin{pmatrix} l_{11} & l_{12} & . & . & l_{1M} \\ l_{21} & l_{22} & . & . & l_{2M} \\ l_{31} & l_{32} & . & . & . \\ . & . & . & . & . \\ l_{M1} & l_{M2} & . & . & l_{MM} \end{pmatrix} \begin{pmatrix} x(1) & x(2) & . & . & x(N-M+1) \\ x(2) & x(3) & . & . & x(N-M+2) \\ . & . & . & . & . \\ . & . & . & . & . \\ x(M) & x(M+1) & . & . & x(N) \end{pmatrix}$$

The M new series $x'_{(\tau)}$, $x'_{(\tau+1)}$, ... $x'_{(N-M+1)}$, ($1< \tau < M$) are called the *principal components* which are actually the projections of the data vectors on the M principal directions or EOFs ($l_{\tau 1}$, $l_{\tau 2}$, ... $l_{\tau M}$), respectively. They can also be regarded as filtered versions of the original series. The associated EOFs correspond to the filters (moving average filters) (Chatfield, 1995). Thus while the EOFs define the dominant modes of variability, the associated principal components provide information relating to variations in amplitude that are not obtainable from conventional spectrum analysis. In brief, the PCs in combination with the associated eigenvalues and EOFs provide information relating to the various modes of variability and their individual contributions to the total variability of the observations.

To analyze the data of core C4B according to the above principles, an SSA software program written by E. Cook (Lamont-Doherty Earth Observatory) was used. As can be seen from the above discussion, the calculations require the choice of a parameter M (window length). The choice is clearly an arbitrary one and has to be made subjectively so as to balance "resolution" against "variance" (Chatfield, 1995). If M is too small, important features may be smoothed out, while if M is too large, spectral "peaks" in variance will be split into several components with neighboring frequencies. Thus a compromise value must be chosen.

7.3 Analysis Results and Discussion

SSA analysis of the C4B $\delta^{18}O$ data was run multiple times at different values of M. It turned out that values of 48months<M<96months did not significantly influence recognition of the dominant oscillatory modes. As I am mainly interested in oscillatory behavior within the ENSO frequency band I chose M at 72 months.

SSA results are presented for the unfiltered data and for a low-pass filtered series. For the unfiltered data, the 14 most significant eigenvectors and their associated variance and periods are listed in Table 7.1a.

Table 7.1a. Singular Spectrum Analysis of unfiltered $\delta^{18}O$ data from Clipperton Atoll (1906 - 1994)

Eigenvector	Variance (%)	Cumulative Variance (%)	Period (year)
1	27.10	27.10	trend
2, 5, 6	19.77	46.87	3-8
3, 4	16.17	63.04	1
7-9, 13, 14	13.28	76.32	1-3
11, 12	3.75	80.07	<1

$\delta^{18}O$ (n=1055), M=72 months (data not filtered)

The first 14 eigenvectors account for 80.07% of the total variance in the time series. The most pronounced cycle is the long-term trend which accounts for 27.10% of the total variance. The interannual cycle (between 3-8 years) is also significant and contributes 19.77% to the total variance. The annual cycle also explains 16.17% of the total variability, which demonstrates the regularity of the seasonal nature of climatic forcing in this region. Another two eigenvectors represent the high-frequency cycles (1-3 years and less than 1 year, respectively) which only explain 13.28% and 3.75% of the total variance, respectively.

To isolate the interannual and interdecadal cycles in the $\delta^{18}O$ record, the analysis was repeated in which the series was pre-filtered using a smoothing filter which removed periods ≤ 2 years. The results of this analysis are presented in Table 7.1b. With the removal of frequencies <2 years, six leading eigenvalues, eigenvectors (EOFs) and principal components (PC) and the associated variances and periods are recognized.

Table 7.1b. Singular Spectrum Analysis of filtered $\delta^{18}O$ data from Clipperton Atoll (1906 -1994)

Eigenvector	Eigenvalue	Variance (%)	Cumulative Variance (%)	Period (year)
1	0.383	54.67	54.67	Trend
2	0.127	18.07	72.74	12.5
3	0.084	11.92	84.66	4.8
4	0.049	7.03	91.69	3.9
5	0.024	3.44	95.13	3.0
6	0.016	2.29	97.42	2.2

$\delta^{18}O$(n=1055), M=72 months (data filtered at 2 years)

The six leading eigenvalues represent the variances of the six leading principal components which account for 97.42% of the total variance in the 2 year filtered time series (Fig. 7.3a & Fig. 7.3b). The first eigenvalue clearly is the most important one which explains over half of the variance of the total variability while the sixth eigenvalue contributes only 2.29% to the total variance. The 2nd eigenvalue is also important and contributes 18.07% to the total variance and the 3th, 4th, and 5th eigenvalues represent 11.92%, 7.03% and 3.44% to the total variability, respectively. The associated 6 eigenvectors and principal components are shown in Fig. 7.4a and Fig 7.4b. From the first to sixth eigenvectors, the dominant modes change from low-frequency to high-frequency. The first eigenvector which has period of about 125 years actually represents a long-term trend of the full record. The second eigenvector which has a period of about 12.5 years represents a interdecadal variation while the third, fourth and fifth eigenvectors show the interannual changes which are all in the ENSO band. The last eigenvector has a period of only about 2.2 years. As for the principal components (PC) they not only show the periods but the amplitudes of variability as well. Generally, from the first to the sixth principal components, the amplitudes of variability vary from maximum to minimum although for each PC the amplitude changes substantially during the whole record.

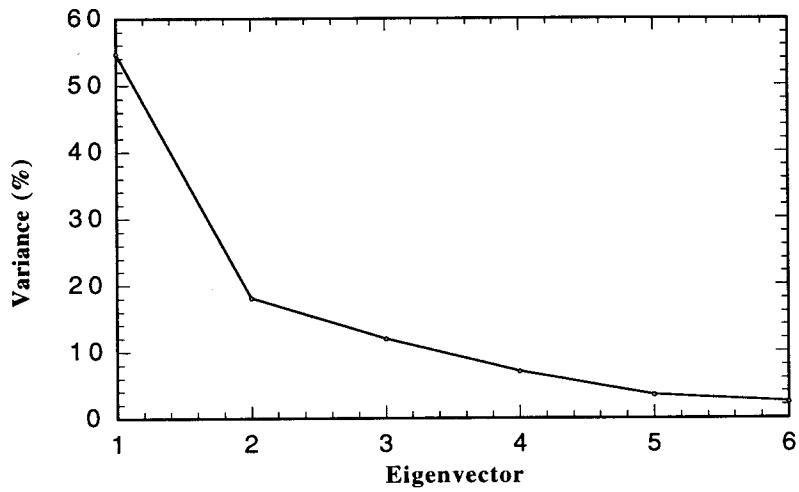

Fig. 7.3b The variance of six leading PC of oxygen isotopic data from Clipperton Atoll

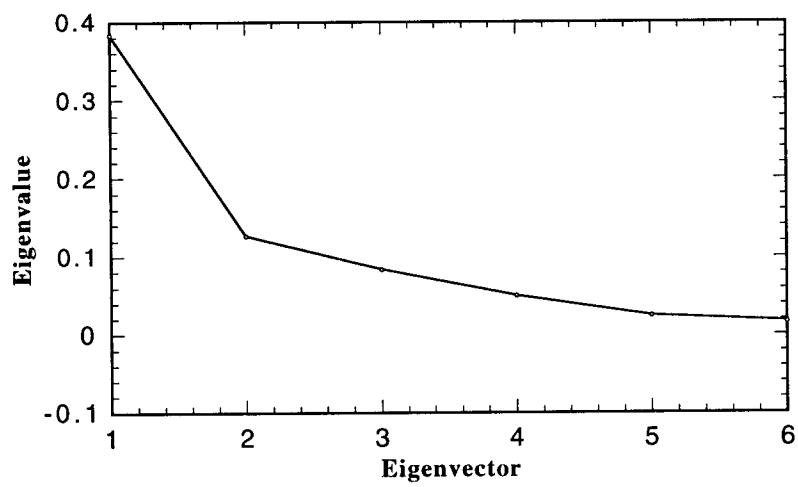

Fig. 7.3a The six leading eigenvalues of the oxygen isotopic data from Clipperton Atoll

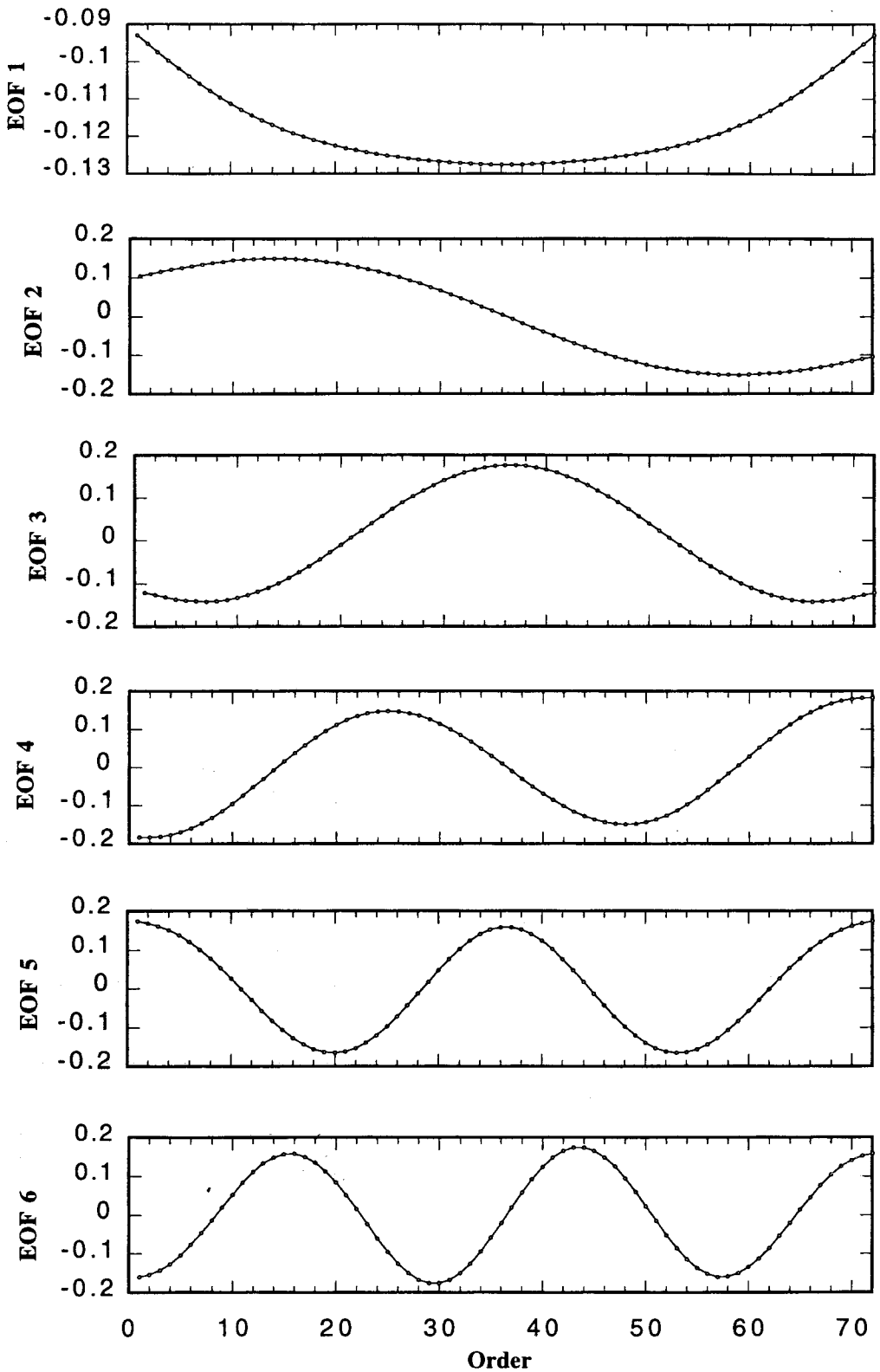

Fig. 7.4a The six leading eigenvectors (EOFs) of the $\delta^{18}O$ data from Clipperton Atoll

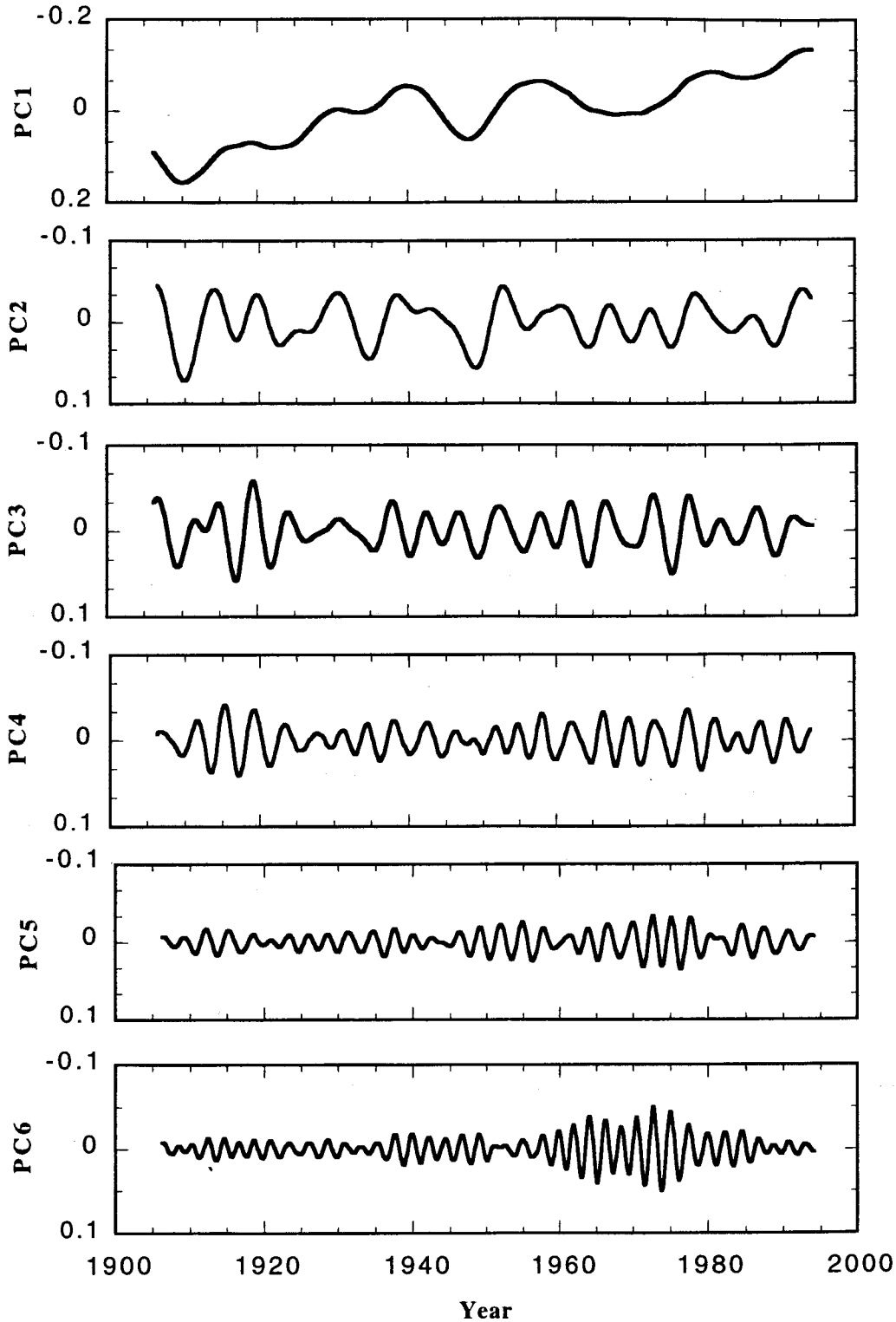

Fig. 7.4b The six leading principal components (PC) of the $\delta^{18}O$ data from Clipperton Atoll

In summary, six leading eigenvalues and associated eigenvectors (EOFs) and principal components (PC) are identified which include a long-term trend, a interdecadal cycle, three interannual cycles and a high-frequency (2.2 yr) variation, respectively. What is most interesting to this study is the interannual cycles (periods 3-5 years) since they may be related to the ENSO phenomenon. Therefore, the interannual cycles are interpreted first and then the other cycles.

7.3.1 The interannual bands

Three principal components have interannual average periods: PC_3, 4.8 years; PC_4, 3.9 years; and PC_5, 3.0 years, respectively (see Table 7.1b). The amplitudes of these three PCs are all in the range of 0.05‰ to -0.05‰ and generally decrease from PC_3 to PC_5 (see Fig. 7.4b). PC_3 and PC_4 have some similarity in that their amplitude vary with the same characteristic period.

It is known that the ENSO-event frequency-band is usually between 3 to 9 years (Trenberth, 1976; Rasmusson et al., 1990; Barnett, 1991) and PC_3, PC_4 and PC_5 are all in the ENSO band, so it is valid to add them together in order to analyze their combined ENSO features. The sum of these interannual principal components can be compared with the historical records of ENSO and SST and also the time series records from other areas.

Comparison with historical records

"El Niño event years" have been identified by Quinn et al. (1987) and Quinn (1992) on the basis of historical evidence from coastal South America for specific climatic, oceanographic, and biological phenomena. These are now indicated at their appropriate time positions in the plot of the combined interannual principal components of $\delta^{18}O$ data (Fig. 7.5) (where the dark arrows represent the strong to very strong ENSO "warm phase" events) (Quinn et al., 1987; Quinn,

1992). As can be seen from the figure, most of the ENSO events can be identified in the 4B $\delta^{18}O$ ENSO band; strong amplitudes are generally coincident with years of strong ENSO events, whereas weak amplitudes correlate with identified weak ENSO events. Of the nine documented strong to very strong ENSO events in the period of 1906 to 1994, six of which (in the years of 1911-12, 1913-15, 1918-20, 1957-58, 1965-66, and 1972-73) are clearly shown in the plot and the magnitudes of the $\delta^{18}O$ peaks all exceed 0.05‰ and almost reach 0.1‰. However, three strong ENSO events (1925-26, 1939-40 and 1982-83) have no counterpart in the plot which shows only 0.01-0.02‰ anomalies (Fig. 7.5).

Also plotted in Fig. 7.5 for comparison is the combined interannual principal components of the SST anomaly series from the Clipperton region (Kaplan et al., in press). The plot represents the sum of a total of 4 principal SST components (eigenvectors 2, 3, 4, and 5) with periods of 3-8 years which were obtained using the same SSA method described earlier to a 2-year filtered series of the original SST series (see Table 7.2). It can be seen that the interannual variation of $\delta^{18}O$ shows good correlation with that of SST (see Fig. 7.5). For most of the period 1906-1994,

Table 7.2. Singular Spectrum Analysis of filtered monthly SST Anomaly Data (1906-1991)

Eigenvector	Variance (%)	Cum Variance (%)	Period (year)
1	38.84	38.84	trend
2, 3, 4, 5	55.46	94.30	3-8
6, 7	4.33	98.63	2

SST (n=1029), M=72 months (data filtered at 2 years)

the variation of the former is synchronous with that of the latter; the minima of $\delta^{18}O$ coincide with the warm SST anomalies, while the maxima of $\delta^{18}O$ coincide with the cool SST anomalies.

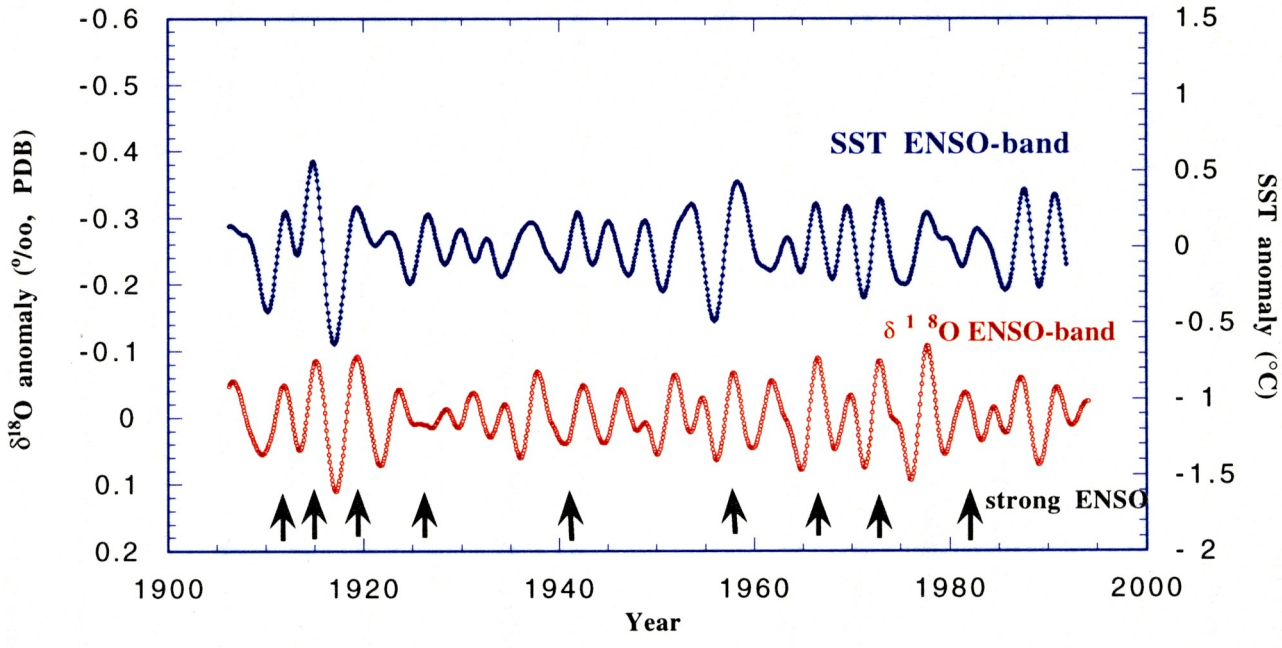

Fig. 7.5 Comparison of oxygen isotope-ENSO-band with ENSO historical instrumental records and SST-ENSO-band in the period 1906-1994

The six documented strong ENSO events recognized in the plot of $\delta^{18}O$ are also recorded as anomalies of more than 0.5°C on the plot of SST anomaly (corresponds with the variation of 0.05‰ to 0.1‰ in $\delta^{18}O$). Furthermore, the amplitudes of variability in both series vary with the same characteristic period; before 1920 and after 1950, both have stronger amplitudes than between these two periods, while after 1980, the amplitudes of both become weaker. It is also interesting to note that of the three strong documented ENSO events (1925-26, 1940-41 and 1982-83) which were not identified on the plot of $\delta^{18}O$, two are also not recognizable as SST anomalies. For the 1982-83 ENSO year, it has been indicated that the effect of the 1982-83 event was weak at Clipperton's geographic location and actually smaller than the intensity of the 1986-1987 event (Glynn et al., 1996). This is clearly shown in both the plots of interannual $\delta^{18}O$ and SST variations. This appears also to be the case with the 1940-41 event, which is not shown in either the $\delta^{18}O$ or SST record.

Therefore, comparisons with the historical records of ENSO events and SSTs suggest that the coral $\delta^{18}O$ record at Clipperton is generally sensitive to ENSO variability. Since this is the first near-century-length monthly coral record in this region of the open eastern Pacific, the good correlation between $\delta^{18}O$ and ENSO events may provide the basis for making use of long-term coral $\delta^{18}O$ data to compensate for the sparsely documented ENSO record in the east Pacific. Furthermore this result may also support the reliability of the instrumental OS-SST data. However, because Clipperton Atoll is located outside of the Niño3 region, although generally recorded in coral $\delta^{18}O$, ENSO events sometimes may have showed local features with only weak effects in the vicinity of Clipperton. Deser and Wallace (1987) suggested that there exist strong local controls on the climate of the eastern equatorial Pacific. Clipperton coral $\delta^{18}O$ appears to support this opinion. It is likely that at Clipperton the ENSO events were relatively strong before

1920 and between 1950-1980, while between 1920-1950 and after 1980, the ENSO events were relatively weak. The strongest ENSO events appears to have occurred in the periods of 1910-1920 and 1965-1980 while the weakest ENSOs in the periods of 1925-1935 and 1980-1985.

Comparison with other coral records

Comparison of different coral time series may provide the opportunity to examine in more detail the climatic coupling between eastern and western Pacific. The concept of El Niño and the Southern Oscillation as a coupled phenomenon has gained wide acceptance and it is suggested that the dominant mode of interannual climate variability is the SO which acts as the pacemaker of tropical Pacific SST variation via a direct link with the El Niño phenomenon (Rasmusson and Carpenter, 1982; Philander, 1990). However, Deser and Wallace (1987) indicated that the eastern and western Pacific ENSO components are more loosely coupled than previously implied. They observed that the major negative swings of the Southern Oscillation are not always accompanied by El Niño events. Tudhope et al. (1995) also indicated larger changes in the degree of coupling of the climate of the west Pacific with the Southern Oscillation. They further suggested that from the 1920s to 1950s the western equatorial Pacific was less important in modulating Pacific and global interannual climatic variability than it has appeared to be subsequently. In order to examine in more detail the coupling between eastern and western Pacific, the Clipperton $\delta^{18}O$-ENSO-band is first compared with the $\delta^{18}O$-ENSO-band of another record from Tarawa Atoll (Cole et al., 1993). Tarawa Atoll (1°N, 172°E) is located in the western Pacific (Fig. 7.6) and lies in the heart of the western Pacific warm pool and positive rainfall anomalies generated by the northeastward migration of the Indonesian Low during ENSO events (Cole et al., 1993) (Table 7.3a shows the SSA result for Tarawa Atoll using the same smoothing filter (removed frequencies ≤ 2 years) as for Clipperton Atoll). Fig. 7.7a is a comparison of the Clipperton

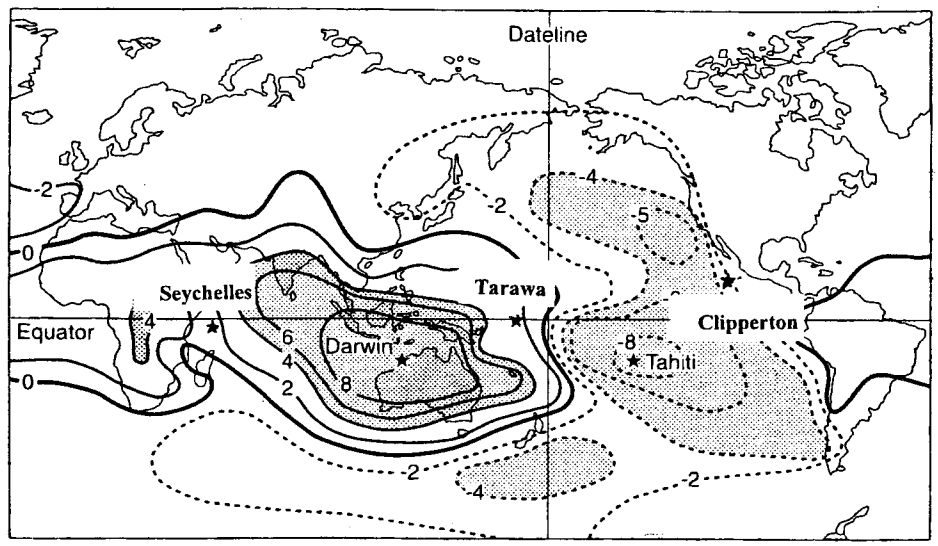

Fig. 7.6 Locations of Clipperton Atoll, Tarawa Atoll and the Seychelles Islands

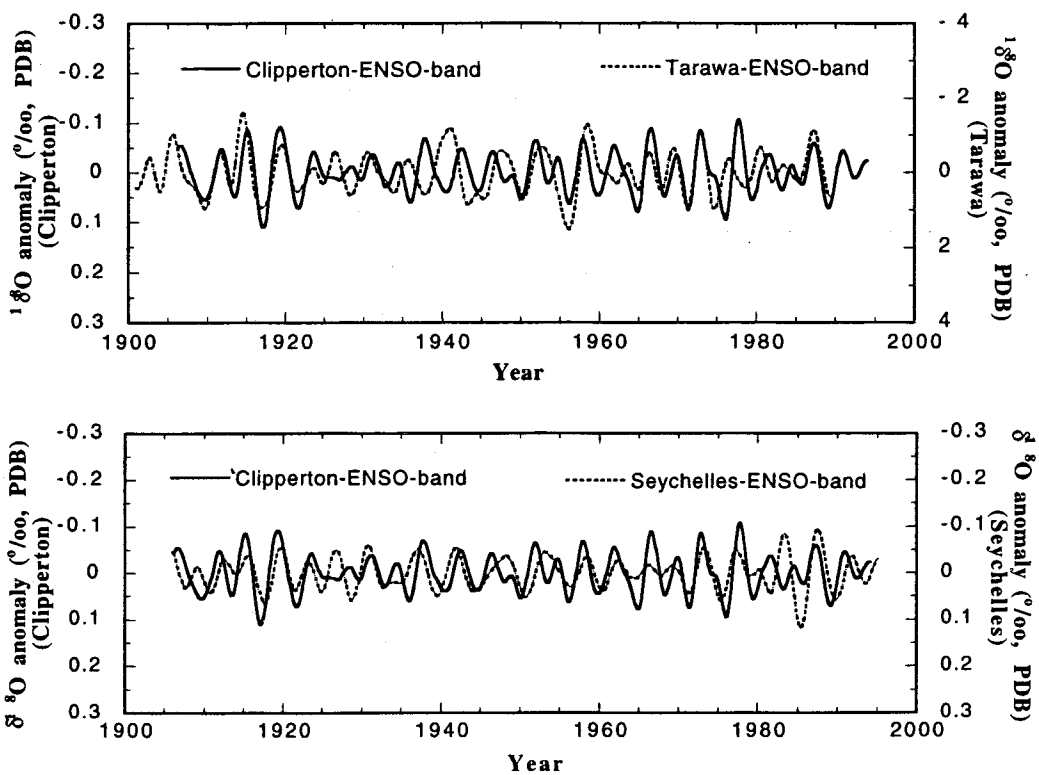

Fig.7.7 Comparisons of Clipperton-ENSO-band with Tarawa-ENSO-band and Seychelles-ENSO-band

interannual PCs and the Tarawa interannual PCs. The coupling of coral $\delta^{18}O$ between Clipperton Atoll and Tarawa Atoll can be examined in two aspects: (1) temporal pattern and (2) variability of amplitude. It can be seen from Fig. 7.7a that both series show the similar characteristic and generally coherent 3-6 year band. Both Clipperton and Tarawa have virtually identical temporal

Table 7.3a Singular Spectrum Analysis of filtered $\delta^{18}O$ data from Tarawa Atoll (1901-1989)

Eigenvector	Variance (%)	Cumulative Variance (%)	Period (Year)
1	34.27	34.27	infinity
2, 3, 4, 5	60.01	94.28	3-6
6, 7	4.63	98.91	~2

$\delta^{18}O$ (n=1062), M=72 months (data filtered at 2 years)

patterns before 1925 and after 1945. This implies that during most of the period the eastern and western Pacific displayed relatively good coupling characteristics. However in the period of 1925-1945 the correlation between the Tarawa $\delta^{18}O$ and the Clipperton $\delta^{18}O$ is relatively poor (see Fig. 7.7a), showing some out-of-phase characteristics. This agrees with Elliott and Angell (1988) and Tudhope et al. (1995). They observed a similar phenomenon that from about 1920 to 1950 the correlation between atmospheric pressures (SO indices) and SSTs was relatively low. Therefore, it suggests that the coupling between the western and eastern Pacific may indeed have been weak during this period. Comparison of the amplitudes of the two $\delta^{18}O$ series also shows that the major negative swings of the Southern Oscillation that occurred in 1940-41 in Tarawa (which shows strong $\delta^{18}O$ anomalies) are not reflected in pronounced anomalies in $\delta^{18}O$ in Clipperton (Fig. 7.7a). Conversely, the El Niño events of 1965-66 recorded in the Clipperton series have no counterpart anomalies in the Tarawa series, suggesting no strong corresponding rainfall anomalies in Tarawa. To summarize, it can be concluded that although ENSO events

have occurred continuously in the entire Pacific ocean during the 20th century, El Niño events and the Southern Oscillation may have been loosely coupled in some years. This may be due to strong local controls on the climate of the eastern equatorial Pacific that sometimes transcend the influence of the Southern Oscillation (Deser and Wallace, 1987; Elliott and Angell, 1988; Tudhope et al., 1995).

To obtain broader information on the teleconnection of ENSO, the Clipperton $\delta^{18}O$-ENSO-band is also compared with another $\delta^{18}O$-ENSO-band from a Seychelles coral (Charles et al., 1997). The Seychelles (5°S, 56°E) are located in the southwest Indian Ocean, an area also recognized as sensitive to ENSO forcing (see Fig. 7.6) (Table 7.3b shows the result for Seychelles islands using the same SSA method). The interannual PC series of the $\delta^{18}O$ record from the Seychelles is now plotted in the same diagram as that of the Clipperton $\delta^{18}O$ record (Fig. 7.7b). As can be clearly

Table 7.3b Singular Spectrum Analysis of filtered $\delta^{18}O$ data from Seychelles Islands (1906-1995)

Eigenvector	Variance (%)	Cumulative Variance (%)	Period (year)
1	58.03	58.03	125
2	14.92	72.95	12.7
3, 4	18.29	91.23	3-5
5, 6	5.3	96.53	~2

$\delta^{18}O$ (n=1070), M=72 months (data filtered at 2 years)

seen, the two series tend to oscillate in the same 3-5 year period and they have virtually an identical temporal pattern for the whole period 1906 to 1994. Even between 1920-50, broad regional connections are still markedly clear with no large mismatches as in the case between Clipperton and Tarawa. As the Seychelles Islands are located in the southwest Indian ocean, and are also characterized by anomalies in SST during ENSOs as at Clipperton, this consistency

implies that the zonal ENSO connection has persisted not only in the Pacific but also in the entire tropical Indian and Pacific oceans for at least 100 years and the relation between the tropical ocean SST and the ENSO may have been essentially constant. However, the corresponding amplitudes of variability of the two series are different. This difference may be due to the effects of the monsoon in the Seychelles Islands which are definitely absent in Clipperton (Charles et al., 1997).

In summary, the comparisons among the interannual PC-series from the above three separate areas suggest that the ENSO has occurred continuously for at least 100 years over the entire tropical ocean and that tropical surface oceanographic conditions have tended to oscillate in the similar characteristic 3-5,6 year period in each area. However, these results suggest that El Niño events and changes in the Southern Oscillation do not always accompany each other. The coral $\delta^{18}O$ record at Clipperton has provided an opportunity to obtain a better understanding of the local climatic controls in the eastern equatorial Pacific. As suggested by Deser and Wallace (1987), the understanding of local climatic changes in east Pacific would constitute an important step toward a full explanation of the ENSO phenomenon.

7.3.2 The long-term trend

The largest component of variance in the Clipperton $\delta^{18}O$ record is the long-term trend (Fig. 7.4b; Table 7.1a, b). As can be seen from Fig. 7.4b, the $\delta^{18}O$ values in C4B have decreased by about 0.28‰ over the whole record, which, if entirely temperature-related, implies that SSTs warmed by about 1.2°C. This range of $\delta^{18}O$ variation in Clipperton core C4B is approximately the same as observed in rough 2 cm sampling of Clipperton cores C6A and C2B (Linsley et al., unpublished data) during the same period (Fig. 7.8). This consistent range of $\delta^{18}O$ long-term

trend in three cores from Clipperton suggests that there has been little long-term drift of the biologically mediated $\delta^{18}O$ vital effect. However, although the pattern of this long-term trend in C4B is similar to that of the instrumental SST record, especially for the periods before 1915 and after 1935 (Fig. 7.9a), the magnitude of inferred warming is substantially larger than what was actually recorded. According to the SST record, SST has increased by only about 0.5°C in the total period. A similar effect was observed in the $\delta^{18}O$ data from the Seychelles Islands in southwestern equatorial Indian Ocean (Charles et al., 1997). These authors also inferred an identical structure but apparently larger inferred warming than the actual SST increase. Comparison of a long-term trend from the Clipperton $\delta^{18}O$ record with that of the Seychelles $\delta^{18}O$ record reveals a striking fit between them (Fig. 7.9b). Between 1906 and 1994 both the amplitude and the range of variability in the two trends are almost exactly the same (both varies from 0.14 to -0.14‰ and totally 0.28‰). This similarity of both long-term trends also suggests little long-term biological effects on coral $\delta^{18}O$. Furthermore, it also implies that besides the influence of SST, the variability in $\delta^{18}O$ might have been synchronously affected by some other common tropical climate factor over both the Indian and eastern Pacific Oceans. It is known that due to the CO_2 "greenhouse effect", increased evaporation and rainfall would lower the salinity and/or $\delta^{18}O$ of sea water and thus in turn lower $\delta^{18}O$ in coral over long periods of time. Since both Clipperton and Seychelles are in the atmospheric convergence zones, it is possible that the additional effects of higher SST and more rain (lower $\delta^{18}O_{water}$) have contributed to the long term trend observed here. However, currently there is no direct measurement of the variation of $\delta^{18}O_{water}$ from both areas to demonstrate this. Deciphering these changes requires additional sites and longer records.

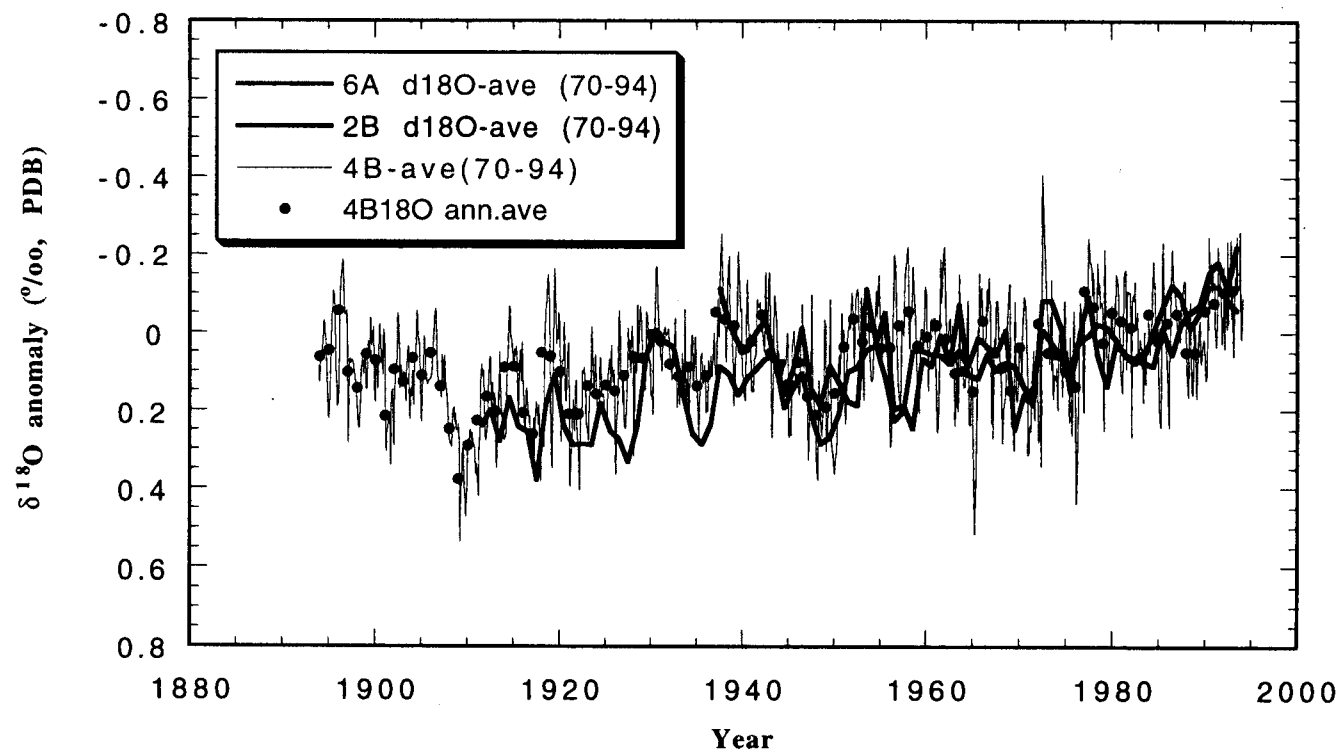

Fig. 7.8 Comparison of oxygen isotope long-term trend among 2B, 4B, and 6A

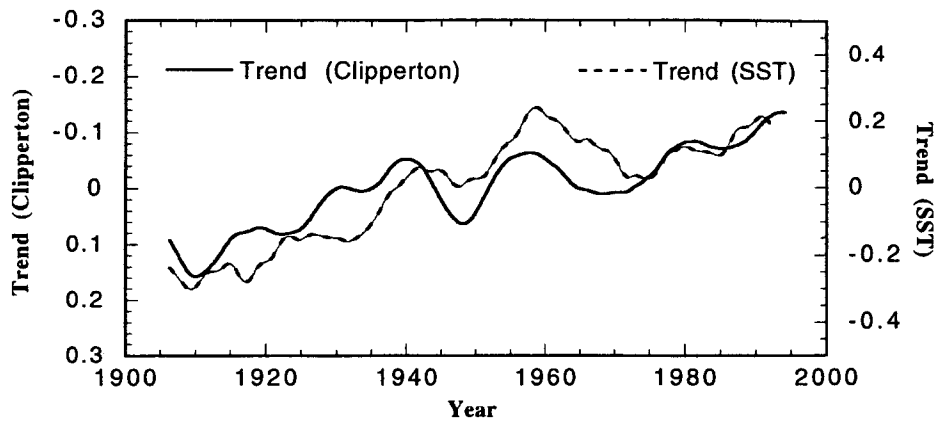

Fig. 7.9a Comparison of oxygen isotope long-term trend with SST long-term trend in Clipperton

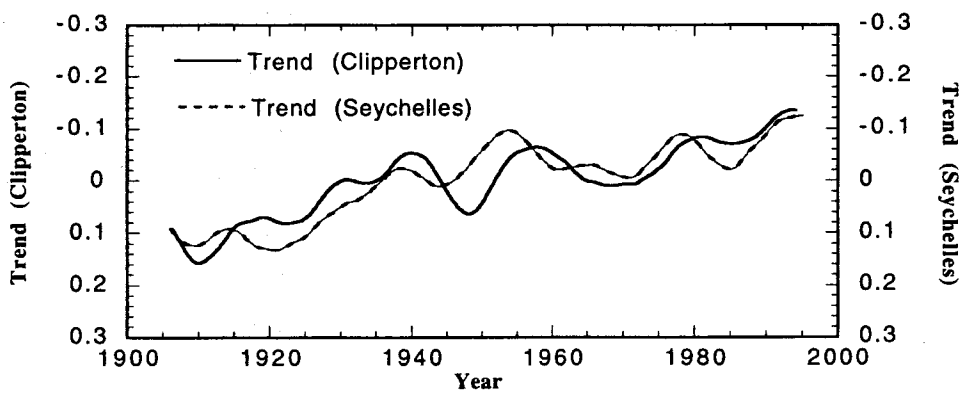

Fig.7.9b Comparison of oxygen isotope long-term trend in Clipperton Atoll with that in Seychelles islands

7.3.3 The interdecadal band

Decadal modes are common in long tropical Pacific climate records. However, the origin of these decadal shifts is still mostly unknown. Dunbar et al. (1994) suggested a possible long-term solar cycle-SST link operating at ENSO and decadal periodicity. However, due to the lack of correlation with sunspot number and modeled solar irradiance, Linsley et al. (1994) did not agree with a direct link between solar insulation variability and tropical climate. In order to evaluate the dominant coral 12.5-year component, an attempt was made to relate it to changes in solar irradiance related to the sunspot cycle. However, plots of sun spot number and modeled solar irradiance, and $\delta^{18}O$ interannual band do not correlate, shifting in-phase and out-of-phase over the length of the time series. Furthermore, this potential link lacks a widely accepted mechanism to translate changes in solar irradiance into climate effects.

Alternatively, quite a few authors have suggested a possible correlation between this interdecadal cycle and ENSO. As early as 1983, Barnett observed a interdecadal change in the atmospheric circulation over the tropical Pacific during 1937-1946 and 1977-1988, respectively. Cooper et al. (1989) and Trenberth (1990) suggested an interdecadal climate variability in ENSO, while Trenberth and Shea (1987) and Elliot and Angell (1988) postulated the long-term changes in the relative strength of the SO. Recently, Jacobs et al. (1994) demonstrated from independent modeling and observations that extremely long-lived El Niño events can last for decades. Zhang et al. (1997) also reported the similar spatial signatures in the global SST and wind stress between interannual and interdecadal components. For the $\delta^{18}O$ data from Clipperton, in fact, the frequency of the interdecadal $\delta^{18}O$ component is not constant over the total period (see Fig. 7.4b). It is also apparent that the periodicities of both 1910-23 and 1965-75 are approximately 5-7 years and thus they are mostly likely related to ENSO and it may be, as suggested by Barnett

(1983), that ENSO recurrence intervals may shift through time. Therefore, it is possible that ENSO at Clipperton may relate to the interdecadal climate patterns and teleconnections. And the climate variability in this area may be linked across time-scales from years to decades and this may reflect important reorganizations of the tropical ocean-atmosphere climate system (Trenberth and Shea, 1987; Jacobs et al., 1994).

7.4 Summary

The above analysis suggests that the Clipperton coral $\delta^{18}O$ record contains strong interannual cycles reflecting ENSO events as well as other interdecadal cycles and a long term trend. Comparison of the ENSO components with the historic records of ENSO and SST shows that the coral $\delta^{18}O$ records at Clipperton are generally sensitive to ENSO variability, although it also shows some local characteristics. Comparison with other coral isotopic records from other regions in Indian and Pacific Oceans further suggests that the ENSO has occurred persistently for at least 100 years over the entire tropical ocean and that ENSO has oscillated in the same characteristic 3- to 6-year frequency band. Although more annually resolved tropical climate records are needed to draw definite conclusions, the interdecadal cycle in the Clipperton coral $\delta^{18}O$ record suggests that it may have been related to the ENSO events while the long-term trend may in part reflect the global temperature rise as a result of the CO_2 "greenhouse effect".

CHAPTER 8 CONCLUSIONS

1. The effect of SST on coral skeletal $\delta^{18}O$ in the Clipperton region appears to have played a more important role than that of the precipitation, and SST may have been the main factor that influenced coral $\delta^{18}O$ compared with precipitation.

2. The relationship between $\delta^{13}C$ in corals and SST is more complicated. Although there appears to be some negative correlation between SST and $\delta^{13}C$, this relationship is not as apparent as with $\delta^{18}O$. The intensity of solar radiation also shows some negative correlation with $\delta^{13}C$, suggesting that radiation may not always result in enrichment in ^{13}C as is generally suggested.

3. The $\delta^{18}O$ record contains strong interannual cycles reflecting ENSO events as well as other interdecadal cycles and a long-term trend. Comparison of the ENSO components with the historic records of ENSO and SST shows that the coral $\delta^{18}O$ record at Clipperton is generally sensitive to ENSO variability, although it also shows some local characteristics. ENSO events appear to have been relatively strong before 1920 and between 1950-1980, while between 1920-1950, and after 1980, they were relatively weak.

4. Comparison with other coral isotopic records from the western Pacific and Indian Ocean further suggests that the ENSO has occurred persistently for at least 100 years over the entire tropical ocean and that ENSO has oscillated in the same characteristic 3- to 6-year frequency band for this time period. However, El Niño events and the Southern Oscillation do not appear to have been always synchronous with each other in the eastern Pacific and the Indian Oceans.

5. The pattern of the long-term trend of $\delta^{18}O$ is identical to that of the instrumental SST records but its magnitude is much larger than that of the SST. The interdecadal cycles in the $\delta^{18}O$ record may also have been related to the ENSO events while the long-term trend may in part reflect the global temperature rise as the result of the CO_2 "greenhouse effect". $\delta^{13}C$ also shows a similar long-term trend, and the comparison with an established model of variation of $\delta^{13}C$ in DIC suggests that it may reflect the variation of $\delta^{13}C$ in DIC over the entire period.

REFERENCES

Allison, N., Tudhope, A. W., and Fallick, A. E., **1996**, Factors influencing the stable carbon and oxygen isotopic composition of *Porites lutea* coral skeletons from Phuket, South Thailand. *Coral Reefs*, 15, 43-57

Barnes, D. J., **1970**, Coral skeletons: An explanation of their growth and structure. *Science*, 170, 1305-1308

Barnes, D. J., **1971**, A study of growth, structure and form in modern coral skeletons. unpublished *Ph.D.Thesis*, University of Newcastle upon Tyne, 180 pp

Barnes, D. J., and Chalker, B. E., **1990**, Calcification and photosynthesis in reef-building corals and algae. *In: Coral Reefs*. Dubinsky, Z, ed., Eldrvier Science publishing Company Inc.

Barnes, D. J., and Lough, J. M., **1992**, Systematic variations in the depth of skeleton occupied by coral tissue in massive colonies of *Porites* from the Great Barrier Reef. *Journal of Exp. Mar. Biol. Ecol.*, 159, 113-128

Barnes, D. J., Taylor, R. B., and Lough J. M., **1995**, On the inclusion of trace materials into massive coral skeletons. Part II: Distortions in skeletal records of annual climate cycles due to growth processes. *Journal of Exp. Mar. Biol. Ecol.*, 194, 251-275

Barnett, T. P., **1983**, Interaction of the monsoon and Pacific trade wind systems at interannual time scales. Part III, A partial anatomy of the Southern Oscillation, *Mon. Weather Rev.*, 112, 2388-2400

Barnett, T. P., **1991**, The interaction of multiple time scales in the tropical system. *J. Climate*, 4, 269-285

Bjerknes, J., **1966**, A possible response of the atmospheric Hedley circulation to equatorial anomalies of ocean temperature. *Tellus*, 18, 820-829

Bjerknes, J., **1972**, large-scale atmospheric response to the 1964-65 Pacific equatorial warming. *J. Phys. Oceanogr.*, 2, 212-217

Cane, M. A., Zebiak, S. E., and Dolan, S. C., **1986**, Experimental forecasts of El Niño. *Nature*, 321, 827-832

Charles, C. D., Hunter, D. E., and Fairbanks, R. G., **1997**, Interaction between the ENSO and the Asian Monsoon in a coral record of tropical climate. *Science*, 277, 925-928

Chatfield, C., **1995**, Problem solving: A statistician's guide (2nd ed.)

Cohen, A. L., and Hart, S. R., **1997**, The effect of colony topography on climatic signals in coral skeleton. *Geochim. Cosmochim. Acta*, 61, No. 18, 3905-3912

Cole, J. E., and Fairbanks, R. G., **1990**, The Southern Oscillation recorded in the $\delta^{18}O$ of corals from Tarawa Atoll. *Paleoceanography*, 5, 669-683

Cole, J. E., Fairbanks, R. G., and Shen, G. T., **1993**, Recent variability in the Southern Oscillation: Isotopic results from a Tarawa Atoll coral. *Science*, 260, 1790-1793

Cook, E. R., **1992**, Using tree rings to study past El Niño/Southern Oscillation influences on climate. *In* El Niño: Historical and paleoclimatic aspects of the Southern Oscillation, H.F. Diaz and V. Markgraf, eds., *Cambridge university Press*, New York, 202-214

Cooper, N. S., Whysall, K. D. B., and Bigg, G. R., **1989**, Recent decadal climate variations in the tropical Pacific. *International Journal of Climatology*, 9, 221-242

Craig, H., and Gordon, L. I., **1965**, Isotopic oceanography: Deuterium and oxygen 18 variations in the ocean and the marine atmosphere. *In* Marine Geochemistry, D. R. Schink and J. T. Corless, eds., *University of Rhode Island*, 227-374

Deser, C., and Wallace, J. M., **1987**, El Niño events and their relation to the Southern Oscillation: 1925-1986. *Journal of Geophysical Research*, 92, 19189-14196

Druffel, E. M., Dunbar, R. B., Wellington, G. M., and Minnis, S. A., **1990**, Reef-building corals and identification of ENSO warming episodes, *In* Global Ecological Consequences of the 1982-83 El Niño Southern Oscillation, P. Glynn, ed., *Elsevier Oceanogra. Ser.*, 52, 233-253

Dunbar, R. B., and Wellington, G.M., **1981**, Stable isotopes in a branching coral monitor seasonal temperature variation. *Nature*, 293, 453-455

Dunbar, R. B., Wellington, G. M., Colgan, M. W., and Glynn, P. W., **1994**, Eastern Pacific sea surface temperature since 1600 A.D.: the $\delta^{18}O$ record of climate variability in Galapagos corals. *Paleoceanography*, 9, No2, 291-315

Elliott, W. P., and Angell, J. K., **1988**, Evidence for changes in Southern Oscillation relationships during the last 100 years. *Journal of Climate*, 1, 729-737

Enfield., D. B., **1989**, El Niño, past and present. *Rev. Geophy.*, 27, 159-187

Epstein, S., Buchsbaum, R., Lowenstam, H. A., and Urey, H. C., **1953**, Revised carbonate-water isotopic temperature scale. *Bull. Geol. Soc. Amer.*, 64, 1315-1326

Erez, J., **1978**, Vital effect on stable-isotope composition seen in foraminifera and coral skeletons. *Nature*, 273, 199-202

Erez, J., and Honjo, S., **1981**, Comparison of isotopic composition of planktonic foraminifera in plankton tows, sediment traps, and sediments. *Paleogeo. Paleoclim. Paleoecol.*, 33, 129-156

Evans, M. N., Fairbanks, R. G., and Rubenstone, J. L., **in press**, A proxy index of climate teleconnections from the central equatorial Pacific. *Nature*

Fairbanks, R. G., and Dodge, R. E., **1979**, Annual periodicity of the $^{18}O/^{16}O$ and $^{13}C/^{12}C$ ratios in the coral *Montastrea annularis*. *Geochim. Cosmochim. Acta*, 43, 1009-1020

Fairbanks, R. G., Evans, M. N., Rubenstone, J. L., Mortlock, R. A., Broad, K., Moore, M. D., and Charles, C. D., **1997**, Evaluating climate indices and their geochemical proxies measured corals. *Coral Reefs*, 16, S93-S100

Falkowski, P.G., Jokiel, P. L., and Kinzie, R. A., **1990**, Irradiance and corals. In: Ecosystems of the world, Coral Reefs, *Elsevier Science Publishers,* Dubinsky ed.

Glantz, M. H., **1996**, Currents of change: El Niño's impact on climate and society. Cambridge, Cambridge University Press, 194 pp.

Glynn, P. W., and Wellington, G. M., **1983**, Corals and coral reefs of the Galapagos islands. Burkeley, *University of California Press*, 330 pp

Glynn, P. W., Veron, J. E., and Wellington, G. M., **1996**, Clipperton Atoll (eastern Pacific): Oceanography, geomorphology, reef-building coral ecology and biogeography. *Coral Reefs*, 15, 1-29

Godfrey, M. G., Roebuck, E. M., and Sherlock, A. J., **1986**, Revision statistics. Baltimore, Edward Arnold, 225 pp

Goreau, T. F., **1959**, The physiology of skeleton formation in corals. I. A method for measuring the rate of calcium deposition by corals under different conditions. *Biol. Bull.*, 116, 59-75

Goreau, T. F., **1961**, Problems of growth and calcium deposition in reef corals. *Endeavour*, 20, 32-39

Goreau, T. F., Goreau, N. I., and Goreau, T. J., **1979**, Corals and coral reefs. *Sci. Amer.*, 241(2), 124-136

Goreau, T. J., **1977**, Coral skeletal chemistry: physiological and environmental regulation of stable isotopes and trace metals in *Montastrea annularis*. *Proc. R. Soc. Lond.*, 196, 291-315

Grossman, E. L., **1982**, Stable isotopic fractionation in live benthic foraminifera from the Southern California borderland. *PhD. dissertation*, Univ. S. California

Grossman, E. L., and Ku, T.L., **1986**, Oxygen and carbon isotope fractionation in biogenic aragonite. *Chem. Geol.*, 59, 59-74

Gutknecht, J., Bisson, M. A., and Tosteson, F. C., **1977**, Diffusion of carbon dioxide through lipid bilayer membranes: Effects of carbonic anhydrase, bicarbonate, and unstirred layers. *J. Gen. Physiol.*, 69, 779-794

Hann, C. T., **1977**, Statistical methods in hydrology. *The Iowa State University Press*, Ames

Hayes, R. L., and Goreau, N. I., **1977**, Intracellular crystal-bearing vesicles in the epidermis of scleractinian corals *Astrangia danae* and *Porites porites*. *Biol. Bull.*, 152, 26-40

Isa, Y., Norikatsu, I., and Yamazato, K., **1980**, Evidence for the occurrence of Ca^{2+} dependent adenosine triphosphatase in a hermatypic coral *Acropora hebes (Dana)*. *Tech. Rep. Sesoko Mar. Sci. Lab. Ryukyu*, 7, 19-25

Isdale, P., **1984**, Fluorescent bands in massive corals record centuries of coastal rainfall. *Nature*, 310, 378-379

Jacobs, G.A., Hurlburt, H.E., Kindle, J.C., Metzger, E.J., Mitchell, J.L., Teague, W.J., and Wlaacraft, A.J., **1994**, Decade-scale trans-Pacific propagation and warming effects of an El Niño anomaly. *Nature*, 370, 360-363

Johnston, I. S., **1980**, The ultrastructure of skeletogenesis in hermatypic corals. *Int. Rev. Cytol.*, 67, 171-214

Kaplan, A., Cane, M., Kushnir, Y., Clement, A. C., Blumenthal, M.B., and Rajagopalan, B, **in press**, Analysis of global sea surface temperature. *J. Geophys. Res.*

Kingsley, R. J., and Watabe, N., **1985**, Ca-ATPase localization and inhibition in the gorgonian *Letptogorgia virgulata* (Lamarck) (Coelenterata: *Gorgonacea*). *J. Exp. Mar. Biol. Ecol.*, 93, 157-167

Land, L. S., Lang, J. C., and Barnes, D. J., **1975**, Extension rate: a primary control on the isotopic composition of West Indian (Jamaican) scleractinian reef coral skeletons. *Mar. Biol.*, 33, 221-233

Lelekin, V.A., and Zvalinsky, V. I., **1981**, Photosynthesis of coral zooxanthellae from different depths. *In*: E.D. Gomez, C.E. Birkeland, R.W. Buddemeier, R.E. Johannes, J.A. Marsh, Jr. and R.Y. Tsuda, eds., The reef and man: Proceedings of the fourth international coral reef symposium, Quezon City, Philippines, , 2, 33-37

Levitus, S., Burgett, R., Boyer, T.P., **1994**, World Ocean Atlas 1994, Volume 3: Salinity. NOAA Atlas NESDIS 3, 3. *U.S. Department of Commerse*, Washington D.C., 99 pp

Linsley, B. K., Dunbar, R. B., Wellington, G. M., and Mucciarone, D. A., **1994**, A coral-based reconstruction of intertropical convergence zone variability over Central America since 1707. *Journal of Geophysical Research*, 99, No. C5, 9977-9994

Linsley, B. K., Messier, R. G., and Dunbar, R. B., **in press**, Assessing between colony and intracolony oxygen isotope variability in the coral porites lobata at Clipperton Atoll. *Coral Reefs*

Lough, M. J., **1992**, An index of the Southern Oscillation reconstructed from western North American tree-ring chronologies. *In* El Niño: Historical and paleoclimatic aspects of the Southern Oscillation, H. F. Diaz, and V. Markgraf, eds., 215-226, *Cambridge University Press*, New York

McCarty, H. B., Peters, E. C., McMannus, J. W., and Pilson, M. Q., **1984**, When is a hermatype not a hermatype? *In*: Advances in Marine Science, Proceedings of a joint meeting of the Atlantic Reef Committee, Rosenstiel School of Marine and Atmospheric Science, Univ. of Miami, Miami, and the International Society for Reef Studies; Miami, Florida, 26-28 Oct. 1984, 78-79

McConnaughey, T. A., **1989a**, ^{13}C and ^{18}O isotopic disequilibria in biological carbonates: I, Patterns. *Geochim.Cosmochim. Acta*, 53, 151-162

McConnaughey, T. A., **1989b**, ^{13}C and ^{18}O isotopic disequilibrium in biological carbonates: II. *In vitro* simulation of kinetic isotope effects. *Geochimica et Cosmochimica Acta,* 53, 163-171

McConnaughey, T. A., Burdett, J., Whelan, J. F., and Paull, C. K., **1997**, Carbon isotopes in biological carbonates: Respiration and photosynthesis. *Geochimica et Cosmochimica Acta*, 61, No. 3, 611-622

Mitchell, T. P., and Wallace, J. M., **1990**, The annual cycle in equatorial convection and sea surface temperature. *J. Climate*, 5, 1140-1155

O'Neil, J. R., Clayton, R. N., and Mayeda, T. K., **1969**, Oxygen isotope fractionation in divalent metal carbonates. *J. Chem. Phys.*, 51, 5547-5558

Philander, S. G., **1990**, El Niño, La Niña, and the Southern Oscillation. *Academic Press*, San Diego, 293 pp.

Quay, P. D., Tibrook, B., and Wong, C. S., **1992**, Oceanic uptake of fossil fuel CO_2: Carbon-13 evidence. *Science*, 256, 74-79

Quinn, W. H., **1992**, A study of Southern Oscillation-related climatic activity for A.D. 622-1990 incorporating Nile River flood data, *In* El Niño: Historical and paleoclimatic aspects of the Southern Oscillation. H. F. Diaz, and V. Markgraf, eds., *Cambridge University Press*, New York, 119-150

Quinn, W. H., Neal, V.T., and Ahtunez de Mayolo, S.E., **1987**, El Niño occurrences over the past four and a half centuries. *J. Geophys. Res.*, 92, 449-461

Rasmusson, E.M., and Carpenter, T. H., **1982**, Variations in tropical sea surface temperature and surface wind fields associated with the Southern Oscillation/El Niño. *Mon.Wea.Rev.*, 110, 354-384

Rasmusson, E.M., Wang, X., and Ropelewski, C. F., **1990**, The biennial component of ENSO variability. *J. Mar. Syst.*, 1, 71-96

Reynolds, R. W., **1988**, A real-time global sea surface temperature analysis. *J. Climate*, 1, 75-86

Reynolds, R. W., and Smith, T. M., **1994**, Improved global sea surface temperature analyses. *J. Climate*, 7, 929-948. 1996 update accessed via Internet: http://www.ideo.columbia.edu/

Rubinson, M., and Clayton, R. N., **1969**, Carbon-13 fractionation between aragonite and calcite. *Geochim. Cosmochim. Acta*, 33, 689-692

Shackleton, N. J., **1965**, The high-precision isotopic analysis of oxygen and carbon in carbon dioxide. *J. Sci. Instrum.*, 42, 689-692

Shen, G. T., Campbell, T. M., and McConnaughey, T., **in press**, Precipitation of trace elements in reef corals: Influences of extension rate and species variability. *Geochimica et Cosmochimica Acta*

Simkiss, K., **1976**, Cellular aspects of calcification. In: N. Watabe and K.M. Wilbur (Editors), The Mechanisms of Mineralization in the Invertebrates and Plants. Columbia, *University of South Carolina Press,* 1-31

Skirrow, G., **1975**, The dissolved gases-carbon dioxide. *In*: Chemical Oceanography, 2, N. Watabe and K. M. Wilbur, eds., Academic Press, 1-31

Stephens, B. B., Keeling, R. F., Heimann, M., Six, K. D., Murnane, R., and Caldeira, K., **1998**, Testing global ocean carbon cycle models using measurements of atmospheric O_2 and CO_2 concentration. *Global Biogeochemical Cycles*, 12, No.2, 213-230

Spencer, R. W., **1993**, Global oceanic precipitation from the MSU during 1979-91 and comparisons to other climatologies. *J. Climate*, 6, 1301-1326

Swart, P. K., **1983**, Carbon and oxygen isotope fractionation in scleractinian corals: A review. *Earth Sci. Rev.*, 19, 51-80

Swart, P. K., Leder, J. J., Szmant, A. M., and Dodge, R. E., **1996**, The origin of variations in the isotopic record of scleractinian corals: II. Carbon. *Geochimica et Cosmochimica Acta*, 60, 2871-2885

Tarutani, T., Clayton, R., and Mayeda, T. K., **1969**, The effect of polymorphism and magnesium substitution on oxygen isotope fractionation between calcium carbonate and water. *Geochim. Cosmochim. Acta*, 33, 987-996

Thompson L. G., Mosley-Thompson, E., and Thompson, P. A., **1992**, Reconstructing interannual climate variability from tropical and subtropical ice-core records. *In* El Niño: Historical and paleoclimatic aspects of the Southern Oscillation. H. F. Diaz, and V. Markgraf, eds., *Cambridge University Press*, New York, 295-322

Trenberth, K. E., **1976**, Spatial and temporal variations in the Southern Oscillation. *Quart J. R. Meteorol. Soc.*, 102, 639-653

Trenberth, K. E., **1990**, Recent observed interdecadal climate changes in the Northern Hemisphere. *Bull. Am. Meteorol. Soc.*, 71, 988-0993

Trenberth, K. E., and Shea, D. J., **1987**, On the evolution of the Southern Oscillation. *Mon. Weather Rev.*, 115, 3078-3096

Troup, A. J., **1965**, The Southern Oscillation. *Quart. J. Roy. Meteor. Soc.*, 91, 490-506

Tudhope, A. W., Shimmield, G. B., Chilcott, C. P., Jebb, M., Fallick, A. E., and Dalgleish, A. N., **1995**, Recent changes in climate in the far western equatorial Pacific and their relationship to the Southern Oscillation; oxygen isotope records from massive corals, Papua New Guinea. *Earth and Planetary Science Letters*, 136, 575-590

Turner, J.V., **1982**, Kinetic fractionation of carbon-13 during calcium carbonate precipitation. *Geochim. Cosmochim. Acta*, 46, 1183-1191

Vautard, R., and Ghil, M., **1989**, Singular spectrum analysis in nonlinear dynamics, with applications to paleoclimatic time series. *Physica* D 35, 395-424

Vautard, R., Yiou, P., and Ghil, M., **1992**, Singular-spectrum analysis: a toolkit for short, noisy chaotic signals. *Physica* D 58, 95-126

Walsh, T. W., **1975**, The carbon and oxygen stable isotope ratios of the density bands recorded in reef coral skeletons. *unpublished M. S. thesis*, Univ. Hawaii, Honolulu

Weber, J. N., and Woodhead, P. M. J., **1970,** Carbon and oxygen isotope fractionation in the skeletal carbonate of reef-building corals. *Chem. Geol.*, 6, 93-117

Weber, J. N., and Woodhead, P. M. J., **1972**, Temperature dependence of oxygen-18 concentration in reef coral carbonates, *Journal of Geophysical research*, 77, 463-473

Weber, J. N., Deines, P., Weber, P. H., and Baker, P. A., **1976**, Depth-related changes in the $^{13}C/^{12}C$ ratio of skeletal carbonate deposited by the Caribbean reef-frame-building coral *Montastraea annularis*. *Geochim. Cosmochim. Acta*, 40, 31-39

Wellington, G. M., Dunbar, R. B., and Merlen G., **1996**, Calibration of stable isotope signatures in Galapagos corals. *Paleoceanography* 11, 467-480

Wells, J. W., **1969**, The formation of dissepiments in zooantharian corals. *In*: K.S.W. Campbell, ed., Stratigraphy and Paleontology, Canberra, Australian National University Press, 17-26

Winter, A., Goenaga, C., and Maul, G. A., **1991**, Carbon and oxygen isotope time series from an 18-year old Caribbean reef coral. *J. Geophys. Res.*, 96, 16673-16678

Zhang, Y., Wallace, J. M., and Battisti, D. S., **1997**, ENSO-like interdecadal variability: 1900-93. *J. Climate*, 10, 1004-1020

Appendix

$\delta^{18}O$ and $\delta^{13}C$ data from *Porites lobata* at Clipperton Atoll in the period 1906-1994

depth	Year A.D.	$\delta^{13}C$	$\delta^{18}O$		depth	Year A.D.	$\delta^{13}C$	$\delta^{18}O$
1	1994.19	-3.67	-5.75		48	1992.35	-3.13	-5.80
2	1994.19	-3.33	-5.69		49	1992.32	-3.16	-5.76
3	1994.18	-3.23	-5.69		50	1992.29	-3.12	-5.67
4	1994.14	-3.33	-5.78		51	1992.27	-3.10	-5.78
5	1994.09	-3.44	-5.69		52	1992.24	-3.22	-5.61
6	1994.04	-3.45	-5.61		53	1992.21	-3.00	-5.62
7	1993.99	-3.40	-5.69		54	1992.18	-2.90	-5.59
8	1993.95	-3.34	-5.68		55	1992.12	-2.65	-5.83
9	1993.90	-3.47	-5.99		56	1992.05	-2.73	-5.73
10	1993.85	-3.64	-5.88		57	1991.98	-3.20	-5.61
11	1993.80	-3.46	-5.81		58	1991.92	-3.10	-5.62
12	1993.75	-3.39	-5.74		59	1991.85	-3.45	-5.69
13	1993.71	-3.17	-5.75		60	1991.78	-3.44	-5.77
14	1993.66	-3.32	-5.78		61	1991.72	-3.46	-5.75
15	1993.61	-3.38	-5.75		62	1991.65	-3.38	-5.80
16	1993.56	-3.48	-5.74		63	1991.58	-3.33	-5.85
17	1993.52	-3.60	-5.94		64	1991.52	-3.53	-5.87
18	1993.49	-3.48	-5.88		65	1991.50	-3.35	-5.81
19	1993.46	-3.32	-5.77		66	1991.48	-2.89	-5.82
20	1993.43	-3.31	-5.76		67	1991.46	-2.94	-5.74
21	1993.40	-3.56	-5.73		68	1991.45	-3.13	-5.69
22	1993.37	-3.58	-5.79		69	1991.43	-3.36	-5.75
23	1993.33	-3.33	-5.79		70	1991.41	-4.28	-5.77
24	1993.30	-3.19	-5.79		71	1991.39	-3.00	-5.63
25	1993.27	-3.45	-5.76		72	1991.37	-2.80	-5.61
26	1993.24	-3.22	-5.66		73	1991.36	-3.02	-5.64
27	1993.21	-3.20	-5.63		74	1991.34	-2.87	-5.67
28	1993.18	-3.25	-5.56		75	1991.32	-2.99	-5.52
29	1993.14	-3.39	-5.63		76	1991.30	-2.98	-5.62
30	1993.09	-3.25	-5.64		77	1991.28	-3.23	-5.64
31	1993.04	-2.81	-5.75		78	1991.27	-3.30	-5.54
32	1992.99	-2.94	-5.76		79	1991.21	-3.05	-5.64
33	1992.95	-3.14	-5.68		80	1991.16	-2.75	-5.72
34	1992.90	-3.18	-5.71		81	1991.11	-2.92	-5.78
35	1992.85	-3.66	-5.94		82	1991.05	-3.04	-5.84
36	1992.80	-3.66	-5.78		83	1991.00	-3.16	-5.67
37	1992.75	-3.41	-5.84		84	1990.95	-3.19	-5.83
38	1992.71	-3.52	-5.84		85	1990.89	-3.73	-5.74
39	1992.66	-3.42	-5.75		86	1990.84	-3.65	-5.76
40	1992.61	-3.59	-5.67		87	1990.78	-3.26	-5.82
41	1992.56	-3.63	-5.82		88	1990.73	-3.09	-5.89
42	1992.52	-3.62	-5.90		89	1990.68	-3.18	-5.72
43	1992.49	-3.40	-5.77		90	1990.62	-2.92	-5.79
44	1992.46	-3.59	-5.71		91	1990.57	-3.28	-5.74
45	1992.43	-3.72	-5.61		92	1990.52	-3.72	-5.94
46	1992.41	-3.85	-5.66		93	1990.49	-3.73	-5.69
47	1992.38	-3.57	-5.69		94	1990.47	-3.38	-5.71

95	1990.45	-3.24	-5.65		207.5	1985.97	-3.33	-5.57
96	1990.42	-3.36	-5.65		210	1985.90	-3.45	-5.62
97	1990.40	-3.00	-5.67		212.5	1985.82	-3.65	-5.73
98	1990.37	-3.01	-5.65		215	1985.75	-3.62	-5.73
99	1990.35	-2.97	-5.73		217.5	1985.67	-3.63	-5.60
100	1990.33	-3.03	-5.77		220	1985.60	-3.72	-5.93
102.5	1990.27	-3.21	-5.48		222.5	1985.49	-3.51	-5.79
105	1990.12	-3.42	-5.57		225	1985.38	-3.25	-5.51
107.5	1989.97	-3.46	-5.63		227.5	1985.27	-3.44	-5.39
110	1989.82	-3.31	-5.59		230	1985.16	-3.53	-5.45
112.5	1989.67	-3.19	-5.56		232.5	1985.05	-3.14	-5.59
115	1989.52	-3.49	-5.69		235	1984.95	-3.61	-5.68
117.5	1989.45	-3.26	-5.63		237.5	1984.84	-3.46	-5.58
120	1989.39	-3.30	-5.65		240	1984.73	-3.47	-5.78
122.5	1989.33	-2.91	-5.49		242.5	1984.62	-3.42	-5.76
125	1989.27	-2.58	-5.59		245	1984.52	-3.38	-5.84
127.5	1989.17	-3.26	-5.44		247.5	1984.41	-3.15	-5.68
130	1989.08	-3.41	-5.61		250	1984.29	-3.37	-5.67
132.5	1988.99	-3.71	-5.72		252.5	1984.18	-3.19	-5.58
135	1988.89	-3.37	-5.61		255	1984.05	-3.17	-5.69
137.5	1988.80	-3.50	-5.49		257.5	1983.92	-3.31	-5.62
140	1988.70	-3.22	-5.47		260	1983.78	-3.54	-5.59
142.5	1988.61	-3.45	-5.57		262.5	1983.65	-3.07	-5.47
145	1988.52	-3.49	-5.74		265	1983.52	-3.39	-5.66
147.5	1988.39	-3.05	-5.66		267.5	1983.45	-3.40	-5.43
150	1988.27	-2.68	-5.46		270	1983.39	-3.37	-5.66
152.5	1988.12	-2.31	-5.60		272.5	1983.33	-3.18	-5.55
155	1987.97	-2.61	-5.76		275	1983.27	-3.09	-5.55
157.5	1987.82	-2.95	-5.79		277.5	1983.14	-3.30	-5.64
160	1987.67	-2.94	-5.69		280	1983.02	-3.19	-5.59
162.5	1987.52	-3.01	-5.74		282.5	1982.89	-3.06	-5.55
165	1987.41	-3.10	-5.57		285	1982.77	-2.79	-5.71
167.5	1987.29	-3.33	-5.70		287.5	1982.64	-3.28	-5.61
170	1987.18	-3.11	-5.61		290	1982.52	-3.12	-5.79
172.5	1987.02	-3.21	-5.67		292.5	1982.43	-3.29	-5.71
175	1986.85	-3.36	-5.77		295	1982.35	-3.44	-5.75
177.5	1986.68	-3.73	-5.77		297.5	1982.27	-3.32	-5.73
180	1986.52	-3.64	-5.87		300	1982.18	-2.40	-5.32
182.5	1986.48	-3.39	-5.77		302.5	1982.09	-2.86	-5.76
185	1986.45	-3.48	-5.74		305	1981.99	-3.17	-5.74
187.5	1986.41	-3.30	-5.69		307.5	1981.90	-3.12	-5.75
190	1986.37	-3.38	-5.61		310	1981.80	-3.47	-5.75
192.5	1986.34	-3.35	-5.58		312.5	1981.71	-3.38	-5.77
195	1986.30	-3.28	-5.57		315	1981.61	-2.94	-5.55
197.5	1986.27	-2.79	-5.61		317.5	1981.52	-3.16	-5.84
200	1986.19	-3.00	-5.39		320	1981.43	-3.38	-5.79
202.5	1986.12	-3.03	-5.44		322.5	1981.35	-3.27	-5.78
205	1986.04	-3.55	-5.57		325	1981.27	-2.69	-5.63

327.5	1981.18	-2.84	-5.47		447.5	1976.60	-3.18	-5.73
330	1981.02	-2.78	-5.55		450	1976.50	-3.10	-5.67
332.5	1980.85	-2.85	-5.66		452.5	1976.39	-2.88	-5.39
335	1980.68	-3.07	-5.77		455	1976.29	-2.83	-5.27
337.5	1980.52	-3.47	-5.80		457.5	1976.18	-2.62	-5.20
340	1980.47	-2.95	-5.76		460	1976.05	-2.84	-5.47
342.5	1980.43	-3.02	-5.69		462.5	1975.92	-3.02	-5.76
345	1980.39	-3.24	-5.72		465	1975.78	-3.12	-5.45
347.5	1980.35	-3.33	-5.72		467.5	1975.65	-2.63	-5.35
350	1980.31	-3.03	-5.60		470	1975.52	-2.69	-5.66
352.5	1980.27	-2.52	-5.63		472.5	1975.43	-2.71	-5.37
355	1980.14	-2.66	-5.63		475	1975.35	-2.91	-5.58
357.5	1980.02	-2.90	-5.72		477.5	1975.27	-2.85	-5.58
360	1979.89	-2.68	-5.64		480	1975.18	-2.34	-5.60
362.5	1979.77	-3.02	-5.66		482.5	1975.09	-2.66	-5.51
365	1979.64	-2.94	-5.51		485	1974.99	-3.03	-5.69
367.5	1979.52	-3.31	-5.54		487.5	1974.90	-3.06	-5.76
370	1979.46	-3.06	-5.61		490	1974.80	-3.16	-5.66
372.5	1979.41	-2.97	-5.61		492.5	1974.71	-3.06	-5.46
375	1979.35	-2.91	-5.67		495	1974.61	-2.75	-5.62
377.5	1979.29	-2.86	-5.99		497.5	1974.52	-3.30	-5.58
380	1979.24	-2.70	-5.54		500	1974.45	-3.03	-5.54
382.5	1979.18	-2.70	-5.35		502.5	1974.38	-2.76	-5.65
385	1979.09	-2.80	-5.69		505	1974.32	-2.56	-5.71
387.5	1978.99	-2.97	-5.70		507.5	1974.25	-2.94	-5.54
390	1978.90	-2.94	-5.75		510	1974.18	-2.81	-5.43
392.5	1978.80	-3.03	-5.69		512.5	1974.05	-3.10	-5.56
395	1978.71	-3.01	-5.77		515	1973.92	-3.15	-5.51
397.5	1978.61	-3.31	-5.74		517.5	1973.78	-3.16	-5.54
400	1978.52	-3.47	-5.84		520	1973.65	-2.90	-5.44
402.5	1978.35	-2.84	-5.58		522.5	1973.52	-3.12	-5.81
405	1978.18	-2.51	-5.59		525	1973.45	-2.87	-5.51
407.5	1978.07	-2.76	-5.85		527.5	1973.39	-2.99	-5.78
410	1977.96	-2.92	-5.73		530	1973.33	-2.70	-5.59
412.5	1977.85	-2.86	-5.81		532.5	1973.27	-2.72	-5.56
415	1977.74	-3.17	-5.83		535	1973.12	-2.59	-5.63
417.5	1977.63	-3.15	-5.83		537.5	1972.97	-2.96	-5.73
420	1977.52	-2.91	-5.90		540	1972.82	-3.24	-5.83
422.5	1977.45	-2.84	-5.77		542.5	1972.67	-2.84	-5.90
425	1977.38	-3.05	-5.73		545	1972.52	-3.09	-6.06
427.5	1977.32	-2.51	-5.68		547.5	1972.45	-3.02	-5.69
430	1977.25	-2.53	-5.79		550	1972.38	-2.83	-5.18
432.5	1977.18	-2.41	-5.70		552.5	1972.32	-3.18	-5.56
435	1977.09	-2.77	-5.75		555	1972.25	-2.61	-5.60
437.5	1976.99	-2.43	-5.23		557.5	1972.18	-2.45	-5.33
440	1976.89	-3.23	-5.73		560	1972.07	-2.36	-5.38
442.5	1976.79	-2.88	-5.61		562.5	1971.96	-2.54	-5.56
445	1976.70	-2.93	-5.68		565	1971.85	-2.75	-5.62

567.5	1971.74	-2.71	-5.42		687.5	1966.68	-2.52	-5.80
570	1971.63	-2.63	-5.42		690	1966.60	-2.79	-5.68
572.5	1971.52	-2.91	-5.62		692.5	1966.52	-2.99	-5.77
575	1971.45	-2.85	-5.53		695	1966.35	-2.49	-5.59
577.5	1971.39	-2.82	-5.69		697.5	1966.18	-2.27	-5.62
580	1971.33	-2.47	-5.32		700	1966.09	-2.47	-5.63
582.5	1971.27	-2.41	-5.41		702.5	1965.99	-2.63	-5.69
585	1971.12	-2.42	-5.40		705	1965.90	-2.82	-5.83
587.5	1970.97	-2.78	-5.28		707.5	1965.80	-2.67	-5.64
590	1970.82	-2.94	-5.62		710	1965.71	-2.66	-5.82
592.5	1970.67	-3.30	-5.72		712.5	1965.61	-2.85	-5.61
595	1970.52	-2.95	-5.74		715	1965.52	-2.86	-5.67
597.5	1970.45	-2.92	-5.68		717.5	1965.41	-2.54	-5.30
600	1970.39	-3.09	-5.73		720	1965.29	-2.09	-5.23
602.5	1970.33	-2.74	-5.57		722.5	1965.18	-2.14	-5.12
605	1970.27	-2.54	-5.52		725	1965.07	-2.77	-5.27
607.5	1970.08	-2.74	-5.62		727.5	1964.96	-2.72	-5.55
610	1969.89	-2.60	-5.50		730	1964.85	-2.84	-5.56
612.5	1969.70	-2.71	-5.45		732.5	1964.74	-2.59	-5.44
615	1969.52	-2.77	-5.74		735	1964.63	-2.65	-5.36
617.5	1969.46	-2.70	-5.31		737.5	1964.52	-3.19	-5.73
620	1969.41	-2.60	-5.42		740	1964.41	-2.65	-5.73
622.5	1969.35	-2.77	-5.35		742.5	1964.29	-2.43	-5.55
625	1969.29	-3.00	-5.47		745	1964.18	-2.40	-5.52
627.5	1969.24	-2.77	-5.60		747.5	1964.05	-2.75	-5.49
630	1969.18	-2.46	-5.35		750	1963.92	-2.70	-5.56
632.5	1969.07	-2.60	-5.50		752.5	1963.78	-2.93	-5.53
635	1968.96	-2.86	-5.77		755	1963.65	-2.54	-5.55
637.5	1968.85	-2.66	-5.75		757.5	1963.52	-2.30	-5.82
640	1968.74	-2.75	-5.66		760	1963.41	-2.31	-5.33
642.5	1968.63	-2.61	-5.65		762.5	1963.29	-2.40	-5.62
645	1968.52	-2.89	-5.49		765	1963.18	-2.08	-5.46
647.5	1968.41	-2.21	-5.47		767.5	1963.10	-2.17	-5.46
650	1968.29	-2.12	-5.43		770	1963.02	-2.37	-5.40
652.5	1968.18	-2.28	-5.35		772.5	1962.93	-2.39	-5.57
655	1968.05	-2.55	-5.50		775	1962.85	-2.31	-5.61
657.5	1967.92	-2.59	-5.59		777.5	1962.77	-2.74	-5.68
660	1967.78	-2.73	-5.62		780	1962.68	-2.48	-5.56
662.5	1967.65	-2.81	-5.73		782.5	1962.60	-2.56	-5.57
665	1967.52	-2.70	-5.72		785	1962.52	-2.75	-5.70
667.5	1967.41	-2.72	-5.56		787.5	1962.35	-2.56	-5.64
670	1967.29	-2.50	-5.68		790	1962.18	-2.30	-5.59
672.5	1967.18	-2.23	-5.34		792.5	1962.09	-2.48	-5.63
675	1967.10	-2.29	-5.61		795	1961.99	-2.97	-5.87
677.5	1967.02	-2.57	-5.38		797.5	1961.90	-3.09	-5.86
680	1966.93	-2.37	-5.63		800	1961.80	-2.76	-5.85
682.5	1966.85	-2.57	-5.74		802.5	1961.71	-3.10	-5.81
685	1966.77	-2.68	-5.73		805	1961.61	-3.07	-5.72

807.5	1961.52	-3.00	-5.85		927.5	1956.07	-2.25	-5.38
810	1961.41	-2.65	-5.63		930	1955.96	-2.34	-5.48
812.5	1961.29	-2.49	-5.45		932.5	1955.85	-2.95	-5.50
815	1961.18	-2.52	-5.38		935	1955.74	-2.39	-5.61
817.5	1961.07	-2.64	-5.48		937.5	1955.63	-2.53	-5.59
820	1960.96	-2.70	-5.59		940	1955.52	-2.54	-5.71
822.5	1960.85	-2.82	-5.69		942.5	1955.43	-2.61	-5.62
825	1960.74	-2.91	-5.68		945	1955.35	-2.12	-5.66
827.5	1960.63	-2.76	-5.64		947.5	1955.27	-2.28	-5.65
830	1960.52	-3.01	-5.69		950	1955.18	-2.59	-5.52
832.5	1960.41	-2.84	-5.66		952.5	1955.07	-2.50	-5.71
835	1960.29	-2.56	-5.59		955	1954.96	-2.48	-5.65
837.5	1960.18	-2.21	-5.48		957.5	1954.85	-2.63	-5.81
840	1960.09	-2.30	-5.64		960	1954.74	-2.62	-5.74
842.5	1959.99	-2.61	-5.68		962.5	1954.63	-2.97	-5.67
845	1959.90	-2.72	-5.80		965	1954.52	-3.00	-5.76
847.5	1959.80	-2.45	-5.70		967.5	1954.41	-2.46	-5.62
850	1959.71	-2.45	-5.64		970	1954.29	-2.16	-5.67
852.5	1959.61	-2.69	-5.60		972.5	1954.18	-2.33	-5.52
855	1959.52	-3.07	-5.66		975	1954.05	-2.59	-5.52
857.5	1959.35	-2.45	-5.64		977.5	1953.92	-2.79	-5.56
860	1959.18	-2.29	-5.42		980	1953.78	-2.92	-5.62
862.5	1958.96	-2.44	-5.55		982.5	1953.65	-2.86	-5.74
865	1958.74	-2.65	-5.72		985	1953.52	-2.74	-5.74
867.5	1958.52	-2.57	-5.82		987.5	1953.41	-2.68	-5.62
870	1958.41	-2.45	-5.69		990	1953.29	-2.55	-5.62
872.5	1958.29	-2.33	-5.69		992.5	1953.18	-2.07	-5.45
875	1958.18	-2.47	-5.59		995	1953.10	-2.07	-5.58
877.5	1958.09	-2.49	-5.69		997.5	1953.02	-2.07	-5.60
880	1957.99	-2.34	-5.90		1000	1952.93	-2.35	-5.76
882.5	1957.90	-2.69	-5.83		1002.5	1952.85	-2.44	-5.72
885	1957.80	-3.04	-5.81		1005	1952.77	-2.43	-5.57
887.5	1957.71	-2.73	-5.81		1007.5	1952.68	-2.63	-5.66
890	1957.61	-2.55	-5.73		1010	1952.60	-2.74	-5.73
892.5	1957.52	-2.80	-5.62		1012.5	1952.52	-2.73	-5.76
895	1957.35	-2.60	-5.68		1015	1952.41	-3.02	-5.75
897.5	1957.18	-2.29	-5.43		1017.5	1952.29	-2.37	-5.71
900	1957.05	-2.44	-5.48		1020	1952.18	-1.98	-5.53
902.5	1956.92	-2.16	-5.53		1022.5	1952.07	-1.88	-5.63
905	1956.78	-2.37	-5.62		1025	1951.96	-2.18	-5.75
907.5	1956.65	-2.62	-5.80		1027.5	1951.85	-2.32	-5.71
910	1956.52	-2.62	-5.85		1030	1951.74	-2.63	-5.64
912.5	1956.46	-2.93	-5.75		1032.5	1951.63	-2.72	-5.67
915	1956.41	-2.80	-5.69		1035	1951.52	-2.82	-5.65
917.5	1956.35	-2.81	-5.69		1037.5	1951.41	-2.31	-5.60
920	1956.29	-2.14	-5.52		1040	1951.29	-1.94	-5.46
922.5	1956.24	-2.35	-5.71		1042.5	1951.18	-2.12	-5.40
925	1956.18	-2.21	-5.31		1045	1951.09	-1.86	-5.54

1047.5	1950.99	-2.07	-5.72		1167.5	1945.74	-2.48	-5.50
1050	1950.90	-2.70	-5.53		1170	1945.63	-2.62	-5.66
1052.5	1950.80	-2.42	-5.74		1172.5	1945.52	-2.73	-5.62
1055	1950.71	-2.51	-5.56		1175	1945.43	-2.61	-5.62
1057.5	1950.61	-2.52	-5.53		1177.5	1945.35	-2.59	-5.58
1060	1950.52	-2.44	-5.60		1180	1945.27	-2.14	-5.35
1062.5	1950.41	-2.10	-5.54		1182.5	1945.18	-2.08	-5.44
1065	1950.29	-2.15	-5.33		1185	1945.05	-2.20	-5.32
1067.5	1950.18	-1.96	-5.33		1187.5	1944.92	-2.29	-5.69
1070	1950.02	-2.11	-5.28		1190	1944.78	-2.30	-5.58
1072.5	1949.85	-2.06	-5.33		1192.5	1944.65	-2.27	-5.55
1075	1949.68	-2.19	-5.37		1195	1944.52	-2.57	-5.58
1077.5	1949.52	-2.32	-5.76		1197.5	1944.43	-2.44	-5.55
1080	1949.43	-2.62	-5.51		1200	1944.35	-2.61	-5.53
1082.5	1949.35	-2.54	-5.50		1202.5	1944.27	-1.97	-5.56
1085	1949.27	-2.22	-5.36		1205	1944.18	-2.03	-5.54
1087.5	1949.18	-1.92	-5.40		1207.5	1944.07	-2.35	-5.50
1090	1949.09	-2.08	-5.32		1210	1943.96	-2.29	-5.61
1092.5	1948.99	-2.24	-5.86		1212.5	1943.85	-2.23	-5.53
1095	1948.90	-2.22	-5.50		1215	1943.74	-2.50	-5.66
1097.5	1948.80	-2.67	-5.45		1217.5	1943.63	-2.55	-5.69
1100	1948.71	-2.57	-5.43		1220	1943.52	-3.04	-5.75
1102.5	1948.61	-2.28	-5.38		1222.5	1943.43	-2.67	-5.70
1105	1948.52	-2.69	-5.42		1225	1943.35	-2.26	-5.47
1107.5	1948.41	-2.56	-5.46		1227.5	1943.27	-2.00	-5.44
1110	1948.29	-2.02	-5.57		1230	1943.18	-2.08	-5.36
1112.5	1948.18	-1.68	-5.23		1232.5	1943.09	-2.34	-5.55
1115	1948.05	-1.92	-5.34		1235	1942.99	-2.66	-5.80
1117.5	1947.92	-2.62	-5.42		1237.5	1942.90	-2.80	-5.80
1120	1947.78	-2.55	-5.45		1240	1942.80	-2.52	-5.74
1122.5	1947.65	-2.30	-5.52		1242.5	1942.71	-2.24	-5.62
1125	1947.52	-2.84	-5.76		1245	1942.61	-2.65	-5.71
1127.5	1947.43	-2.82	-5.48		1247.5	1942.52	-2.86	-5.81
1130	1947.35	-2.56	-5.56		1250	1942.35	-2.37	-5.58
1132.5	1947.27	-2.31	-5.37		1252.5	1942.18	-1.86	-5.66
1135	1947.18	-2.08	-5.31		1255	1942.07	-2.12	-5.64
1137.5	1947.05	-2.10	-5.47		1257.5	1941.96	-2.41	-5.66
1140	1946.92	-2.25	-5.55		1260	1941.85	-2.51	-5.73
1142.5	1946.78	-2.43	-5.60		1262.5	1941.74	-2.52	-5.70
1145	1946.65	-2.46	-5.53		1265	1941.63	-2.54	-5.73
1147.5	1946.52	-2.54	-5.73		1267.5	1941.52	-2.58	-5.70
1150	1946.43	-2.58	-5.61		1270	1941.45	-2.35	-5.59
1152.5	1946.35	-2.58	-5.64		1272.5	1941.38	-2.13	-5.50
1155	1946.27	-2.41	-5.49		1275	1941.32	-2.28	-5.74
1157.5	1946.18	-1.96	-5.48		1277.5	1941.25	-2.04	-5.45
1160	1946.07	-1.95	-5.49		1280	1941.18	-1.87	-5.50
1162.5	1945.96	-2.29	-5.54		1282.5	1941.02	-2.34	-5.49
1165	1945.85	-2.05	-5.52		1285	1940.85	-2.40	-5.65

1287.5	1940.68	-2.62	-5.62		1407.5	1935.61	-2.50	-5.52
1290	1940.52	-2.87	-5.79		1410	1935.52	-2.54	-5.60
1292.5	1940.41	-2.57	-5.66		1412.5	1935.43	-2.57	-5.58
1295	1940.29	-1.96	-5.46		1415	1935.35	-2.31	-5.47
1297.5	1940.18	-1.83	-5.50		1417.5	1935.27	-2.06	-5.48
1300	1940.07	-2.46	-5.51		1420	1935.18	-1.84	-5.35
1302.5	1939.96	-2.14	-5.55		1422.5	1935.07	-2.16	-5.49
1305	1939.85	-2.26	-5.72		1425	1934.96	-2.51	-5.52
1307.5	1939.74	-2.55	-5.69		1427.5	1934.85	-2.62	-5.65
1310	1939.63	-2.40	-5.79		1430	1934.74	-2.75	-5.61
1312.5	1939.52	-2.77	-5.86		1432.5	1934.63	-2.51	-5.49
1315	1939.35	-2.32	-5.67		1435	1934.52	-2.73	-5.65
1317.5	1939.18	-1.94	-5.49		1437.5	1934.41	-2.57	-5.63
1320	1939.10	-2.11	-5.57		1440	1934.29	-2.20	-5.53
1322.5	1939.02	-2.40	-5.44		1442.5	1934.18	-1.99	-5.42
1325	1938.93	-2.24	-5.58		1445	1934.09	-2.50	-5.47
1327.5	1938.85	-2.64	-5.66		1447.5	1933.99	-2.44	-5.59
1330	1938.77	-2.48	-5.66		1450	1933.90	-2.39	-5.42
1332.5	1938.68	-2.56	-5.63		1452.5	1933.80	-2.68	-5.52
1335	1938.60	-2.83	-5.70		1455	1933.71	-2.85	-5.74
1337.5	1938.52	-2.69	-5.86		1457.5	1933.61	-2.54	-5.46
1340	1938.35	-2.65	-5.74		1460	1933.52	-2.96	-5.50
1342.5	1938.18	-1.93	-5.56		1462.5	1933.41	-2.64	-5.64
1345	1938.09	-2.10	-5.69		1465	1933.29	-2.33	-5.49
1347.5	1937.99	-2.33	-5.66		1467.5	1933.18	-2.33	-5.52
1350	1937.90	-2.33	-5.74		1470	1933.09	-2.59	-5.44
1352.5	1937.80	-2.66	-5.78		1472.5	1932.99	-2.41	-5.62
1355	1937.71	-2.75	-5.91		1475	1932.90	-2.52	-5.41
1357.5	1937.61	-2.64	-5.82		1477.5	1932.80	-2.55	-5.51
1360	1937.52	-2.93	-5.75		1480	1932.71	-2.58	-5.57
1362.5	1937.41	-2.67	-5.57		1482.5	1932.61	-2.60	-5.68
1365	1937.29	-2.21	-5.77		1485	1932.52	-2.90	-5.54
1367.5	1937.18	-2.19	-5.52		1487.5	1932.45	-2.77	-5.59
1370	1937.07	-2.20	-5.54		1490	1932.38	-2.53	-5.65
1372.5	1936.96	-2.20	-5.55		1492.5	1932.32	-2.51	-5.50
1375	1936.85	-2.52	-5.65		1495	1932.25	-2.41	-5.54
1377.5	1936.74	-2.55	-5.53		1497.5	1932.18	-2.35	-5.55
1380	1936.63	-2.16	-5.53		1500	1932.05	-2.39	-5.59
1382.5	1936.52	-2.57	-5.59		1502.5	1931.92	-2.60	-5.66
1385	1936.43	-2.82	-5.53		1505	1931.78	-2.78	-5.64
1387.5	1936.35	-2.41	-5.54		1507.5	1931.65	-2.65	-5.63
1390	1936.27	-2.08	-5.58		1510	1931.52	-2.43	-5.66
1392.5	1936.18	-2.40	-5.42		1512.5	1931.35	-2.90	-5.64
1395	1936.09	-2.02	-5.46		1515	1931.18	-2.54	-5.54
1397.5	1935.99	-2.40	-5.43		1517.5	1931.09	-2.18	-5.59
1400	1935.90	-2.25	-5.56		1520	1930.99	-2.19	-5.57
1402.5	1935.80	-2.44	-5.55		1522.5	1930.90	-2.43	-5.66
1405	1935.71	-2.48	-5.51		1525	1930.80	-2.30	-5.69

1527.5	1930.71	-2.26	-5.76		1647.5	1926.29	-2.14	-5.43
1530	1930.61	-2.68	-5.81		1650	1926.18	-1.96	-5.26
1532.5	1930.52	-2.41	-5.82		1652.7	1926.08	-2.28	-5.37
1535	1930.45	-2.30	-5.66		1655	1925.99	-2.11	-5.58
1537.5	1930.38	-2.25	-5.57		1657.5	1925.90	-2.29	-5.51
1540	1930.32	-2.42	-5.69		1660	1925.80	-2.59	-5.52
1542.5	1930.25	-2.32	-5.57		1662.5	1925.71	-2.57	-5.63
1545	1930.18	-1.89	-5.40		1665	1925.61	-2.51	-5.48
1547.5	1930.10	-2.03	-5.51		1667.5	1925.52	-2.40	-5.58
1550	1930.02	-2.27	-5.48		1670	1925.41	-2.41	-5.57
1552.5	1929.93	-1.93	-5.57		1672.5	1925.29	-2.08	-5.50
1555	1929.85	-2.20	-5.57		1675	1925.18	-2.17	-5.39
1557.5	1929.77	-2.36	-5.58		1677.5	1925.07	-2.52	-5.43
1560	1929.68	-2.52	-5.60		1680	1924.96	-2.55	-5.41
1562.5	1929.60	-2.62	-5.68		1682.5	1924.85	-2.62	-5.49
1565	1929.52	-2.65	-5.70		1685	1924.74	-2.63	-5.49
1567.5	1929.41	-2.14	-5.47		1687.5	1924.63	-2.71	-5.47
1570	1929.29	-2.05	-5.54		1690	1924.52	-2.31	-5.59
1572.5	1929.18	-1.93	-5.53		1692.5	1924.43	-2.55	-5.57
1575	1929.09	-2.07	-5.54		1695	1924.35	-2.60	-5.43
1577.5	1928.99	-2.08	-5.67		1697.5	1924.27	-2.22	-5.47
1580	1928.90	-2.20	-5.67		1700	1924.18	-2.09	-5.41
1582.5	1928.80	-2.45	-5.75		1702.5	1924.05	-2.01	-5.52
1585	1928.71	-2.61	-5.60		1705	1923.92	-2.16	-5.60
1587.5	1928.61	-2.27	-5.59		1707.5	1923.78	-2.58	-5.47
1590	1928.52	-2.60	-5.73		1710	1923.65	-2.50	-5.60
1592.5	1928.41	-2.45	-5.48		1712.5	1923.52	-2.59	-5.66
1595	1928.29	-2.19	-5.63		1715	1923.45	-2.97	-5.50
1597.5	1928.18	-2.04	-5.33		1717.5	1923.38	-2.47	-5.54
1600	1928.09	-2.16	-5.33		1720	1923.32	-2.22	-5.49
1602.5	1927.99	-2.41	-5.77		1722.5	1923.25	-1.95	-5.42
1605	1927.90	-2.27	-5.55		1725	1923.18	-2.26	-5.35
1607.5	1927.80	-2.59	-5.52		1727.5	1923.07	-2.22	-5.40
1610	1927.71	-2.24	-5.63		1730	1922.96	-2.39	-5.40
1612.5	1927.61	-2.48	-5.59		1732.5	1922.85	-2.51	-5.48
1615	1927.52	-2.75	-5.66		1735	1922.74	-2.37	-5.56
1617.5	1927.41	-2.46	-5.49		1737.5	1922.63	-2.30	-5.54
1620	1927.29	-2.17	-5.44		1740	1922.52	-3.06	-5.55
1622.5	1927.18	-1.97	-5.39		1742.5	1922.43	-2.41	-5.44
1625	1927.10	-2.02	-5.41		1745	1922.35	-1.98	-5.43
1627.5	1927.02	-2.28	-5.54		1747.5	1922.27	-2.05	-5.36
1630	1926.93	-2.26	-5.44		1750	1922.18	-1.94	-5.22
1632.5	1926.85	-2.40	-5.54		1752.5	1922.07	-2.04	-5.36
1635	1926.77	-2.47	-5.54		1755	1921.96	-2.24	-5.35
1637.5	1926.68	-2.31	-5.53		1757.5	1921.85	-2.57	-5.54
1640	1926.60	-2.24	-5.64		1760	1921.74	-2.34	-5.50
1642.5	1926.52	-2.73	-5.71		1762.5	1921.63	-2.47	-5.38
1645	1926.41	-2.33	-5.48		1765	1921.52	-2.67	-5.48

1767.5	1921.43	-2.19	-5.42		1887.5	1916.90	-2.53	-5.30
1770	1921.35	-2.09	-5.34		1890	1916.80	-2.64	-5.44
1772.5	1921.27	-2.14	-5.34		1892.5	1916.71	-2.70	-5.41
1775	1921.18	-2.43	-5.24		1895	1916.61	-2.82	-5.44
1777.5	1921.07	-2.24	-5.62		1897.5	1916.52	-3.11	-5.47
1780	1920.96	-2.31	-5.61		1900	1916.41	-2.75	-5.51
1782.5	1920.85	-2.02	-5.56		1902.5	1916.29	-2.26	-5.39
1785	1920.74	-2.44	-5.42		1905	1916.18	-1.99	-5.42
1787.5	1920.63	-2.31	-5.57		1907.5	1916.07	-2.34	-5.47
1790	1920.52	-2.52	-5.68		1910	1915.96	-2.65	-5.64
1792.5	1920.46	-2.24	-5.57		1912.5	1915.85	-2.86	-5.50
1795	1920.41	-2.31	-5.59		1915	1915.74	-2.83	-5.65
1797.5	1920.35	-1.99	-5.57		1917.5	1915.63	-2.35	-5.52
1800	1920.29	-2.16	-5.58		1920	1915.52	-2.72	-5.41
1802.5	1920.24	-2.50	-5.49		1922.5	1915.41	-2.64	-5.54
1805	1920.18	-2.55	-5.33		1925	1915.29	-2.59	-5.61
1807.5	1920.10	-2.24	-5.45		1927.5	1915.18	-2.15	-5.58
1810	1920.02	-2.36	-5.70		1930	1915.09	-2.31	-5.61
1812.5	1919.93	-2.50	-5.69		1932.5	1914.99	-2.32	-5.52
1815	1919.85	-2.56	-5.62		1935	1914.90	-2.33	-5.62
1817.5	1919.77	-2.66	-5.66		1937.5	1914.80	-2.36	-5.63
1820	1919.68	-2.28	-5.61		1940	1914.71	-2.44	-5.63
1822.5	1919.60	-2.84	-5.70		1942.5	1914.61	-2.81	-5.71
1825	1919.52	-2.84	-5.83		1945	1914.52	-2.54	-5.71
1827.5	1919.35	-2.40	-5.59		1947.5	1914.45	-2.48	-5.58
1830	1919.18	-2.14	-5.28		1950	1914.38	-2.51	-5.58
1832.5	1919.07	-2.50	-5.37		1952.5	1914.32	-3.06	-5.54
1835	1918.96	-2.60	-5.72		1955	1914.25	-2.46	-5.49
1837.5	1918.85	-2.33	-5.74		1957.5	1914.18	-2.00	-5.36
1840	1918.74	-2.27	-5.82		1960	1914.09	-2.24	-5.38
1842.5	1918.63	-2.66	-5.71		1962.5	1913.99	-2.38	-5.36
1845	1918.52	-2.74	-5.69		1965	1913.90	-2.58	-5.40
1847.5	1918.43	-2.59	-5.65		1967.5	1913.80	-2.53	-5.45
1850	1918.35	-2.46	-5.56		1970	1913.71	-2.69	-5.41
1852.5	1918.27	-2.19	-5.32		1972.5	1913.61	-2.88	-5.51
1855	1918.18	-2.00	-5.37		1975	1913.52	-2.58	-5.60
1857.5	1918.09	-2.10	-5.42		1977.5	1913.41	-2.16	-5.46
1860	1917.99	-2.54	-5.27		1980	1913.29	-2.42	-5.44
1862.5	1917.90	-2.30	-5.25		1982.5	1913.18	-2.15	-5.28
1865	1917.80	-2.54	-5.48		1985	1913.07	-2.59	-5.45
1867.5	1917.71	-2.71	-5.40		1987.5	1912.96	-2.46	-5.50
1870	1917.61	-2.44	-5.45		1990	1912.85	-2.71	-5.44
1872.5	1917.52	-2.81	-5.45		1992.5	1912.74	-2.64	-5.56
1875	1917.41	-2.53	-5.48		1995	1912.63	-2.38	-5.38
1877.5	1917.29	-2.10	-5.28		1997.5	1912.52	-2.64	-5.60
1880	1917.18	-2.02	-5.44		2000	1912.35	-2.22	-5.56
1882.5	1917.09	-2.38	-5.23		2002.5	1912.18	-2.06	-5.40
1885	1916.99	-2.66	-5.44		2005	1912.05	-2.24	-5.38

2007.5	1911.92	-2.40	-5.36		2127.5	1907.52	-2.75	-5.59
2010	1911.78	-2.51	-5.55		2130	1907.43	-2.40	-5.48
2012.5	1911.65	-2.48	-5.52		2132.5	1907.35	-2.18	-5.56
2015	1911.52	-2.77	-5.57		2135	1907.27	-2.38	-5.59
2017.5	1911.45	-2.20	-5.52		2137.5	1907.18	-2.39	-5.46
2020	1911.38	-2.28	-5.40		2140	1907.07	-2.24	-5.51
2022.5	1911.32	-2.69	-5.32		2142.5	1906.96	-2.69	-5.51
2025	1911.25	-2.26	-5.39		2145	1906.85	-2.64	-5.52
2027.5	1911.18	-2.05	-5.19		2147.5	1906.74	-2.59	-5.54
2030	1911.05	-2.18	-5.31		2150	1906.63	-2.74	-5.68
2032.5	1910.92	-2.73	-5.27		2152.5	1906.52	-2.91	-5.71
2035	1910.78	-2.44	-5.35		2155	1906.41	-2.85	-5.64
2037.5	1910.65	-2.45	-5.35		2157.5	1906.29	-2.66	-5.59
2040	1910.52	-2.82	-5.39		2160	1906.18	-2.28	-5.52
2042.5	1910.46	-2.55	-5.38					
2045	1910.41	-2.43	-5.34					
2047.5	1910.35	-2.43	-5.39					
2050	1910.29	-2.35	-5.43					
2052.5	1910.24	-2.10	-5.32					
2055	1910.18	-2.02	-5.37					
2057.5	1910.09	-2.32	-5.37					
2060	1909.99	-2.45	-5.34					
2062.5	1909.90	-2.03	-5.14					
2065	1909.80	-2.32	-5.22					
2067.5	1909.71	-2.31	-5.23					
2070	1909.61	-2.39	-5.28					
2072.5	1909.52	-2.42	-5.38					
2075	1909.45	-2.62	-5.32					
2077.5	1909.38	-2.30	-5.31					
2080	1909.32	-2.01	-5.25					
2082.5	1909.25	-1.80	-5.19					
2085	1909.18	-2.12	-5.09					
2087.5	1909.09	-2.06	-5.44					
2090	1908.99	-2.28	-5.39					
2092.5	1908.90	-2.53	-5.40					
2095	1908.80	-2.60	-5.38					
2097.5	1908.71	-2.35	-5.44					
2100	1908.61	-2.38	-5.41					
2102.5	1908.52	-2.64	-5.46					
2105	1908.41	-2.42	-5.43					
2107.5	1908.29	-2.10	-5.35					
2110	1908.18	-2.07	-5.36					
2112.5	1908.09	-2.11	-5.36					
2115	1907.99	-2.58	-5.38					
2117.5	1907.90	-2.57	-5.43					
2120	1907.80	-2.45	-5.47					
2122.5	1907.71	-2.38	-5.50					
2125	1907.61	-2.68	-5.54					